Approved for public release: distribution unlimited.

LC–DRI Field Experiment and Data Calibration Report

by B. Ma, E. D'Asaro, T. Sanford, and J. Thomson

Technical Report
APL-UW TR 2002
March 2020

Applied Physics Laboratory University of Washington
1013 NE 40th Street Seattle, Washington 98105-6698

Contract: N00014-17-1-2859

ACKNOWLEDGMENTS

The authors thank Drs. Terri Paluszkiewicz, Scott Harper, and Linwood Vincent of the Office of Naval Research for the support from the Waves, Langmuir Cells and the Upper Ocean Boundary Layer Departmental Research Initiative (LC–DRI).

ABSTRACT

The goal of the Waves, Langmuir Cells and the Upper Ocean Boundary Layer Departmental Research Initiative (LC–DRI) is to explore the upper ocean physics necessary to advance our understanding of the fluxes into and across the ocean mixed layer, including surface waves and wave breaking, Langmuir cells, and wave–current interaction. A set of comprehensive observational data was collected during the LC-DRI field experiment from various platforms including autonomous floats, drifter, buoys, and shipboard observations. The field campaign was conducted on the coast of Southern California 21 March – 5 April 2017. The fieldwork, including the event log and instrument deployment, is described in Part I. The inter-calibration between observed CTD data from EM-APEX and MLF floats, SWIFT drifters and R/V *Sproul* are described in Part II. For the MLF vs. EM-APEX calibration, the average salinity of MLF #82 and #83 top and bottom sensors is used as a reference. The calculated salinity offset for EM-APEX #6667, #6672, and #6678 is ~ 0.004 psu, for EM-APEX #6671 and #6674 is ~0.001 psu, and for EM-APEX #6675 is ~−0.001 psu. For seven SWIFT drifters at 0.2, 0.5, and 1.2 m, the calculated temperature offset varies from −0.1 to 0.1°C and the salinity offset varies from −0.003 to 0.2 psu. The salinity data from SWIFT #16 and #17 at 0.2 m exhibited large offsets, which suggest data bias. The comparison of wave energy measurements between SWIFT drifters and a Datawell Waverider buoy moored at CDIP station 299 are described in Part III. Excluding the periods when the mean separation distance was greater than 30 km (periods 3–1, 3, 5, 6, 8, 12), the root-mean-square error (RMSE) of significant wave height (*Hs*) is 0.25 ± 0.08 m, the RMSE of integrated wave energy is 0.057 ± 0.029 m^2, and the average percent error of *Hs* is ~13%. In general, given the temporal, spatial, and spectral differences in the sampling strategy of SWIFT drifters and the CDIP buoy, the comparison suggests no significant bias in either dataset.

The raw data, analysis plots, PPT files, movies and reports for this project are available at ampere.apl.washington.edu/~barry/LCDRI/ (APL-UW VPN is required for the access).

Table of Contents

LIST OF TABLES

LIST OF FIGURES

PART I. FIELD EXPERIMENT

Summary of R/V *Sproul* operations on the 2017 LC–DRI cruise, 19 March – 6 April 2017, Eric D'Asaro, Chief Scientist.

1.1 Operating area

Operations were conducted within a 15-n mi circle centered on R/P *FLIP*, excluding the gray Navy restricted areas when they were in active use.

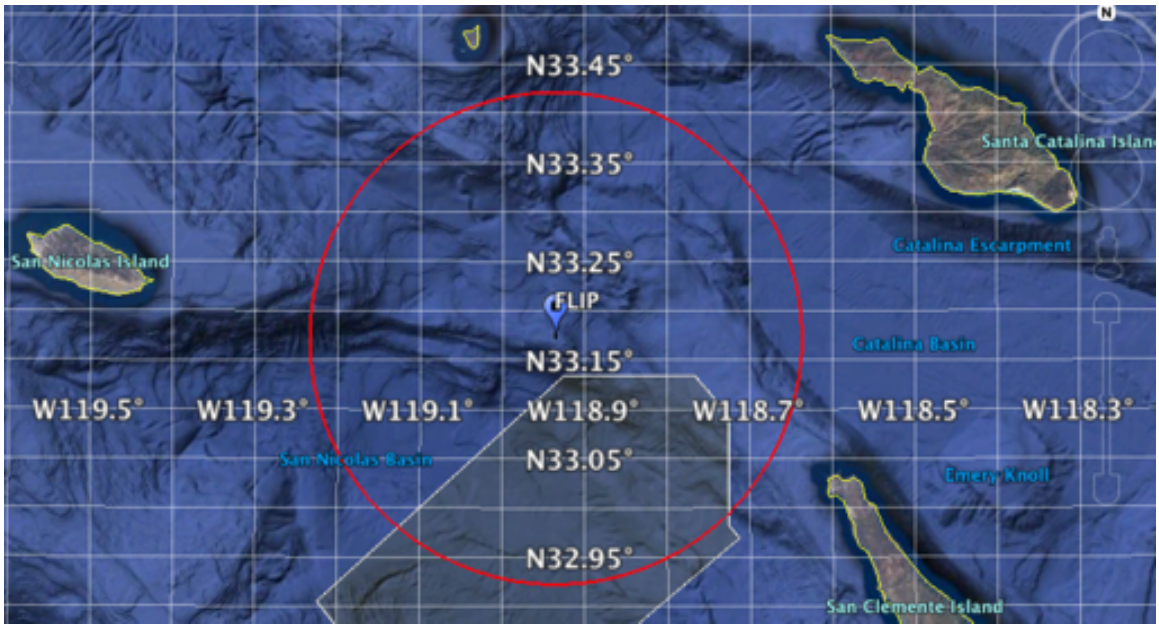

Figure 1.1: LC–DRI operating area.

1.2 Activity log

Times in Pacific daylight time as noted

March 19 (yd 78) – Leave Marfac

March 20 (yd 79) – Arrive in operating area

Weather: wind SE 10–20 kts

8:00 am: test deployment of all instrument types

SWIFT v3 #12

SWIFT v4 #22

MLF #83

EM-APEX #5574

4:00 pm: additional deployments in tight 100-m array

MLF #81 MLF #82

EM-APEX #6678

SWIFT #24 SWIFT #16

March 21 (yd 80)

Weather: fair

Recovered SWIFT #24 and #16

Recovered EM-APEX #6678 and MLF #83

Deployed SWIFTS #11 and #17, EM-APEX #6675, continuing missions for MLF #81 and #82

March 22 (yd 81)

Weather: good, but strong winds expected in the evening and tomorrow

Recovered all but EM-APEX #6678 before noon

Redeployed 12 items in a fancy array, completed by 4:30 pm, including all EM-APEXs except #6678, which is still out, MLF #81, #82, #83, and SWIFT #17 and #12

March 23 (yd 82)

Weather: too stormy to operate; tried to recover SWIFTS, but too dangerous

SWIFT drifters blown southward into the restricted area, others move SW (Fig. 1.4)

March 24 (yd 83)

Weather: improved

Recovered MLFs and most EM-APEXs by 9:15 am

Restricted area was open; recovered SWIFTS and EM-APEX #6678

The weather was forecast to be stormy for the next few days. What to do?

Ship goes to Catalina Harbor.

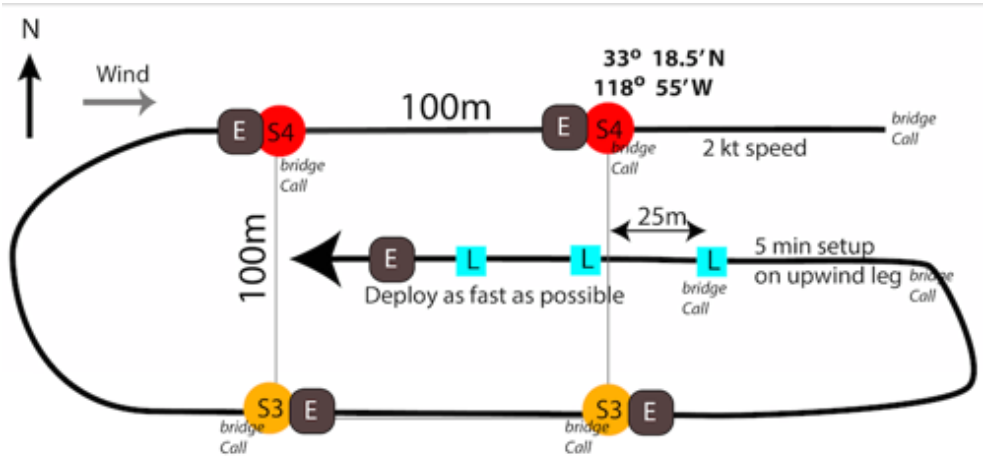

S4, S3 and EM deployments by Alex/Mike off port aft quarter from cart
Moved by Alex, Andrey, Mike

L deployments by Mike/Andrey near port A-frame leg
2 floats staged at CTD, held by John, Eric

Figure 1.2: Cruise track 1.

IDs and times are noted here

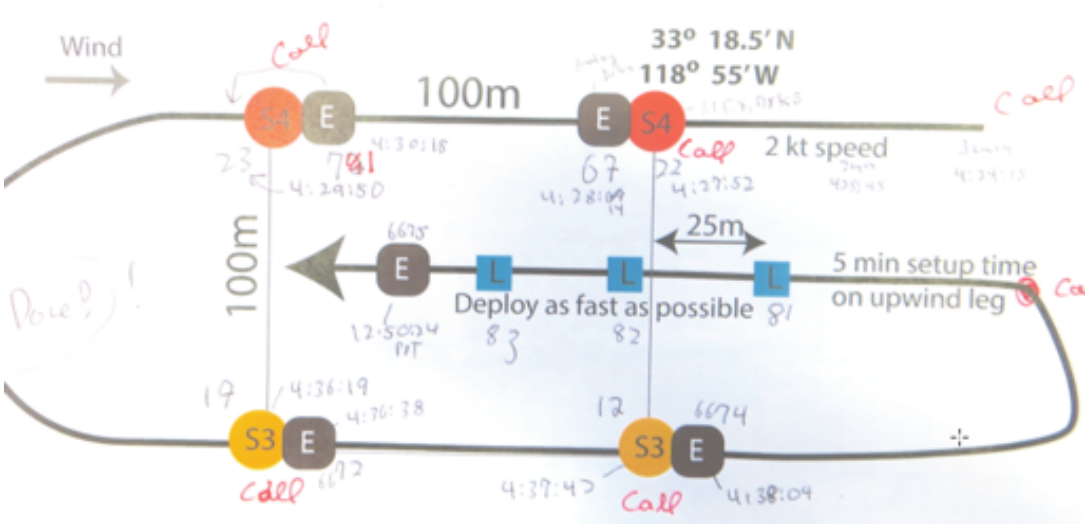

Figure 1.3: Cruise track 2.

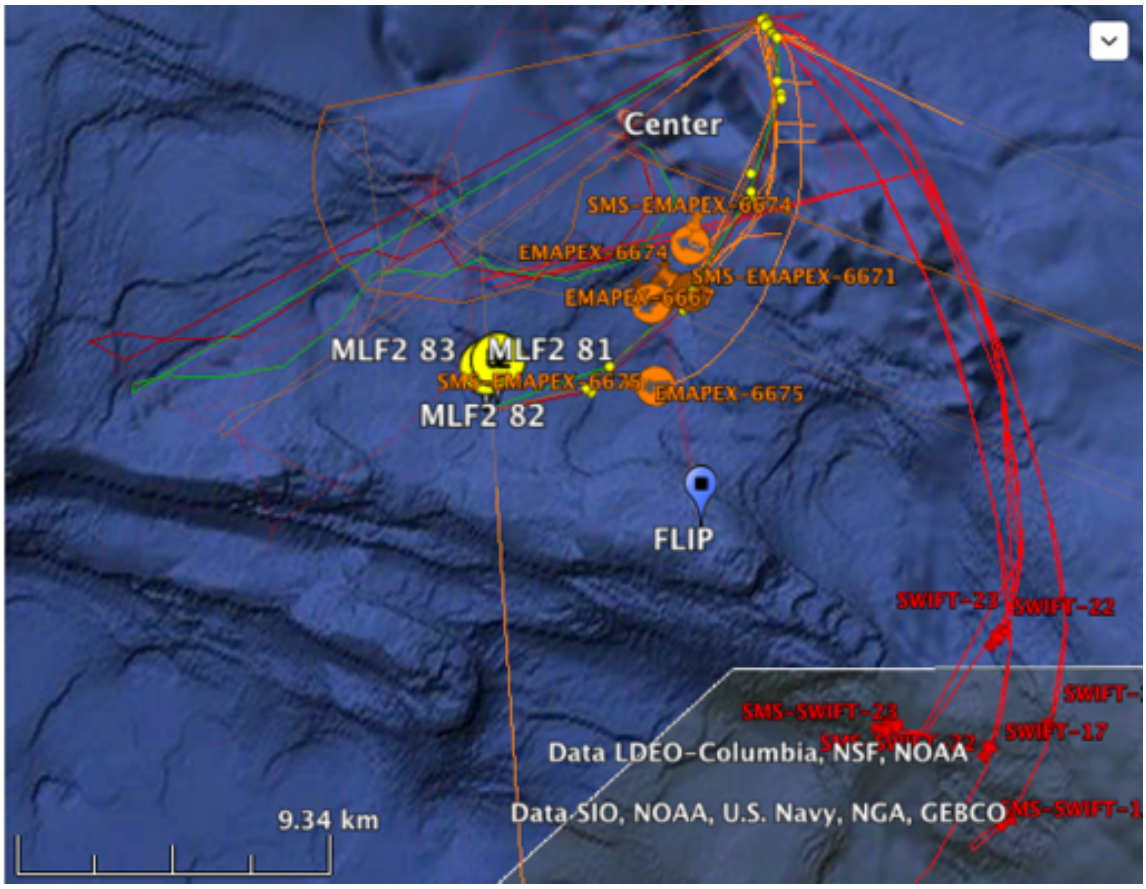

Figure 1.4: Map of asset locations 23 March 2017.

March 25 (yd 84)

Back out for hole between storms

MLF #82, SWIFT #17 and #25

Short deployment 11:00 am – 4:00 pm

March 26 (yd 85)

Deploy: ~8:00 am EM-APEX #6673, SWIFT #25 and #17, MLF #81 and MLF #83

Recover: ~7:00 pm, SWIFT #81 and #82; SWIFT #83 and EM-APEX #6672 stay out for the storm

The ship goes to Catalina Harbor

March 27 – Ship stays at Catalina

March 28 (yd 87)

Short deployments in Catalina Channel

Deploy: ~11:00 am MLF #81 and #82, SWIFT #22, #23, #24, and #25 in a small square

March 29 (yd 88)

Recover: MLF #83 and EM-APEX #6672

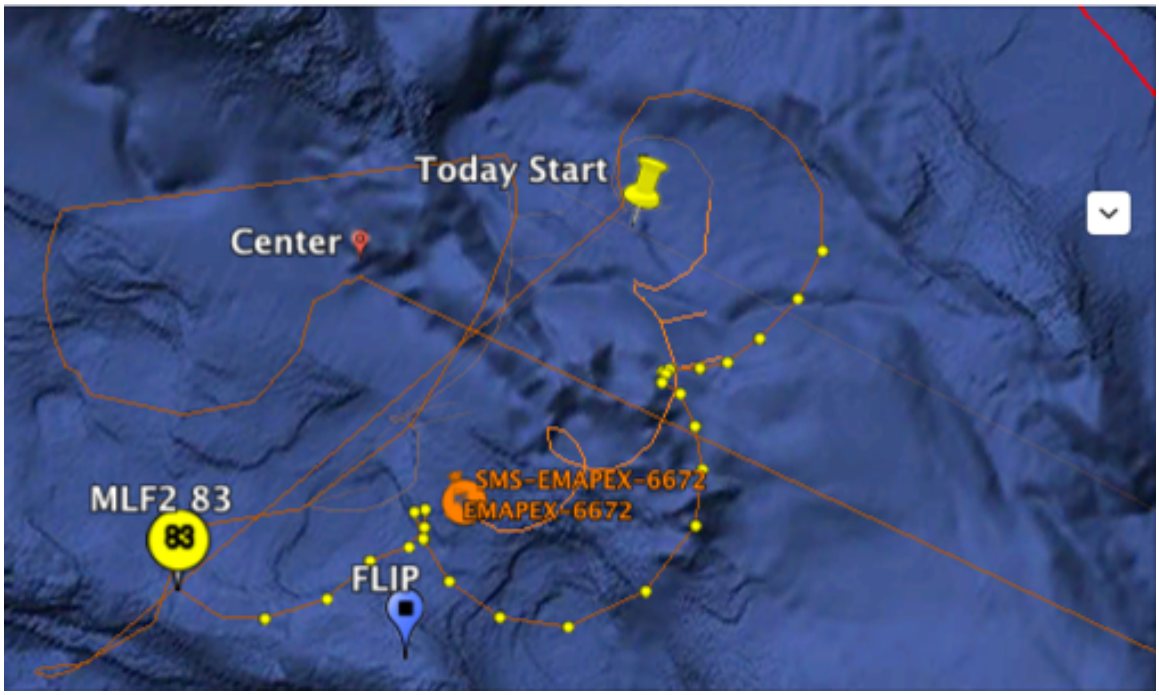

Figure 1.5: Tracks of first 3-day operation.

Deployment (short): all 8 SWIFTS near R/P *FLIP* for intercomparison

Deployed: ~5:30 pm, back at 'START' EM-APEX #6667, #6671, #6675, and #6678; SWIFT #17; MLF #81, #82, and #83

March 30 (yd 89)

Recover: 10:00 am, SWIFT #17

Go to Catalina for the third storm

March 31 (yd 90)

Stay at Catalina

April 1 (yd 91)

Recover: all by 10:00 am

Redeploy: ~2:00 pm, floats for a long period of nicer weather; deploy at three nearby points. “Start” = MLF #81, #82, and #83, EM-APEX #6672 and #6667, SWIFT #12 and #17; “B” = EM-APEX #6675, and #6678; “A” = EM-APEX #6674

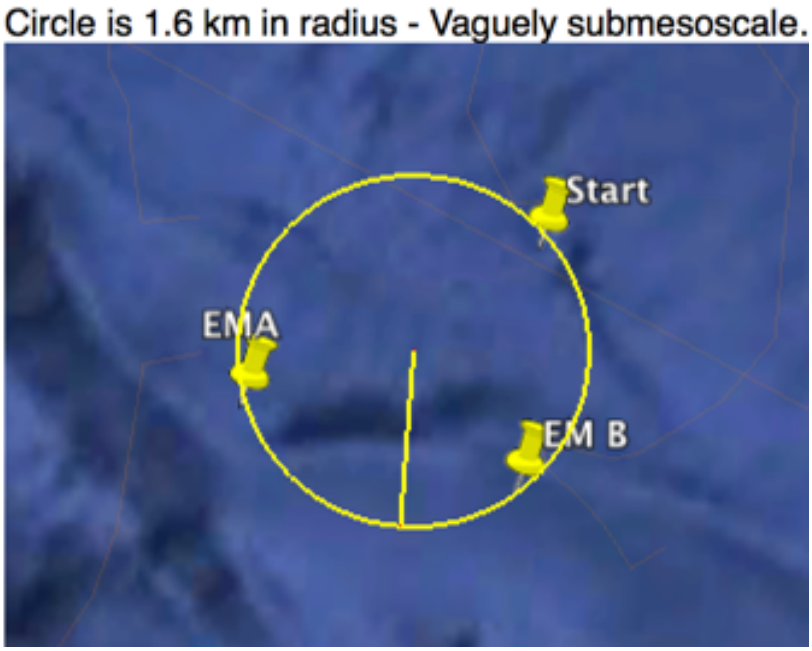

Figure 1.6: 1 April float locations.

April 2 (yd 92)

Naval GPS outage 10–11 am

Floats continue on the mission

Recover and reposition SWIFT #12 and #17 to near Lagrangian

Four SWIFT v4 deployed during the day

April 3 and 4 (yd 93 and 94)

Repeat April 2

April 5 (yd 95)

Recover all assets by 2:00 pm

Head for home

April 6

Demobilize

1.3 Plots

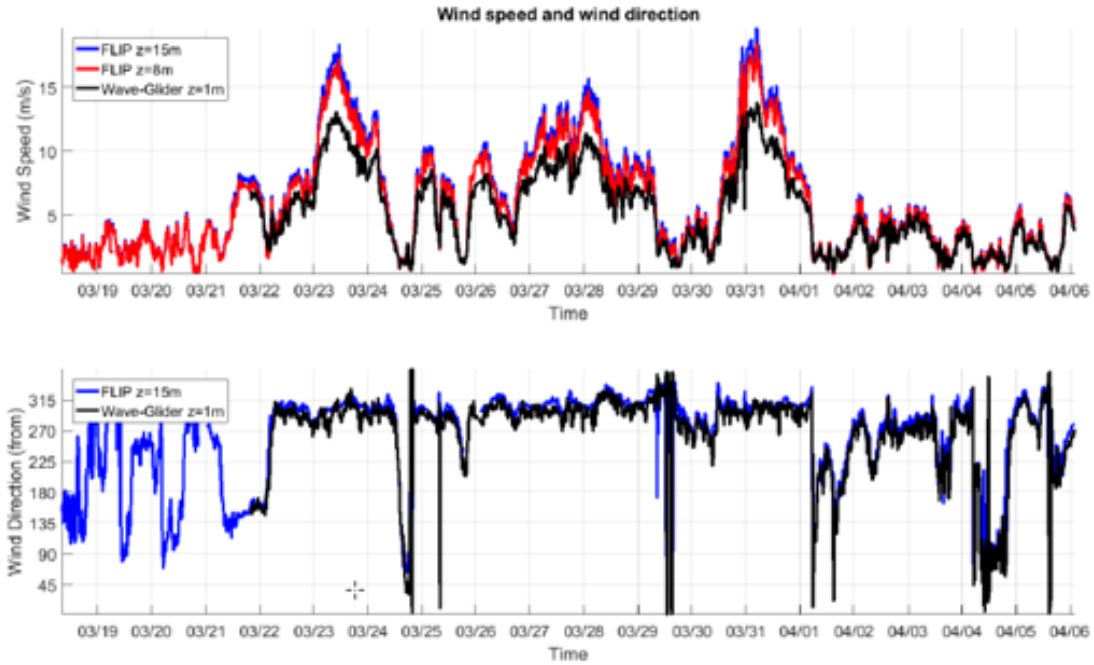

Figure 1.7: R/P FLIP wind speed and direction (similar measurements on R/V Sproul).

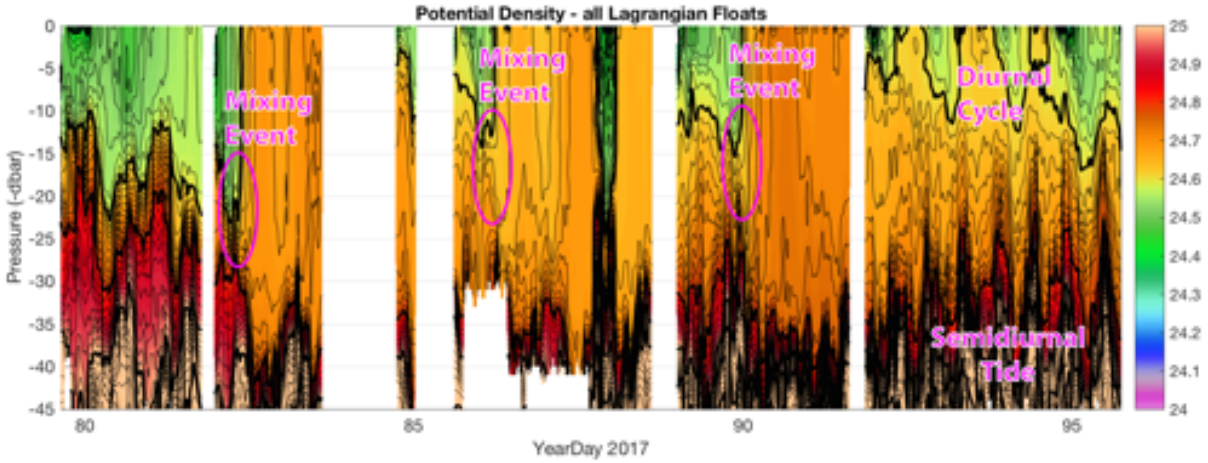

Figure 1.8: Potential density of all Lagrangian floats.

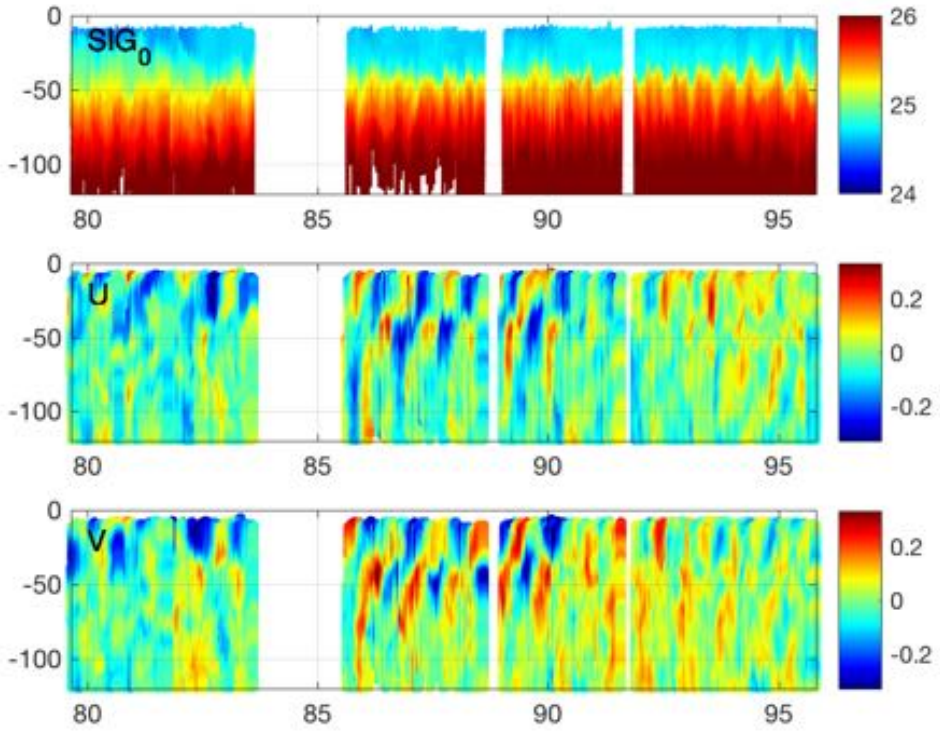

Figure 1.9: EM-APEX density and velocity.

PART II. SALINITY AND TEMPERATURE DATA CALIBRATION

2.1 Introduction

This report contains the calibration of salinity and temperature data for three *Mixed-layer Lagrangian Floats* (MLFs), six *Electromagnetic Autonomous Profiling Explorer* (EM-APEX) floats and seven *Surface Wave Instrument Float with Tracking* (SWIFT) drifters deployed during the LC–DRI field campaign 21 March – 5 April 2017. Several factors affect the accuracy of the temperature and salinity sensors including, 1) instrument resolution and accuracy – these are determined by the type of CTD on the platform and sensor drift over time; 2) lateral gradients of the ocean – if lateral gradients are large it will be difficult to inter-calibrated nearby floats; 3) depth resolution and sampling depth – the EM-APEX takes independent measurement about every 2–3 m, a profiling MLF takes independent measurements about every ~0.2 m, and SWFIT has fixed depth CTDs near the surface; 4) sampling method – the profiling floats vs. drifter and shipboard-underway fixed depth measurements.

MLFs profiled to ~50 m depth and EM-APEXs profiled to ~150 m depth in most of the deployments. SWIFT drifters, however, remain on the sea surface with a fixed depth CTD measuring the near-surface layer. This calibration report is focused on the salinity correction utilizing the temperature–salinity diagram and depth interpolation. Two sets of calibrations are described in this report. The EM-APEX vs. MLF salinity calibration (section 2.6) and the SWIFT vs. MLF temperature and salinity calibration (section 2.7).

2.2 MLF

The Mixed-layer Lagrangian Float (MLF) was developed and built at the Applied Physics Laboratory of the University of Washington (APL-UW) (*D'Asaro* 2003). The 1.5-m-long instrument was designed to measure turbulence in the ocean mixed layer by accurately following the three-dimensional motion of water parcels through a combination of active neutral buoyancy maintenance and high-drag provided by controllable, flexible drogues. Compared to other types of floats (e.g., Argo floats), MLFs have an adaptable automatic buoyancy control and a relatively heavy payload. These floats can provide a uniform sampling of mixed layer turbulence in a fully Lagrangian water-following mode. They can also operate in isopycnal or isopycnal/Lagrangian modes in the pycnocline, or profile across a given depth range. The MLFs used in this experiment are MLF #81, #82, and #83 (Fig. 2.1). The MLF is equipped with two sets of CTDs sensors on both ends of the float separated by 1.5 m, thus the top sensor only measures the water column near the surface (<1.5 m depth). The vertical resolution of MLF CTD data is ~0.1 m.

2.3 EM-APEX

The EM-APEX float combines the standard Teledyne Webb Research Corp. APEX profiling float with an APL-UW developed subsystem that measures the motionally induced electric fields generated by the ocean currents moving through the vertical component of the earth's magnetic field (*Sanford et al*. 2005). The EM-APEX floats used in this experiment are #6667, #6671, #6672, #6674, #6675, and #6678. The vertical resolution of EM-APEX CTD data is ~2–3 m.

2.4 SWIFT

A Lagrangian drifter, the Surface Wave Instrument Float with Tracking (SWIFT), was developed by Jim Thomson's group at APL-UW. It is designed to follow the time-varying free-surface while collecting high-resolution profiles of turbulent velocity (*Thomson* 2012). The wave-following reference frame method (*Gemmrich* 2010) is adapted. The velocity fluctuations are used to estimate the turbulence dissipation rate (*Wiles et al*. 2006). SWIFT drifters used in this experiment are #12 and #13 with CT sensors at 0.5 m depth, SWIFT #16 and #17 with CT sensors at 0.2, 0.5, and 1.2 m depths, and SWIFT #22, #23, #24, and #25 with CT sensors at 0.2 m depth. The SWFIT #25 CT sensor malfunctioned during the experiment, thus it is not included in this report. The raw CT data on the SWIFT has a temporal resolution of 2 s, and the reported data products are ensemble averages every 12 min.

2.5 Experiment location and periods

The LC–DRI field experiment was conducted in the region between San Nicolas Island, Santa Catalina Island, and San Clemente Island on 21 March – 5 April 2017 (Fig. 2.2). The 16-day timespan is separated into five periods, each about 1–3 days. Various numbers of floats and drifters were deployed. All MLFs were deployed in each of the periods, though in period 3 MLF #81 and #82 only were deployed for a few hours in two incidents. Five EM-APEXs were deployed in periods 2 and 5, four EM-APEXs were deployed in period 4, three EM-APEXs were deployed in period 1, though EM-APEX #6678 returned only two profiles in this deployment, and one EM-APEX was deployed in period 3. Four SWIFTs were deployed in periods 1 and 2. All eight SWIFTs were deployed in two incidents in period 3 for a few hours. Six SWIFTs were deployed in period 5 with SWIFT #22, #23, #24, and #25 deployed for a few hours in three incidents, and SWIFT #12 and #17 deployed for ~4 days (Fig. 2.3 and Table 2.1).

2.6 EM-APEX vs. MLF salinity calibration

2.6.1 Description

Data from six EM-APEX and all MLF floats are used for inter-calibration analyses. The averaged float path of MLF #92 and #93 is used as the default reference after an initial inspection of the data quality of these two MLFs. The EM-APEX intercepts within ±1 km of the mean location of MLF #92 and #93 and within ±1 hr are used for comparison. The float paths of each period are shown in Fig. 2.4. The thick black line indicates the reference float MLF_{Ref} (the average path of MLF_{82} and MLF_{83}). The grey patch is the ±1-km width of the black line. The open circles are the float locations represented by different colors. The solid circles are the floats within ±1 km and ±1 hr of MLF_{Ref}. The T–S diagrams are plotted according to each deployment period.

2.6.2 Calibration procedure

Depth selection:

The profiling depth of EM-APEX is ~150 m and MLF is ~50 m. To compare the T–S diagrams of MLF and EM-APEX floats, data at depth 2–40 m for periods 1, 2, and 4, depth 2–35 m for period 3, and 2–20 m for period 5 are used. The depth 2–20 m was adopted for period 5 due to the fact that MLF #81 was set to profile 0–10 m in this deployment. The starting depth of 2 m is selected so that the top CTD of the MLF never rises above the surface. This prevents the biased data to be included in the T–S diagram. The top CTD of the MLF is at the surface for a depth of ~1.4 m.

Reference float (MLF_{Ref}):

The average location and time of MLF_{82} and MLF_{83} are used as a reference float (Eqn. 2.1) because these two floats seem relatively stable over the deployment. We interpolated the MLF_{82} and MLF_{83} locations into uniform time then averaged the locations. The salinity data of the other floats are adjusted to match the average salinity of these two floats (four CTDs, including top and bottom sensors).

$$MLF_{Ref}(x,y,t) = \frac{MLF_{82}(x,y,t) + MLF_{83}(x,y,t)}{2} \tag{2.1}$$

Data selection for calibration:

Each profile T_n (where n is the profile number) is checked against the reference float MLF_{Ref}. Only the data within a ±1 km vicinity and ± 1 hr are used in the calibration (Fig. 2.4, Eqn. 2.2 and 2.3).

$$\left|T_n(x,y) - MLF_{Ref}(x,y,)\right| \leq 1km \tag{2.2}$$

$$\left|T_n(t) - MLF_{Ref}(t)\right| \leq 1h \tag{2.3}$$

Linear least square fits:

Scatter plots of T–S are made for each CTD sensor and the least square fits are applied to the data within ± one standard deviation of the mean potential temperature of

each group. Then the data within two standard deviations of the first fit are used to reproduce the linear fit. In general, about 20–40% of data are excluded from the first fit, and 1–2% of data are excluded from the second fit. Figures 2.5–2.9 [subpanel (a) in each] show the T–S diagram with fitting results of periods 1–5. The number in the legend box indicates the number of points after depth and spatial screening. The first percentage number indicates the portion of data outside the one standard deviation of potential temperature being removed before the first fit. The second percentage number indicates a portion of data outside two standard deviations of data being removed after the first fit. The thin vertical dashed line is the mean potential temperature of each CTD. The thick vertical grey line is the average of mean potential temperature. The grey dashed line is one standard deviation.

Salinity offset adjustment:

The average of the mean potential temperatures is used to determine the salinity offset. This is because the slopes of the fit lines are not necessarily uniform (Fig. 2.5–2.9) [subpanel (b) in each]. The final offset is calculated using the average offset over five periods (Eqn. 2.4).

$$S_{corrected} = S_{obs} + S_{offset} \tag{2.4}$$

2.6.3 Results

A final salinity offset for each float is calculated using the average of periods 1–5 (Table 2.2). The offsets for each calibration interval are shown in Fig. 2.10a. The mean and one standard deviation of the calibration after offsets applied are shown in Fig. 2.10b. Temperature calibration uses the distance of MLF #82 and SWIFTs — 2 km. SWIFT #17 at period 4 seems biased, and was not included in the mean offset calculation. The estimation of salinity accuracy after calibration is ~0.0015 psu (one standard deviation of final fits).

2.7 SWIFT and MLF temperature and salinity calibration

2.7.1 Description

Data from three MLF floats and seven SWIFT drifters are used for temperature and salinity inter-calibration. SWIFT is equipped with fixed depth CT sensors near the surface. SWIFT #12 and #13 have CT sensors at 0.5 m depth, SWIFT #16 and #17 at 0.2, 0.5, and 1.2 m depths, and SWIFT #22, #23, #24, and #25 at 0.2 m depth. Only the MLF top CTD sensor is able to profile the near-surface water column at depths < 1.4 m. Only the MLF top sensor data is used for calibration. MLF #92 was selected as reference float after the initial inspection of data quality. The SWIFT Anderaa CT sensor has temperature accuracy of ±0.05°C and the MLF SBE-41 has temperature accuracy of ±0.002°C. It is important to check the temperature offset before the T–S diagram fits. The

R/V *Sproul* underway CT data, assuming a water intake at 1.2 m depth, is also included in this inter-calibration.

2.7.2 Calibration procedure

Data interpolation:

The MLF and SWIFT temperature, salinity, and location data are first interpolated to uniform 10-min intervals. (The SWIFT data are reported at 12-min intervals.) Then the MLF data are interpolated to SWIFT CT sensor depths.

Finding temperature offsets:

The scatter plots of distance vs. $\Delta T = T(t,x) - T_{mlf92}(t,x)$ (temperature difference from MLF #92) are used to determine the temperature offsets [Fig. 2.11 (a)–(c) period 1, (d)–(f) period 2, (g)–(i) period 3, (j)–(l) period 4, and (m)–(o) period 5]. The mean temperature difference within the 2-km range is calculated as the temperature offset for each period. The average ΔT of period 1–5 is calculated as the final temperature offset of each sensor (Fig. 2.12, Table 2.3). The SWIFT #17 at period 4 seems biased thus it is not included in the average ΔT calculation. The R/V *Sproul* was positioned > 2 km away, yielding no result in temperature offset. Zero temperature offset is used in R/V *Sproul* data.

Data selection for calibration:

Each data sample point S_n (where *n* is the data sample number) is checked against the reference float MLF_{92} . Only data within ±5 km vicinity and within ±5 hr are used in the calibration [Figs. 2.13–2.17; subpanel (c) in each].

$$|S_n(x,y) - MLF_{92}(x,y,)| \leq 5\ km \tag{2.5}$$

$$|S_n(t) - MLF_{92}(t)| \leq 5h \tag{2.6}$$

Linear least squares fits:

Scatter plots of T–S are made for each CTD sensor and the least squares fits are applied using a method similar to that described in section 2.6 (Figs. 2.13–2.17).

Salinity offset adjustment:

The average of the mean potential temperatures is used to determine the salinity offset. The final offset is calculated using the average offsets over five periods (Eqn. 2.4).

2.7.3 Calibration results

Figures 2.13–2.17 show the salinity calibration after applying the temperature offset for each SWIFT drifter. The final salinity offset is acquired by averaging over periods 1–5. (Fig. 2.18, Table 2.4). The results show that SWIFT #16 and #17 at 0.2 m depth have the larger salinity correction values of 3.04 psu and 1.48 psu, respectively. The large

values indicate that at the near-surface depth of 0.2 m the SWIFT data may be contaminated by the bubbles in the water.

At 0.5 m depth, SWIFT #11, #12, #16, and #17 have salinity correction values of ~0.2 psu. At 1.2 m depth, SWIFT #16 and #17 have salinity correction values at ~0.1 and ~0.05 psu, respectively. The values are closely related to the accuracy of the salinity sensor. The R/V *Sproul* has a small salinity correction value of 0.0067 psu, assuming the temperature sensor is correct.

2.8 Summary

Two sets of sensor corrections, MLF vs. EM-APEX and MLF vs. SWIFT, are performed for the LC–DRI field experiment data. The salinity correction value is made by utilizing the T–S diagram and least squares fits with careful data selection. The salinity corrections for MLF vs. EM-APEX are given in Table 2.2. The temperature and salinity corrections for SWIFT are given in Tables 2.3 and 2.4, respectively. For the MLF vs. EM-APEX calibration, the average salinity of MLF #82 and #83 top/bottom sensors is used as a reference. The calculated salinity offset for EM-APEX #6667, #6672, and #6678 is ~ 0.004 psu, for EM-APEX #6671 and #6674 is ~0.001 psu, and for EM-APEX #6675 is ~−0.001 psu. For seven SWIFTs at 0.2, 0.5 and 1.2 m, the calculated temperature offset varies from −0.1 to 0.1°C; the calculated salinity offset varies from −0.003 to 0.2 psu. In general, the correction value is related to the accuracy of the conductivity sensors except for the value for SWIFT #16 and #17 at 0.2 m depth, which is relatively large. This may be due to the bubble entrainment near the surface. A follow-up study is needed to determine the actual causes.

Appendix A: CTD Specifications

A.1. SBE 41 ARGO CTD

The EM-APEX and MLF were equipped with the SBE 41-argo-ctd sensor (Fig. 2.19). The temperature accuracy is ±0.002°C and salinity accuracy is ±0.002 psu (Table 2.5). (±0.05 mS/cm)

A.2. Aanderaa 4319 CT

The SWIFT drifters were equipped with Aanderaa 4319 CT sensors (Fig. 2.20). The temperature accuracy is ±0.05°C (0.09°F)/ ±0.1°C (0.18°F). The conductivity accuracy is ±0.05 mS/cm (4319A) or ±0.018 mS/cm (4319B) (Table 2.6).

PART III. WAVE ENERGY SPECTRUM COMPARISONS

3.1 Introduction

During the experiment, eight SWIFT drifters and a Datawell Waverider MK IIII, moored at Coastal Data Information Program (CDIP) station 299 at San Nicolas Island East, CA, were deployed for surface wave observations. We report the wave products from SWIFT drifters (Lagrangian) and CDIP buoy (Eulerian) platform to determine data quality.

3.2 SWIFT

A Lagrangian drifter, the SWIFT was developed by Jim Thomson's group at APL-UW (Fig. 3.1). It is designed to follow the time-varying free-surface while collecting high-resolution profiles of turbulent velocity (*Thomson* 2012). The wave-following reference frame method (*Gemmrich* 2010) is adapted. The velocity fluctuations are used to estimate the turbulence dissipation rate (*Wiles et al*. 2006). Two versions of the SWIFT were used in this experiment: SWIFT v3 #12, #13, #16 and #17, and SWIFT v4 #22, #23, #24 and #25. The data products used in this report are significant wave height, wave energy spectra, and peak wave direction. The wave products are calculated from GPS and IMU signals, following the methods of *Herbers et al*. (2012) and *Thomson et al*. (2018). The temporal resolution of SWIFT data is 12 min. The wave energy spectra product has 42 frequency bins from 0 to 0.5 Hz at resolution 0.0117 Hz.

3.3 CDIP – wave buoy

CDIP at the Scripps Institution of Oceanography, University of California, San Diego measures, analyzes, archives, and disseminates coastal environment data (Fig. 3.2). During the LC–DRI field campaign, a CDIP wave buoy was deployed in the vicinity of the experiment field. The CDIP data product has a temporal resolution of 30 min. The wave energy spectra have 64 frequency bins. Bins 0–0.1 Hz have resolution of 0.005 Hz and bins 0.1–0.58 Hz have resolution of 0.01 Hz. CDIP buoys are available commercially as Waverider MKII buoys from Datawell, which is based in the Netherlands. The wave products are calculated from the conventional pitch, roll, and heave motions of the buoys.

3.4 Experiment location and periods

The LC–DRI field experiment was conducted in the region between San Nicolas Island, Santa Catalina Island, and San Clemente Island on 21 March – 5 April 2017 (Fig. 3.3). The 16-day timespan is separated into five periods each about 1–3 days. Four SWIFTs were deployed in period 1 and 2, eight SWIFTs were deployed in two incidents in period 3 for a few hours. Six SWIFTs were deployed in period 5 with SWIFT #22, #23, #24, and #25 deployed for a few hours in three incidents and SWIFT #12 and #17

deployed for ~4 days. The deployment times and periods are shown in Figure 3.4 and Table 2.1.

3.5 Data description

The data from SWIFT drifters and the CDIP wave buoy are first interpolated into 10-min uniform intervals. The original SWIFT data have a temporal resolution of 12 min and CDIP data have a temporal resolution of 30 min. Then the CDIP wave energy data are interpolated to the same frequency bins and limits as the SWFITs (0–0.5 Hz with bin size 0.0117 Hz) to calculate the total wave energy $\int E\ df$, the cross product of wave energy $E \times f$, and the cross product of frequency compensated wave energy $E \times f^4$. The compensated $E \times f^4$ spectra are related to the mean square slope of the waves, which provide a high-frequency weighting similar to that of the Stokes drift calculation.

The comparison of each SWIFT deployment is shown in Figs 3.5–3.40. Each subpanel (a) shows the drifter tack and CDIP location; subpanel (b) shows the comparison of wave energy spectra; and (c) shows the comparison of frequency compensated spectra ($E \cdot f^4$). In all, the thick color line is the mean and the thin color line is ± 1 standard deviation, and the thick black line is CDIP mean and the grey shaded area is CDIP ± 1 standard deviation. The time series of the distance between SWIFT and CDIP, Hs, the peak wave direction, $\int E\ df$, $E \times f$, and $E \times f^4$ are shown in subpanels (d)–(i), respectively. The comparison suggests that the data are in agreement when the distance between both platforms is < 30 km. Thus the periods 3–1, 3, 5, 6, 8, and 12 (Figs. 13, 15, 17, 18, 20, and 24, respectively) with separation distance greater than 30 km are not used to estimate data quality.

3.6 Range vs. significant wave height

The scatter plots of distance vs. significant wave height (Hs) and $\Delta Hs = Hs_{swift} - Hs_{CDIP}$ are shown in Fig. 3.41. The upper distance limit is set at 20 km. The subpanels (a)–(b) are period 1, (c)–(d) are period 2, (e)–(f) are period 3, (g)–(h) are period 4, and (i)–(j) are period 5. The ΔHs average of period 1–5 is shown in Fig. 3.42. The result suggests the average ΔHs for SWIFT #22, #23 and #25 is ~ 0.003 m, for SWIFT #24 is ~ –0.05 m, and for SWIFT #11, #12, #16, and #17 is ~ –0.2 m.

3.7 Range vs. total wave energy

The scatter plots of distance vs. total wave energy ($Wave\ E = \int E\ df$) and $\Delta Wave\ E = Wave\ E_{swift} - Wave\ E_{CDIP}$ are shown in Fig. 3.43. The subpanels (a)–(b) are period 1, (c)–(d) are period 2, (e)–(f) are period 3, (g)–(h) are period 4, and (i)–(j) are period 5. The $\Delta Wave\ E$ average over period 1–5 is shown in Fig. 3.44. The result suggests that the average $\Delta Wave\ E$ for SWIFT #22, #23, and #25 is ~ 0.02 m^2, for

SWIFT #24 is ~ –0.01 m^2, for SWIFT #16 is –0.02 m^2, and for SWIFT #11, #12, and #17 is ~ –0.05 m^2.

3.8 Range vs. cross product of compensated energy

To compare the energy in the higher frequency band, the cross product of compensated energy spectra $E \times f^4$ was used. The scatter plots of distance vs. $E \times f^4$ and $\Delta\ (E \times f^4)$ are shown in Fig. 3.45, where

$$\Delta\ (E \times f^4) = E \times f^4{}_{swift} - E \times f^4{}_{CDIP} \quad (1)$$

The subpanels (a)–(b) are period 1, (c)–(d) are period 2, (e)–(f) are period 3, (g)–(h) are period 4, and (i)–(j) are period 5. The $\Delta\ (E \times f^4)$ average over period 1–5 is shown in Fig. 3.46. The result suggests that the average $\Delta\ (E \times f^4)$ is ~–2 x 10^{-3} $m^2\,Hz^3$ except for SWIFT #25, which is ~–5 x 10^{-3} $m^2\,Hz^3$.

3.9 Root mean square error

The root mean square error (RMSE) is calculated as

$$RMSE = \sqrt{\frac{1}{n}\sum_{j=1}^{n}(y_{CDIP} - y_{SWIFT})^2} \quad (2)$$

The RMSE of Hs, $\Delta Wave\ E$, $E \times f$, and $E \times f^4$ between SWIFT and CDIP for each deployment period are shown in Figs. 3.5–3.40. Excluding the periods with a mean separation distance greater than 30 km (periods 3–1, 3, 5, 6, 8, 12), the RMSE of Hs is 0.25 ± 0.08 m, the RMSE of $\Delta Wave\ E$ is 0.057 ± 0.029 m^2, the RMSE of $E \times f$ is 0.49 ± 0.32 m^2, the RMISE of $E \times f^4$ is 0.0054 ± 0.0031 m^2, and RMSE of peak wave direction is 22.4 ± 11.3 degrees.

3.10 Percent error of significant wave height

The percent error (PE) of the significant wave height is calculated as

$$PE = \left[\frac{|\Delta\ (Hs)|}{Hs_{CDIP}}\right] \times 100 \quad (3)$$

The PE in each period is printed on subpanel (e) of Figs. 3.5–3.40. Excluding the periods with a distance greater than 30 km, the average PE of significant wave height is ~13%.

3.11 Summary

These results are expected. The wave heights are scattered around the CDIP values, without many trends by a separation distance. This suggests that the CDIP product can be

used for LC–DRI analysis, with an assumption of spatial and temporal homogeneity within 30 km of this location. The total energy is similar because it is the square of the wave height. No significant bias was found in either dataset.

Appendix B: CTD specifications

The products from the CDIP wave buoy station 229 deployed during the LC–DRI field experiment are shown in Figs. 3.47–3.50 and Table 3.3.

Table 2.1: Five deployment periods

Period	start	end	duration
1	2017–03–20 14:00	2017–03–22 20:00	2 days 8 hr
2	2017–03–23 23:00	2017–03–24 16:00	17 hr
3	2017–03–25 18:00	2017–03–30 00:00	——
4	2017–03–30 01:00	2017–04–01 17:00	2 days 16 hr
5	2017–04–01 20:00	2017–04–05 20:00	4 days

Table 2.2: Salinity correction MLF vs. EM-APEX

Instrument	Mixed Layer float					
Serial #	81		82		83	
	top	bottom	top	bottom	top	bottom
S_{offset} (psu)	0.01211	0.01153	0.00178	0.00001	–0.00429	0.00250
Instrument	EM-APEX float					
Serial #	6667	6671	6672	6674	6675	6678
S_{offset} (psu)	0.00047	0.01220	0.00434	0.00108	–0.00129	0.00413

* final salinity offset for each CTD sensor

** $S_{corrected} = S_{obs} + S_{offset}$

*** reference value is the average of MLF #82 and #83 top/bottom sensors (grey shaded areas).

Table 2.3: Temperature correction for SWIFT

Depth	SWF#11	SWF#12	SWF#16	SWF#17	SWF#22	SWF#23	SWF#24
0.2 m	---	---	–0.0978	0.0138	–0.1790	–0.1262	–0.0714
0.5 m	–0.0244	–0.0961	–0.1168	–0.1022	---	---	---
1.2 m	---	---	–0.0574	–0.0673	---	---	---

* $T_{corrected} = T_{obs} + T_{offset}$; unit: °C

** Reference sensor is MLF #82 CTD top sensor.

Table 2.4: Salinity correction for SWIFT

Depth	SWF#11	SWF#12	SWF#16	SWF#17	SWF#22	SWF#23	SWF#24	R/V Sproul
0.2 m	---	---	3.0405	1.4828	0.0602	–0.0351	–0.0365	---
0.5 m	0.190	0.2601	0.2014	0.2014	---	---	---	---
1.2 m	---	---	0.0917	0.0458	---	---	---	0.0067

* $S_{corrected} = S_{obs} + S_{offset}$; *unit: psu*

** Reference sensor is MLF #82 CTD top sensor.

Table 2.5: Specification of Seabird SBE 41 CTD module for MLF

	Calibration Standard	Initial Accuracy	Typical Stability
Temperature (°C)	ITS-90	± 0.002	0.0002 per year
Conductivity	IAPSO Standard Seawater	± 0.002 (equivalent salinity)	0.001per year (equivalent salinity)
Pressure	Deadweight tester & pressure reference	± 2 dbar	0.8 dbar per year

source: www.seabird.com/sbe41-argo-ctd

Table 2.6: Specifications for SWIFT Aanderaa 4319 CT

Conductivity:	
Range:	0-7.5S/m (0-75mS/cm)
Resolution:	0.0002S/m (0.002mS/cm)
Accuracy:	
4319A	±0.005S/m (±0.05mS/cm)
4319B	±0.0018S/m (±0.018mS/cm)
Response Time (90%):	<3s[1]
Temperature:	
Range:	-5-40°C (23-104°F)[2]
Resolution:	0.01°C (0.018°F)
Accuracy:	±0.05°C (0.09°F)/ (±0.1°C (0.18°F) for interval <30s.)
Response Time (63%):	<10 seconds

source: www.aanderaa.com/media/pdfs/conductivity-sensor-4319.pdf

Table 3.1: Specifications for SWIFT v3

Hull	Anodized aluminum
Power	14 VDC, Alkaline or Lithium D cell packs
Weight	30 kg in air
Dimensions	1.25 m draft, 1.0 m mast, 0.35 m diameter
Shipping crate	1.65 m length, 0.5 m width, 0.5 m depth
Endurance	20 days (Alkaline), 60 days (Lithium)
Tracking (RF)	Garmin Astro DC40 or AIS
Tracking (Iridium)	Geoforce SmartOne (global)
Telemetry	Iridium SBD
Processor	Sutron Xpert
Profiler	2 MHz Nortek Aquadopp HR
Met	Airmar PB200 or RM Young 8100
IMU	Microstrain 3DM-GX3-35
CT	Aanderaa 4319
Camera	123 Camera Y201-TTL
Light	Yellow 1s strobe

Table 3.2: Specifications for SWIFT v4

Hull	Anodized aluminum
Power	14 VDC, Alkaline or Lithium (custom)
Weight	20 kg in air
Dimensions	0.52 m tall, 0.45 m diameter
Shipping crate	0.58 x 0.56 x 0.76 m
Endurance	4 days (Alkaline), 12 days (Lithium)
Tracking (RF)	AIS ship traffic system (10 km range)
Tracking (Iridium)	Geoforce SmartOne (global)
Telemetry	Iridium SBD
Processor	Sutron Xpert
Profiler	Nortek Signature 1000
IMU	SBG Ellipse
CT	Aanderaa 4319
Camera	123 Camera Y201-TTL
Light	Yellow 1s strobe

Table 3.3: CDIP station 229 daily maximum waves

Time series start (UTC)	Time series end (UTC)	Time of max wave (UTC)	C-T wave height (m)	C-T wave period (s)
2017-04-07 00:00:00	2017-04-07 23:59:59	2017-04-07 11:22	3.48	12.50
2017-04-06 00:00:00	2017-04-06 23:59:59	2017-04-06 05:01	2.29	11.70
2017-04-05 00:00:00	2017-04-05 23:59:59	2017-04-05 00:04	2.79	14.10
2017-04-04 00:00:00	2017-04-04 23:59:59	2017-04-04 08:58	3.76	11.70
2017-04-03 00:00:00	2017-04-03 23:59:59	2017-04-03 19:07	3.71	12.50
2017-04-02 00:00:00	2017-04-02 23:59:59	2017-04-02 04:56	2.77	10.90
2017-04-01 00:00:00	2017-04-01 23:59:59	2017-04-01 07:41	4.31	9.40
2017-03-31 00:00:00	2017-03-31 23:59:59	2017-03-31 06:28	7.20	9.40
2017-03-30 00:00:00	2017-03-30 23:59:59	2017-03-30 22:49	5.15	7.00
2017-03-29 00:00:00	2017-03-29 23:59:59	2017-03-29 04:53	4.01	8.60
2017-03-28 00:00:00	2017-03-28 23:59:59	2017-03-28 02:06	5.92	6.20
2017-03-27 00:00:00	2017-03-27 23:59:59	2017-03-27 21:26	4.13	7.00
2017-03-26 00:00:00	2017-03-26 23:59:59	2017-03-26 16:05	3.55	8.60
2017-03-25 00:00:00	2017-03-25 23:59:59	2017-03-25 05:37	3.23	5.50
2017-03-24 00:00:00	2017-03-24 23:59:59	2017-03-24 04:18	4.48	7.80
2017-03-23 00:00:00	2017-03-23 23:59:59	2017-03-23 11:46	5.43	7.80
2017-03-22 00:00:00	2017-03-22 23:59:59	2017-03-22 06:36	2.81	9.40
2017-03-21 00:00:00	2017-03-21 23:59:59	2017-03-21 18:10	1.98	10.20
2017-03-20 00:00:00	2017-03-20 23:59:59	2017-03-20 16:16	2.17	11.70
2017-03-19 00:00:00	2017-03-19 23:59:59	2017-03-19 04:57	1.54	14.10
2017-03-18 00:00:00	2017-03-18 23:59:59	2017-03-18 14:33	2.10	8.60

source: http://cdip.ucsd.edu ; (C-T, crest to trough method)

Figure 2.1: MLFs, EM-APEXs, and SWIFTs on deck of R/V Sproul.

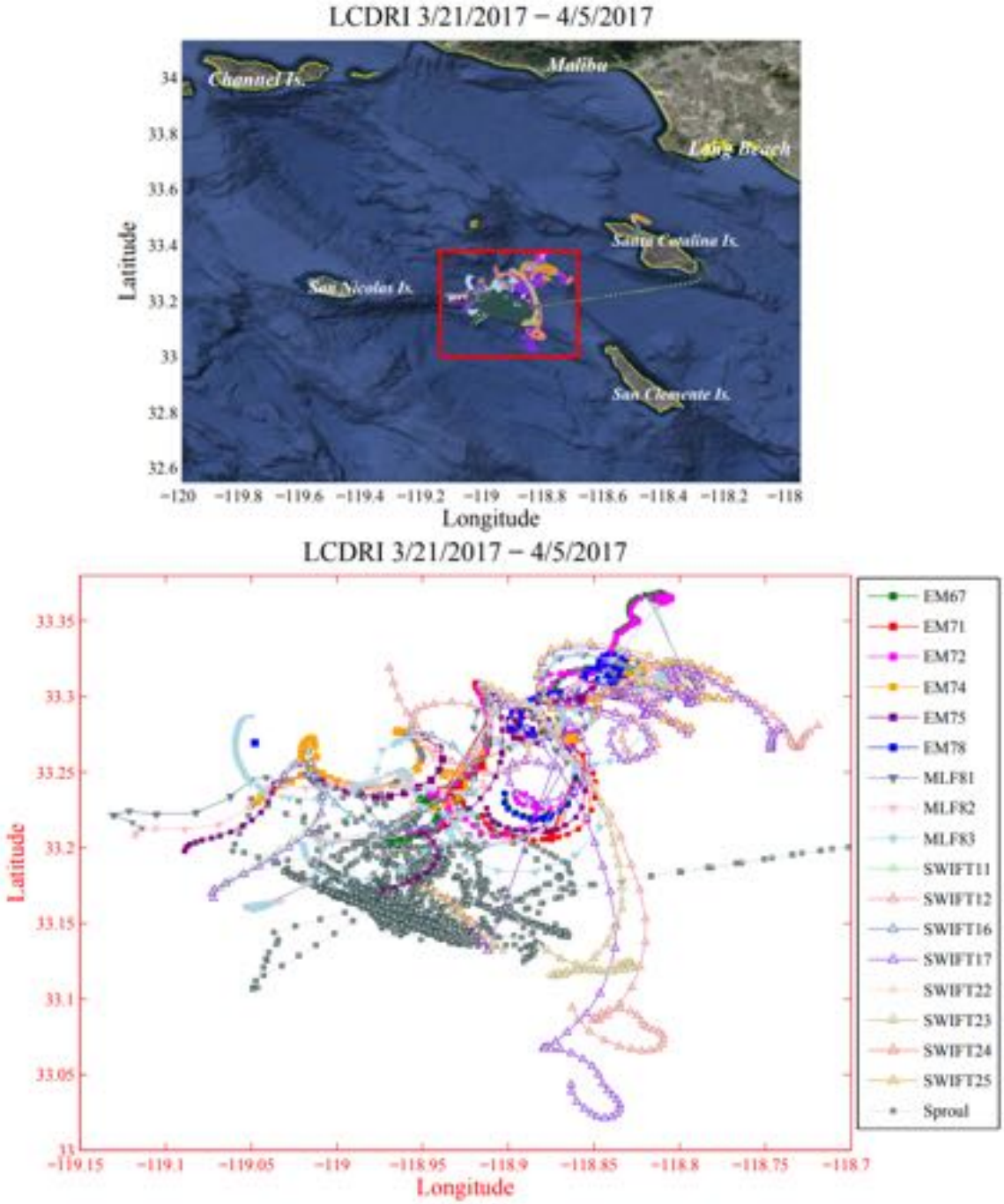

Figure 2.2: LC–DRI assets and R/V Sproul locations.

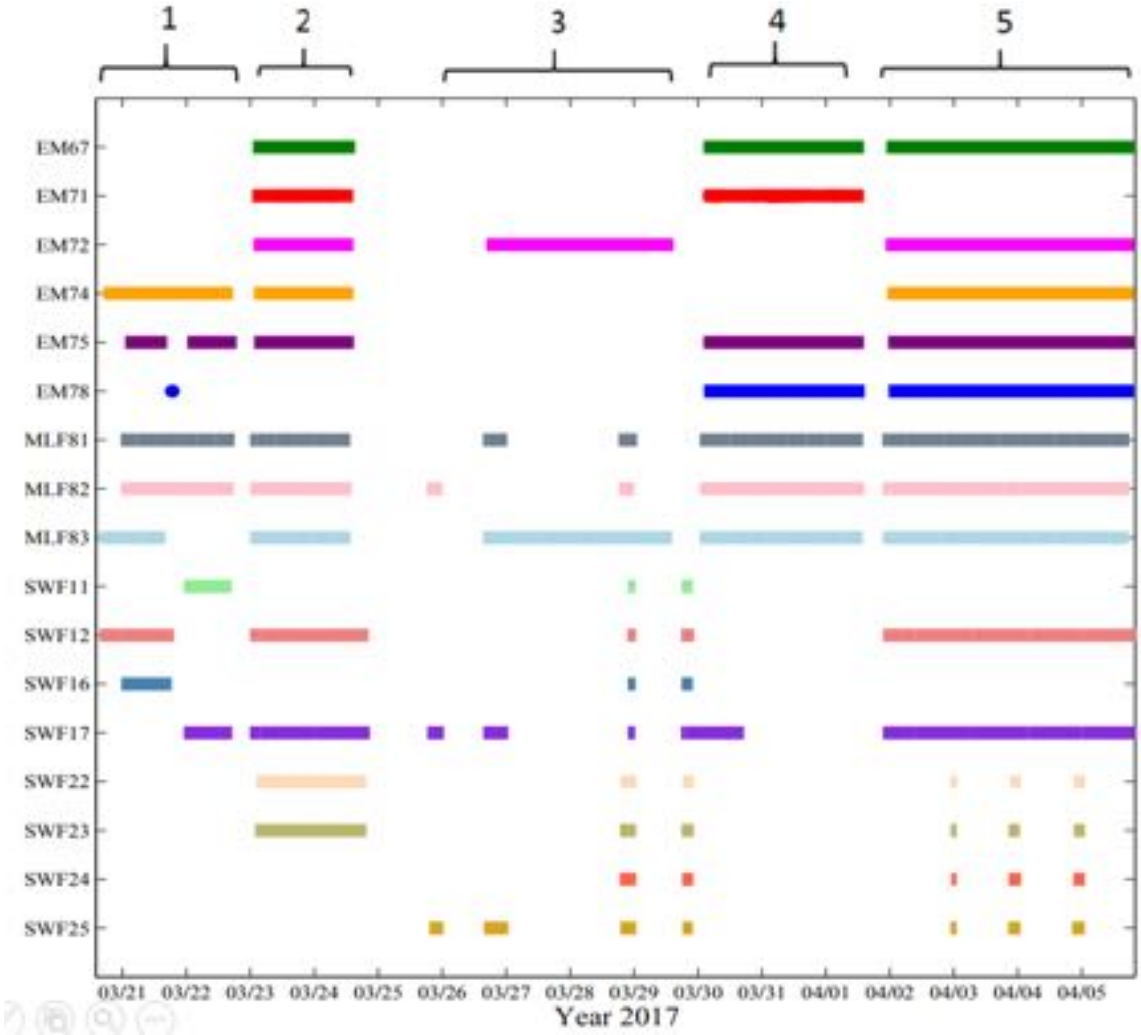

Figure 2.3: Deployment periods of MLFs, EM-APEXs, and SWIFTs.

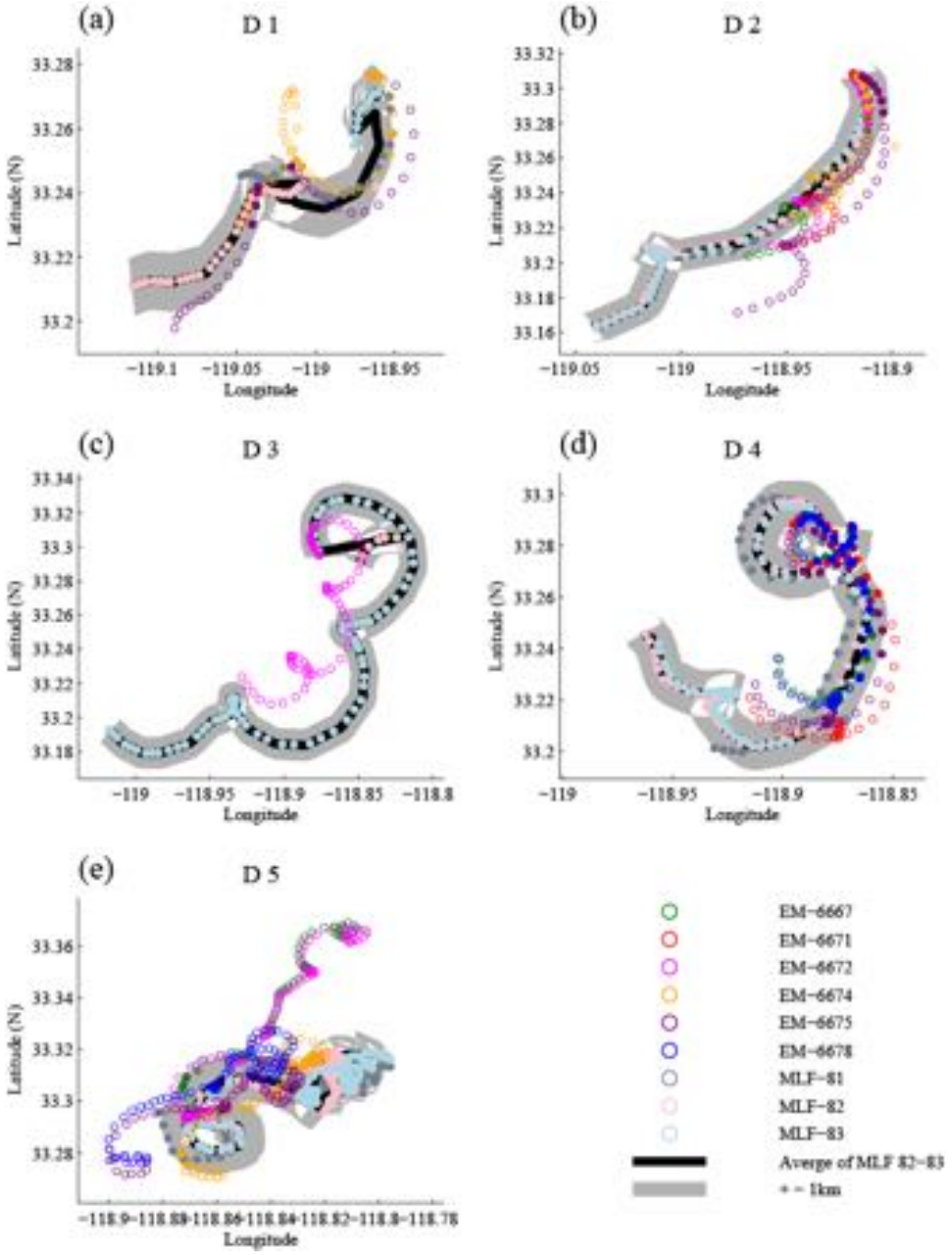

Figure 2.4: The float paths of deployment periods 1–5 (a)–(e).

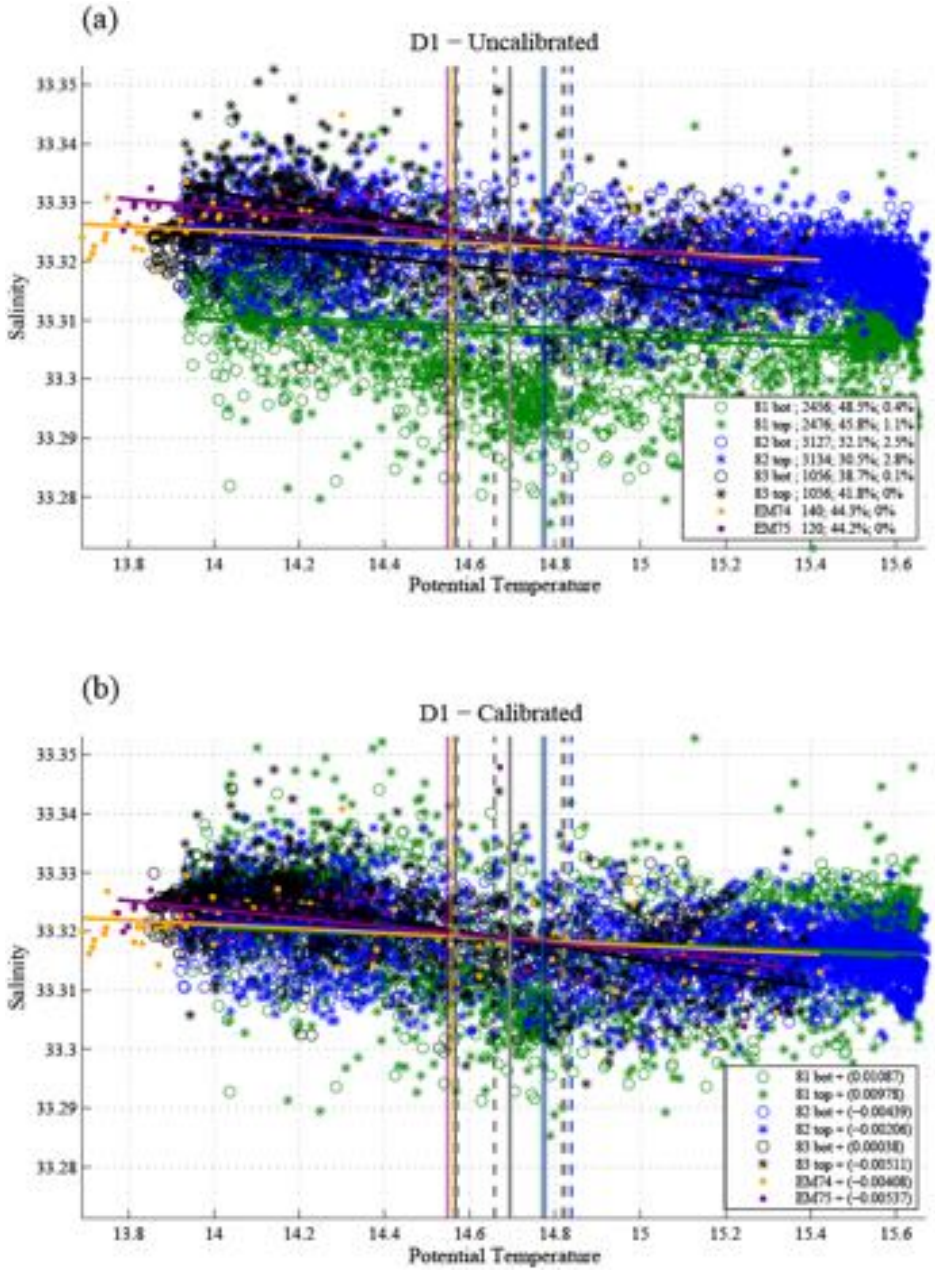

Figure 2.5: The T–S scatter plot for period 1, (a) uncalibrated, (b) calibrated.

.

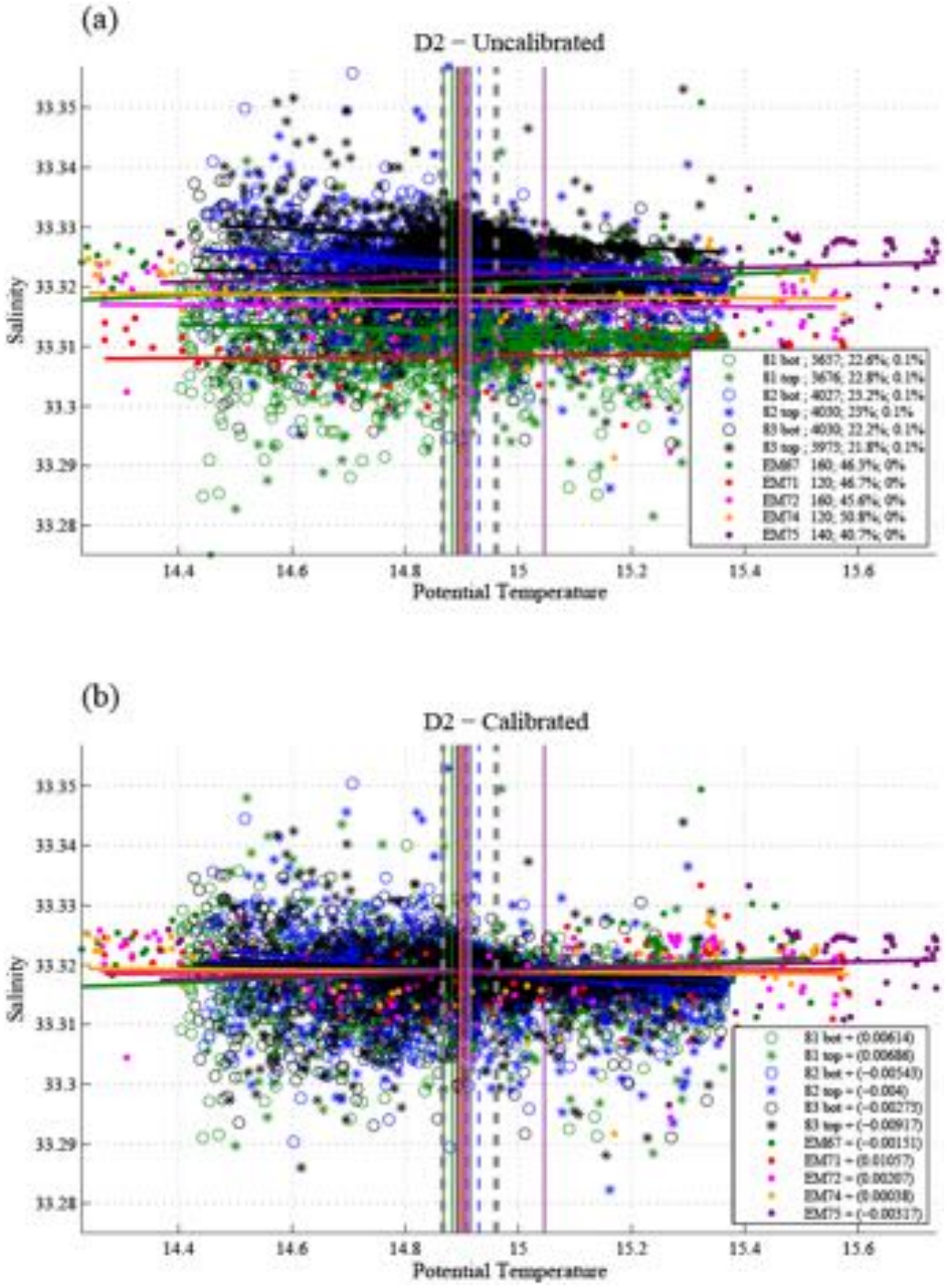

Figure 2.6: The T–S scatter plots for period 2, (a) uncalibrated, (b) calibrated.

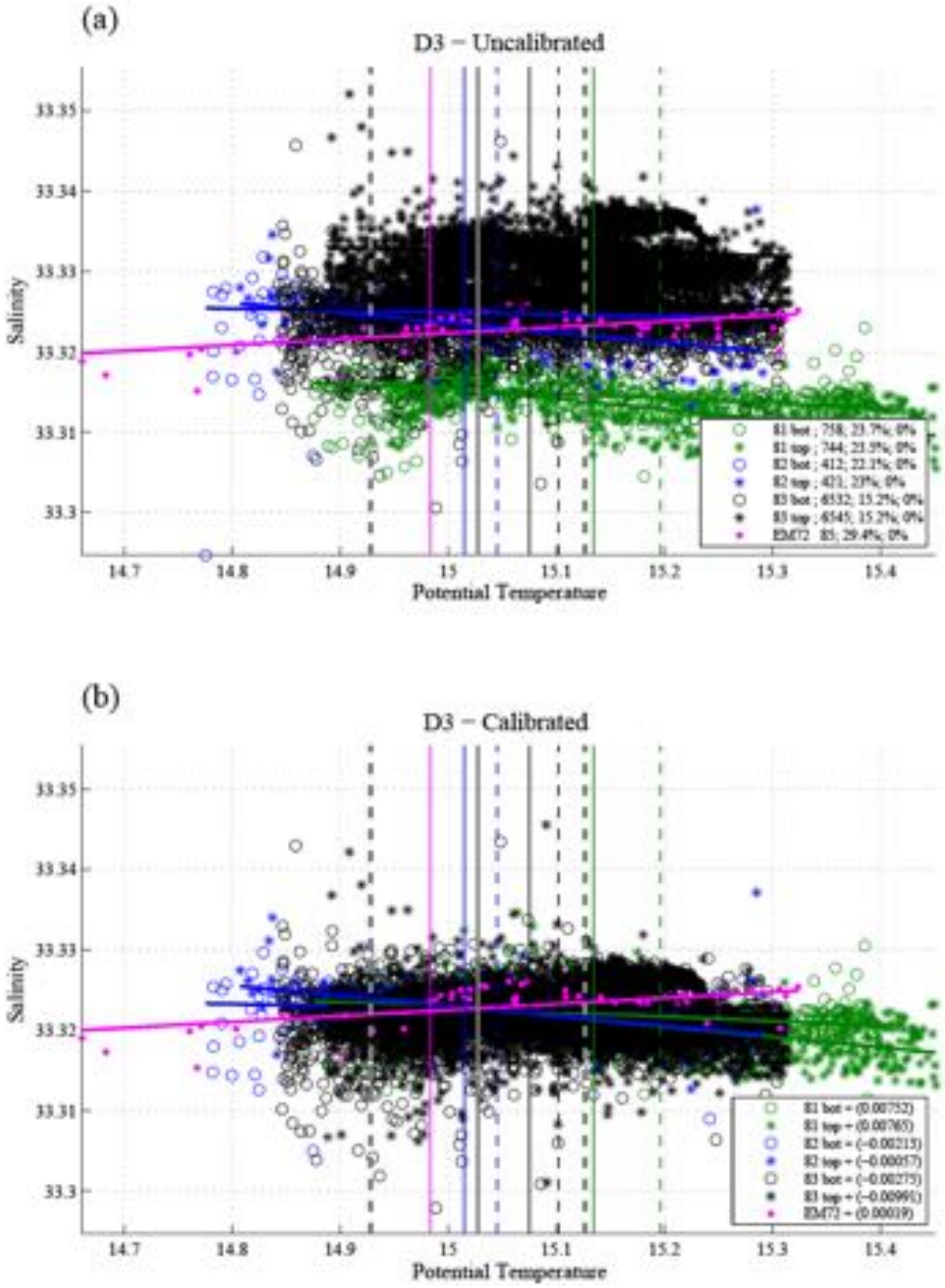

Figure 2.7: The T–S scatter plots for period 3, (a) uncalibrated, (b) calibrated.

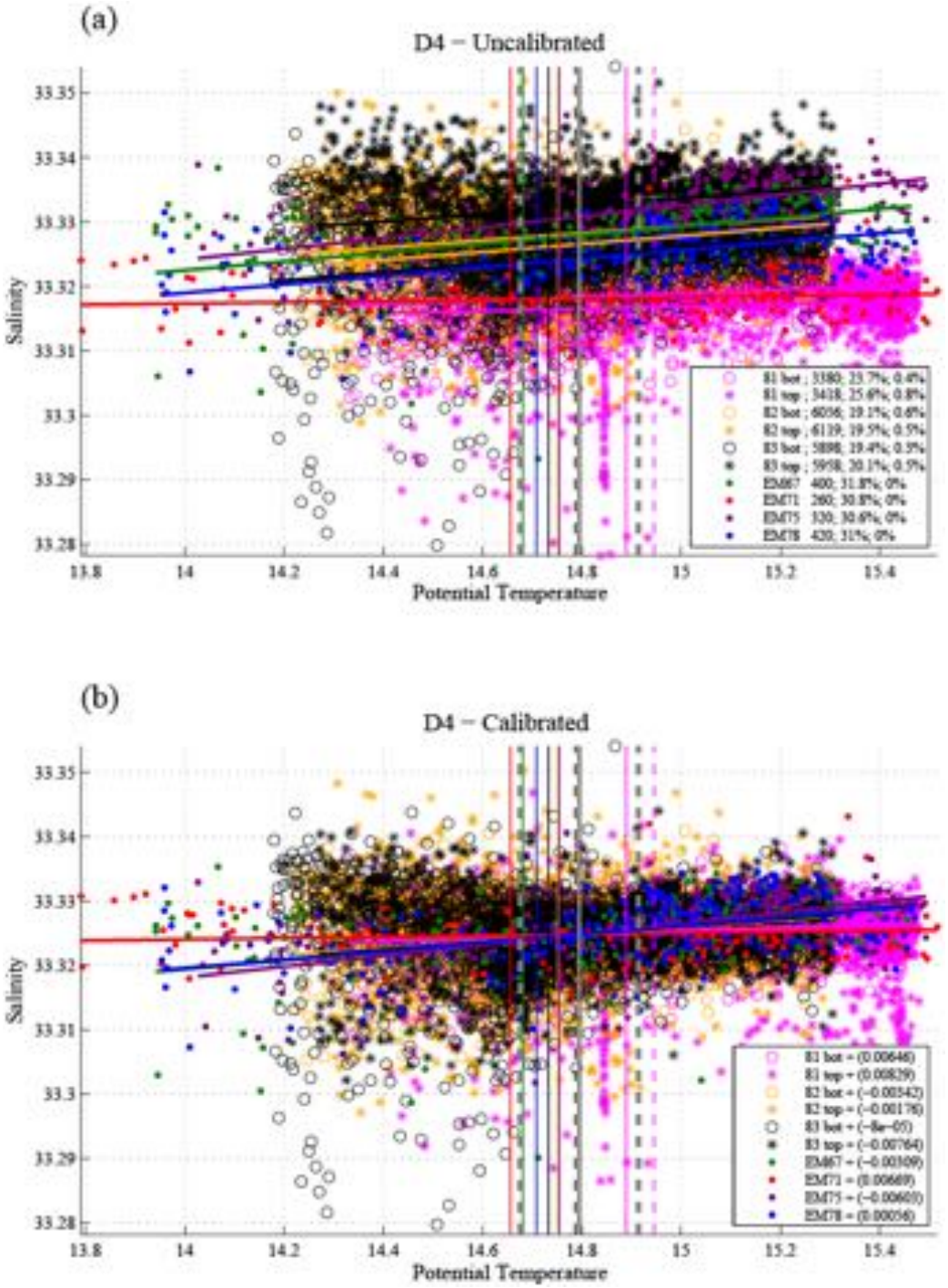

Figure 2.8: The T–S scatter plots for period 4, (a) uncalibrated, (b) calibrated.

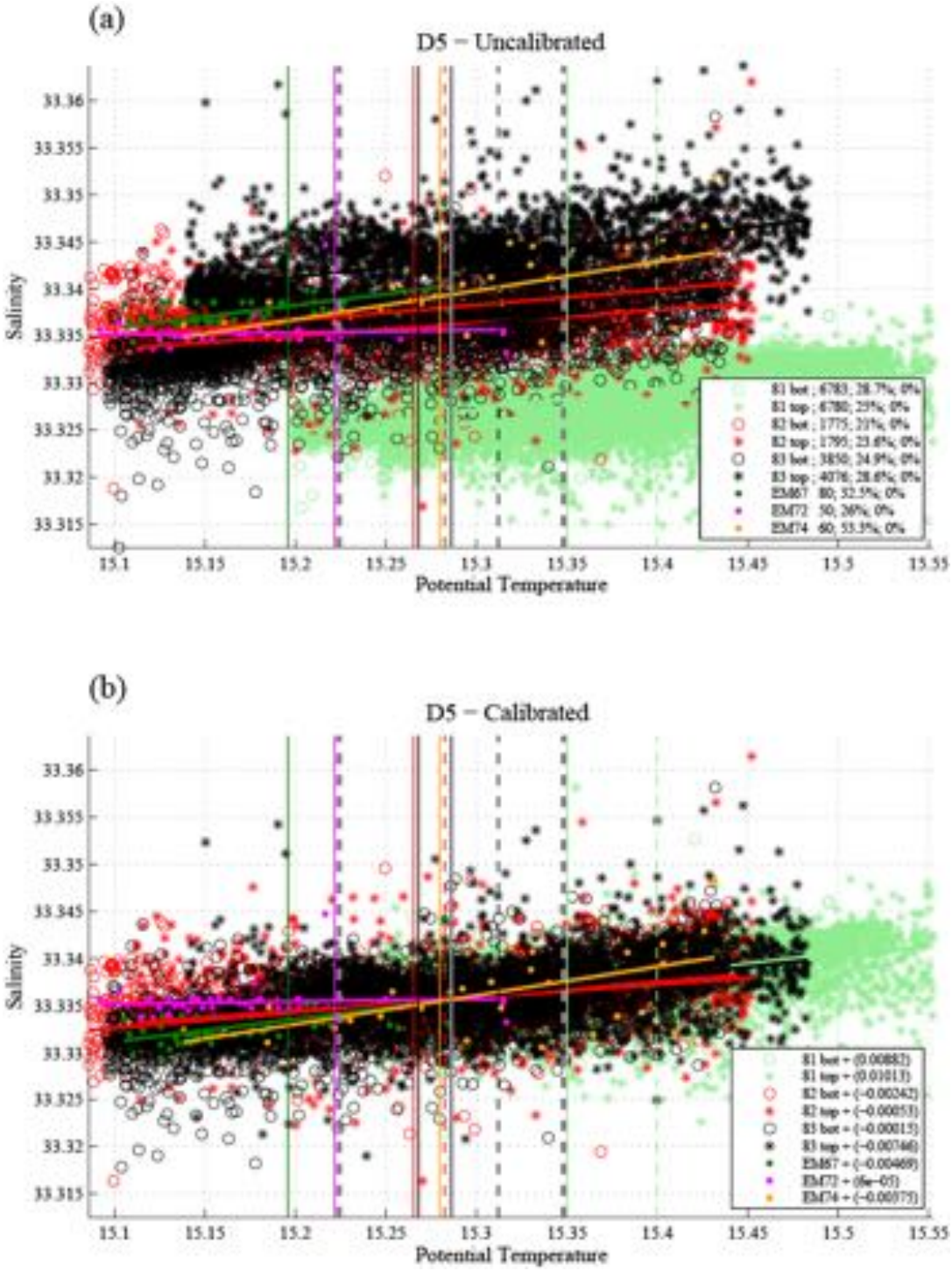

Figure 2.9: The T–S scatter plots for period 5, (a) uncalibrated, (b) calibrated.

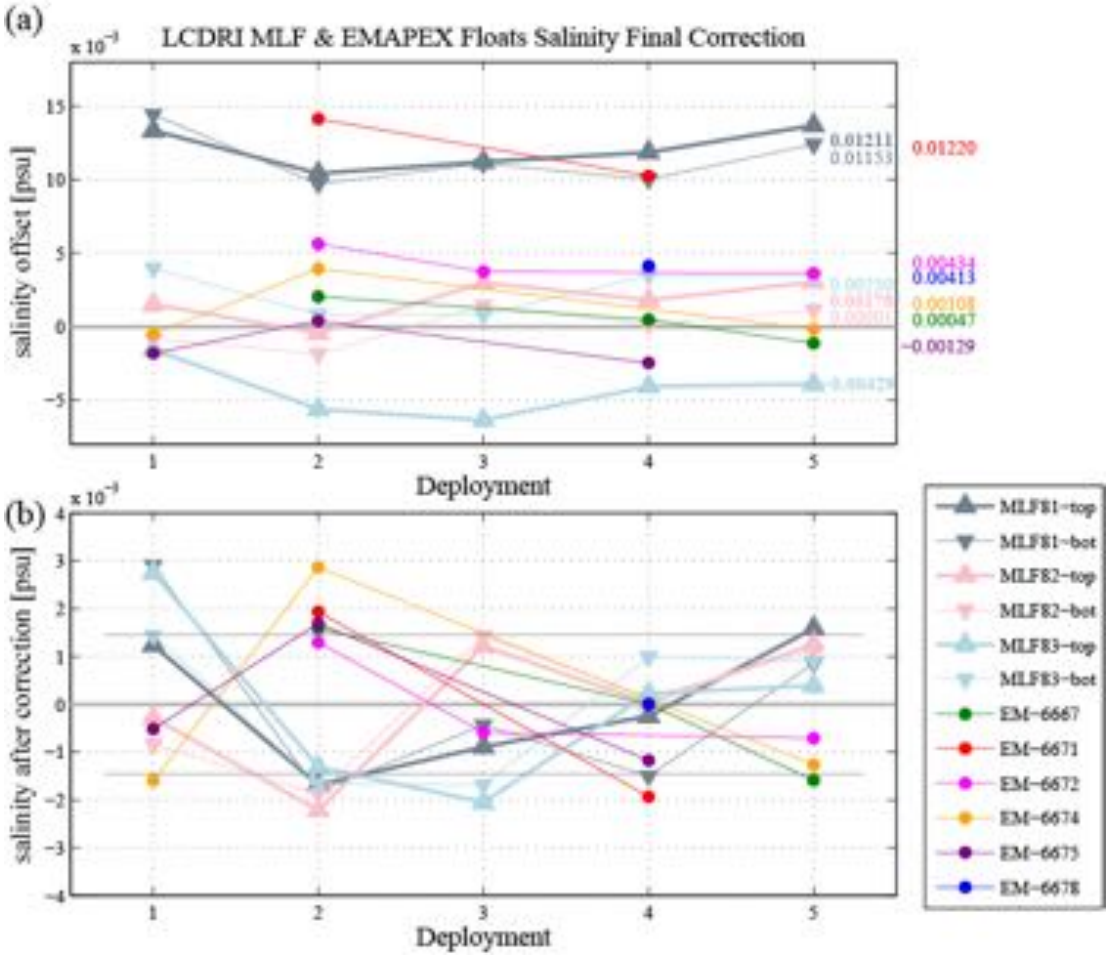

Figure 2.10: (a) The final calibration offset for each CTD sensors. (b) The salinity after calibration adjustment. The thick grey line indicates the mean and the thin grey lines indicate ± one standard deviation.

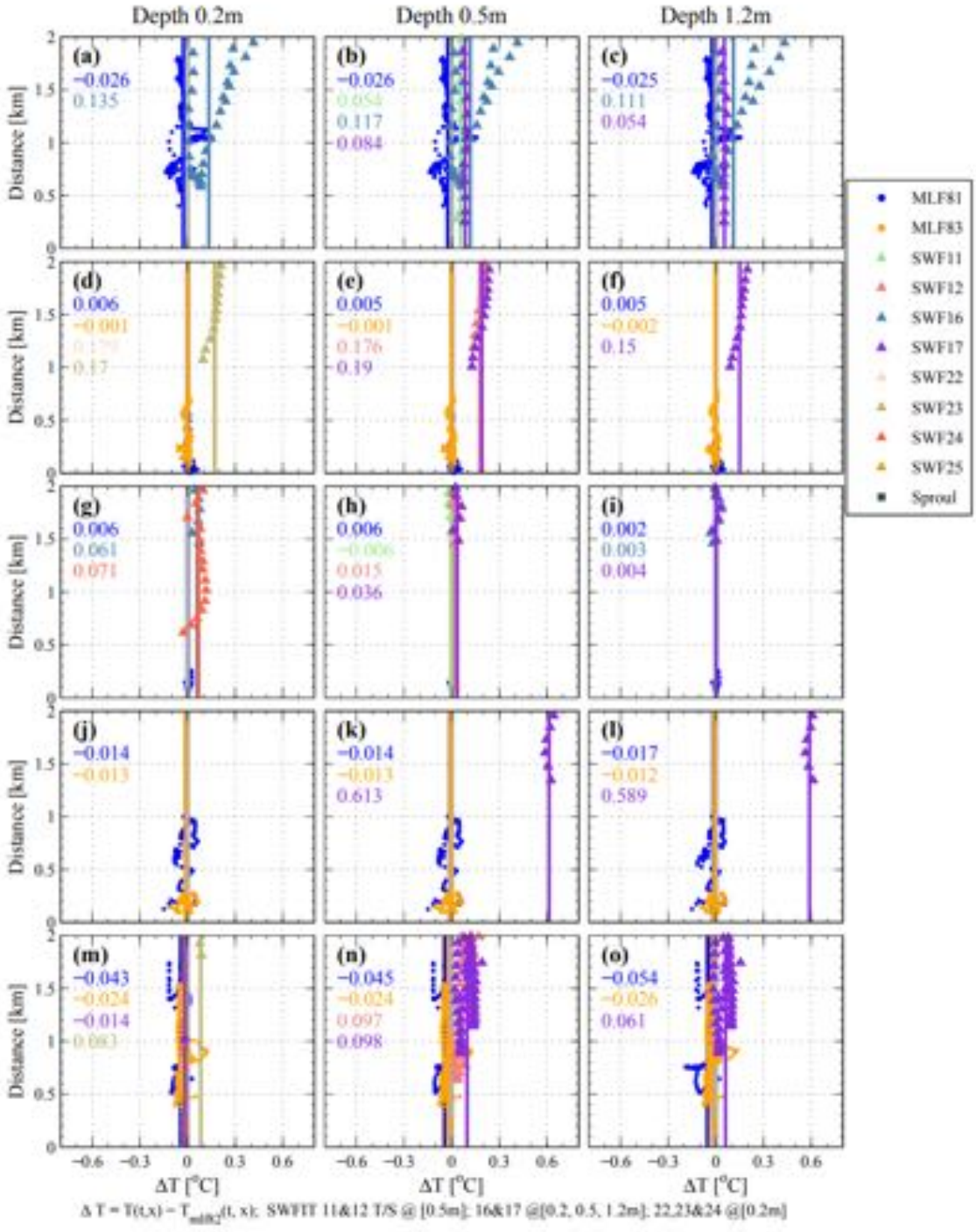

Figure 2.11: Distance and temperature offset between MLF #82 and other floats

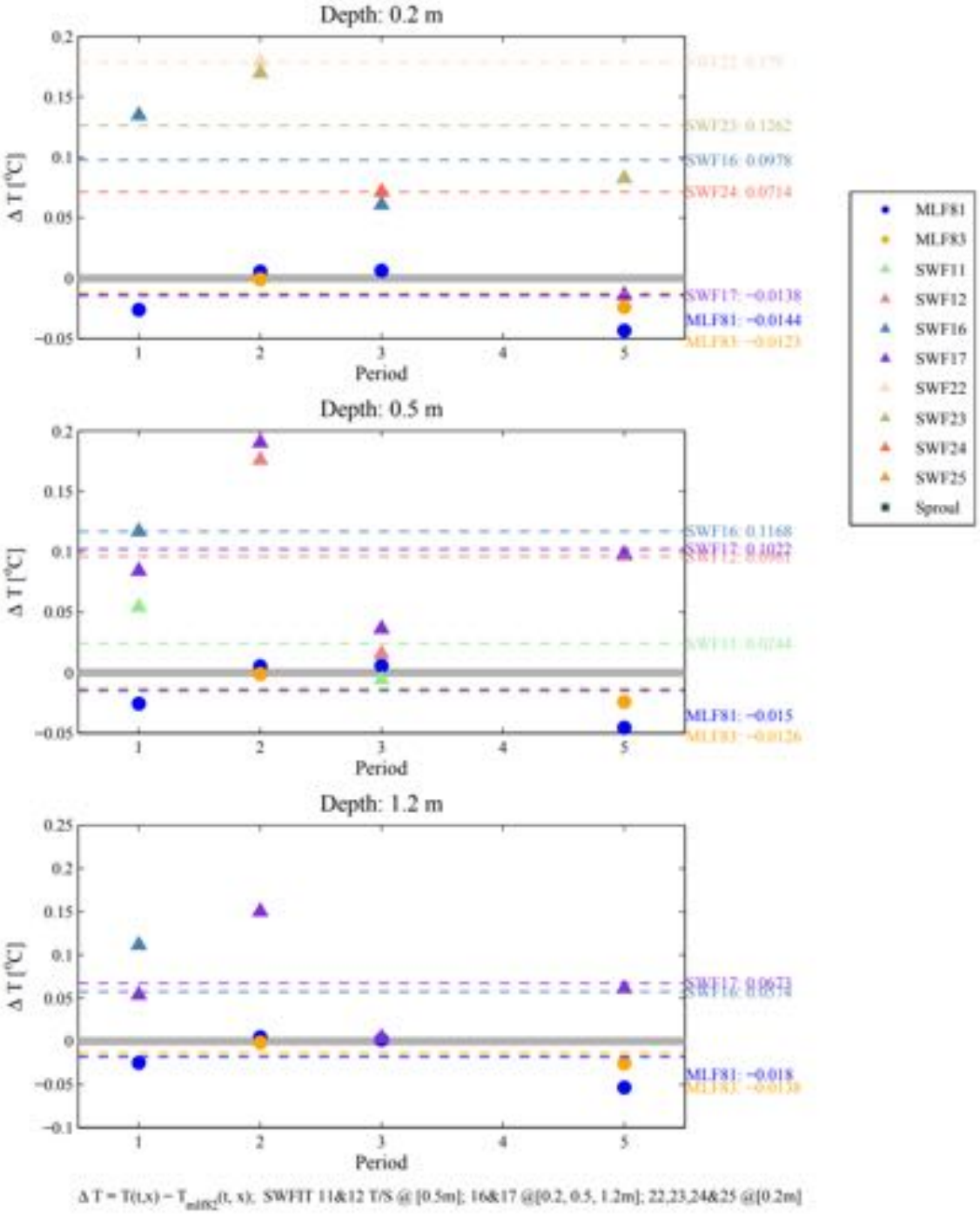

Figure 2.12: The temperature offset for SWIFT at 0.2, 0.5 and 1.2 m depths.

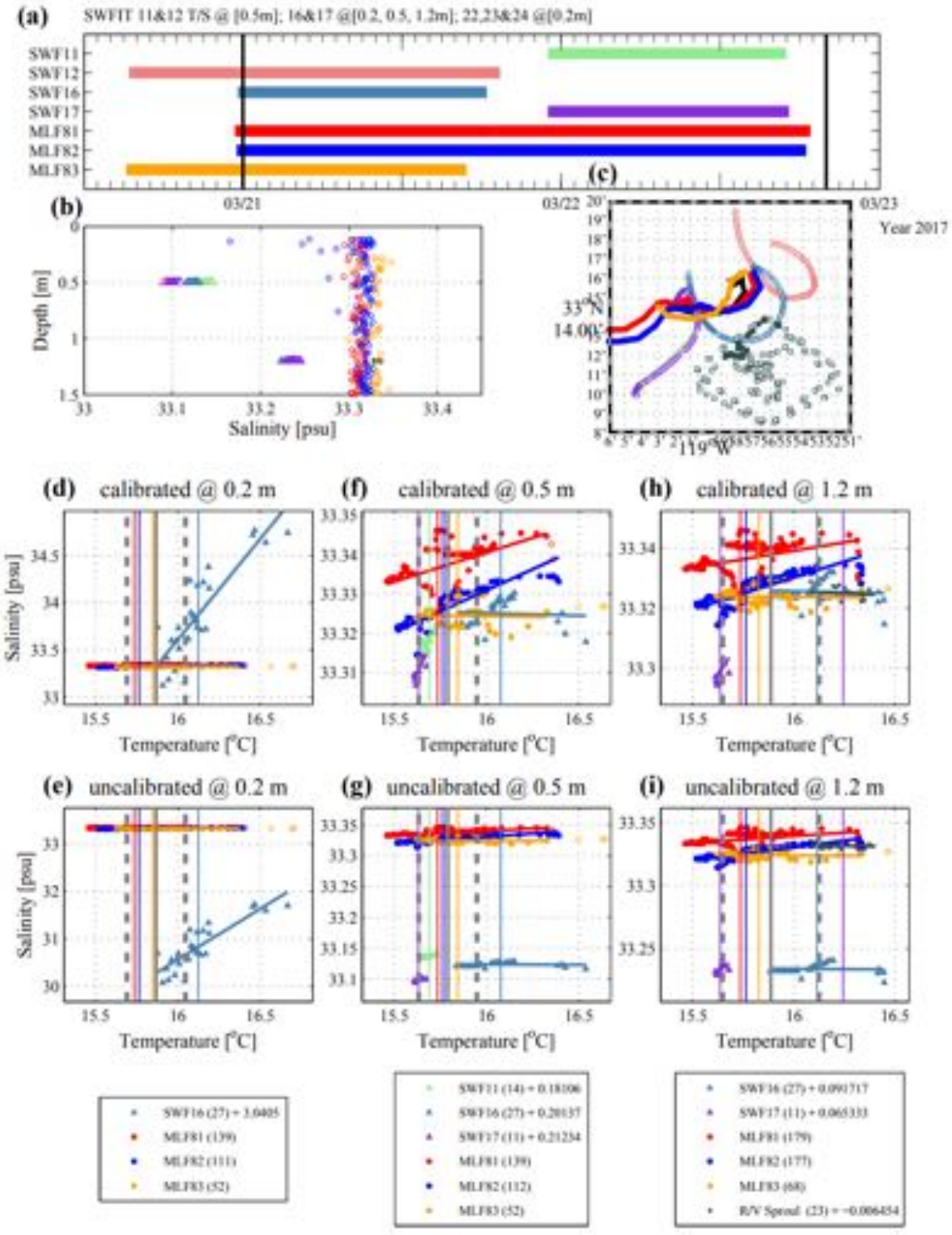

Figure 2.13: SWIFTs vs. MLFs salinity calibration for period 1.

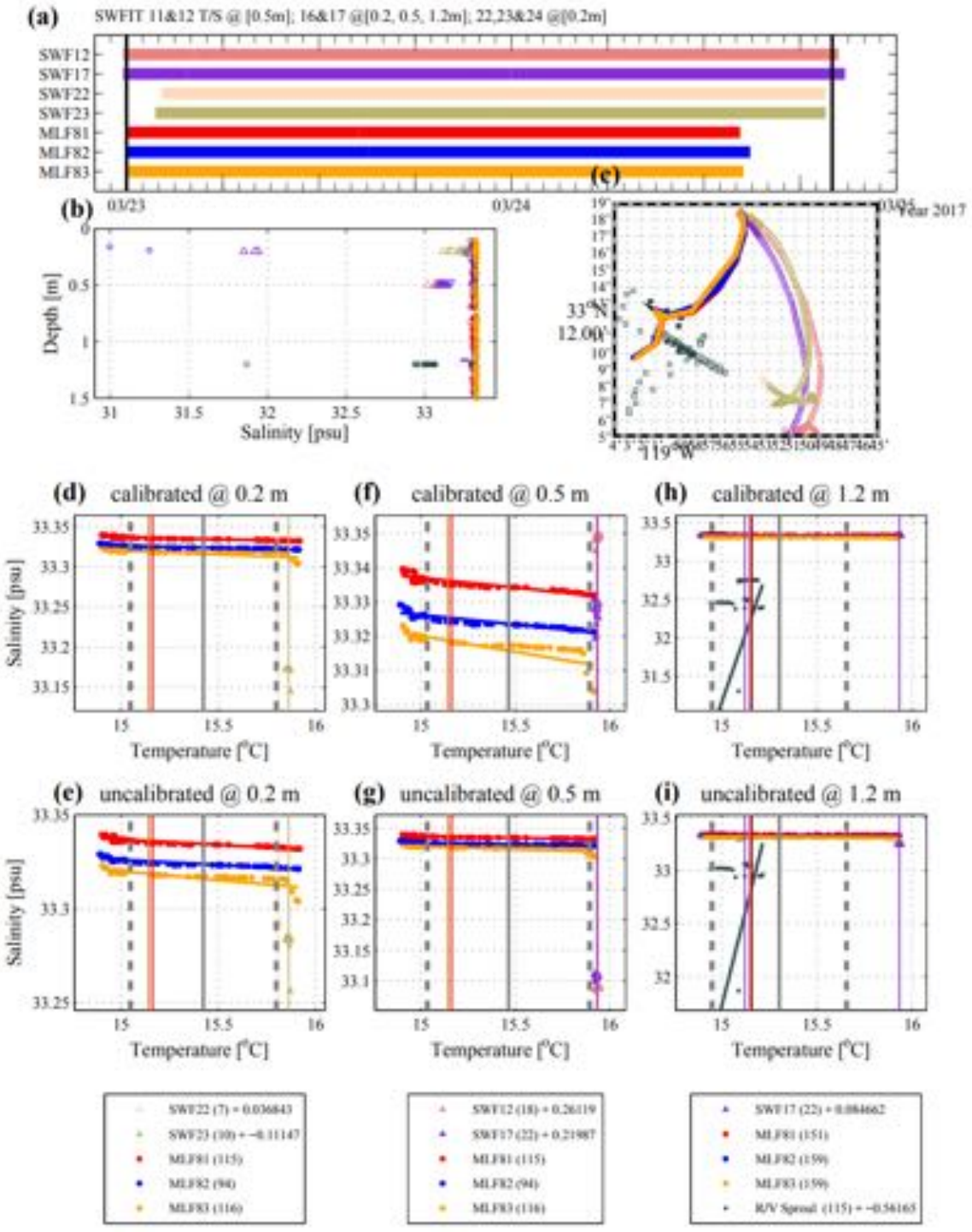

Figure 2.14: SWIFTs vs. MLFs salinity calibration for period 2.

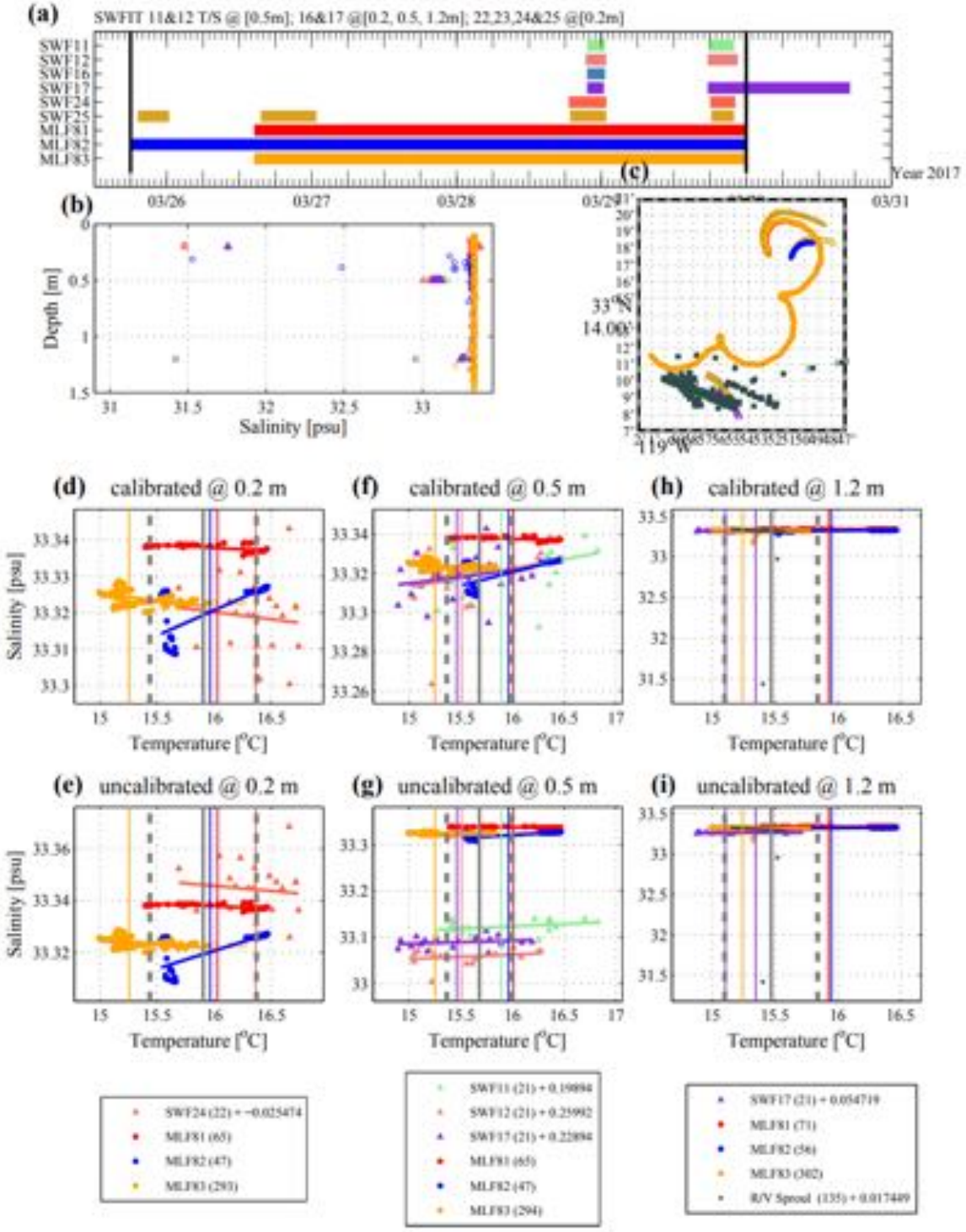

Figure 2.15: SWIFTs vs. MLFs salinity calibration for period 3.

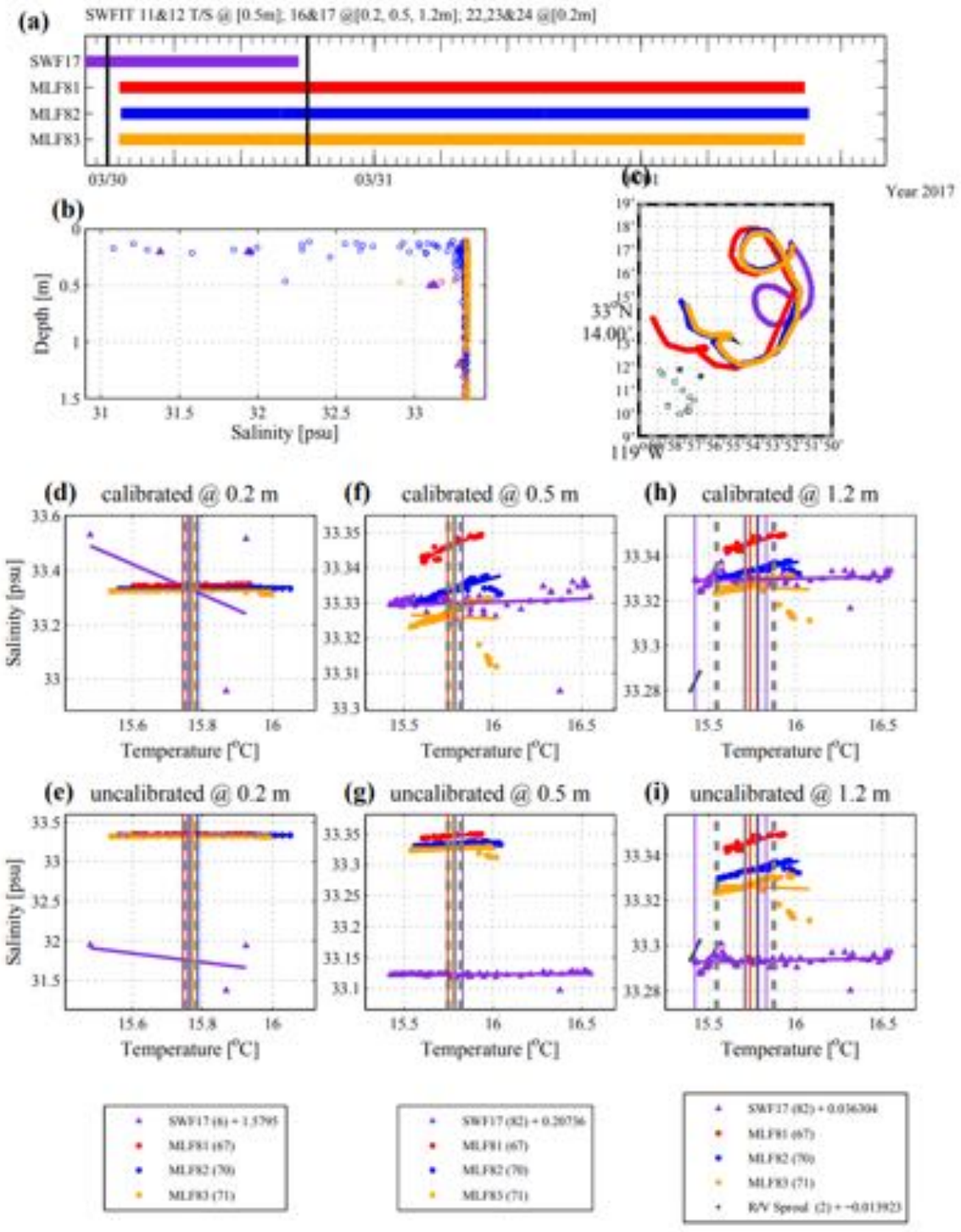

Figure 2.16: SWIFTs vs. MLFs salinity calibration for period 4.

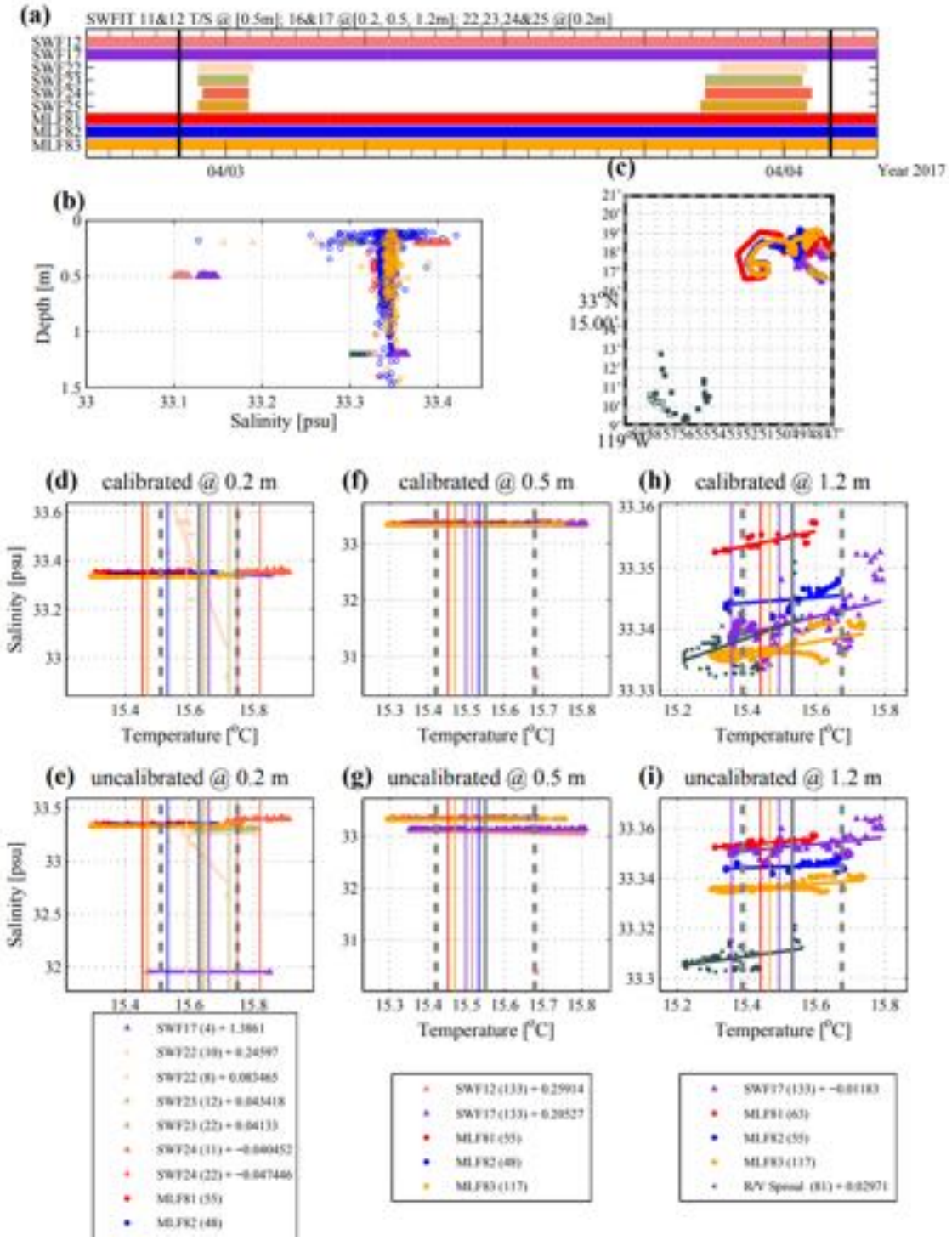

Figure 2.17: SWIFTs vs. MLFs salinity calibration for period 5.

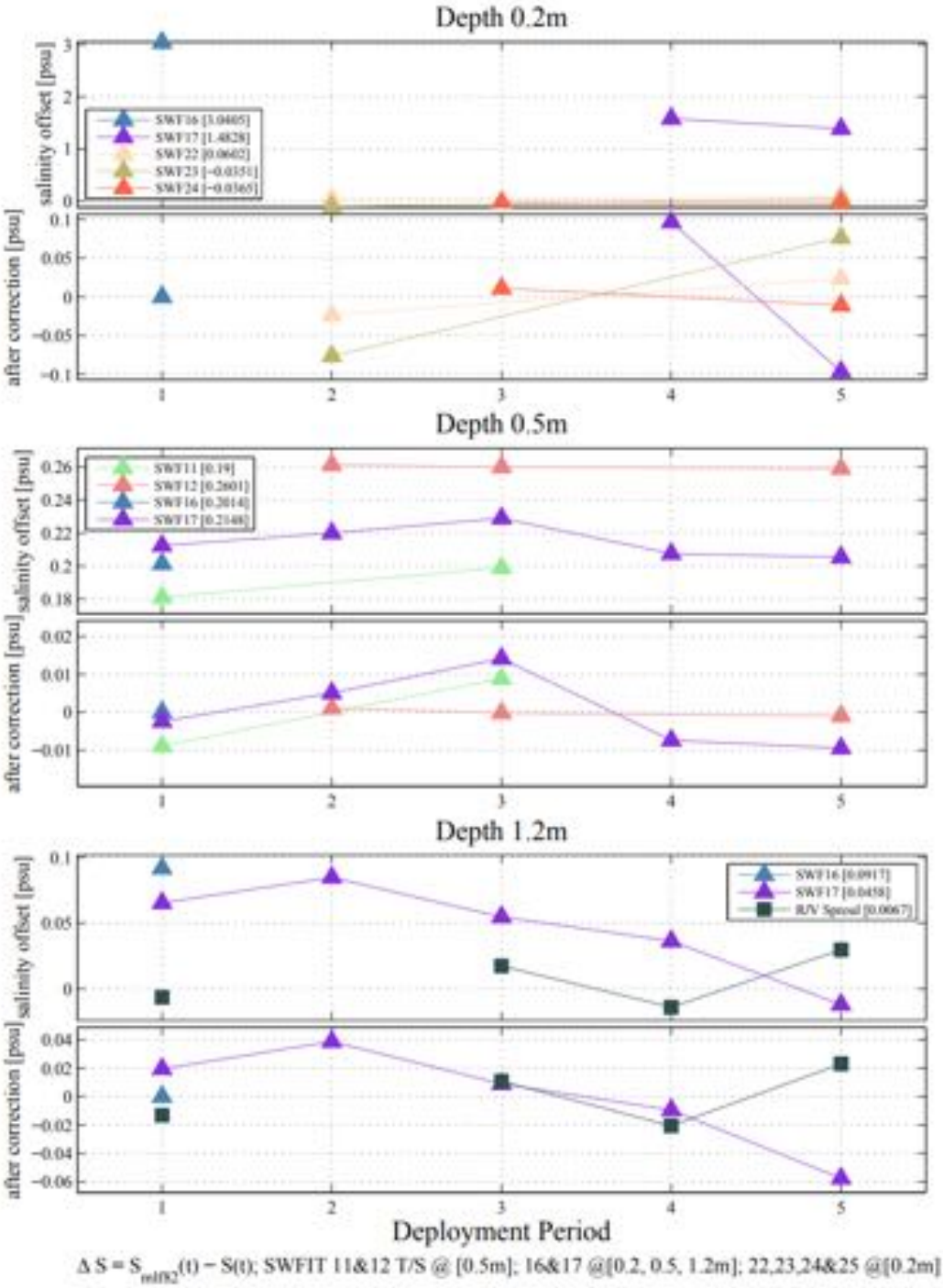

Figure 2.18: Final SWIFT salinity calibration offset.

source: http://www.seabird.com/sbe41-argo-ctd

Photo A. Sea-Bird CTD module with guard installed

Photo B. Module with guard removed to show conductivity cell

Figure 2.19: Sea-Bird SBE 41-ARGO-CTD. Source: www.aanderaa.com/media/pdfs/conductivity-sensor-4319.pdf

Figure 2.20: AANDERAA 4319 CT sensor.

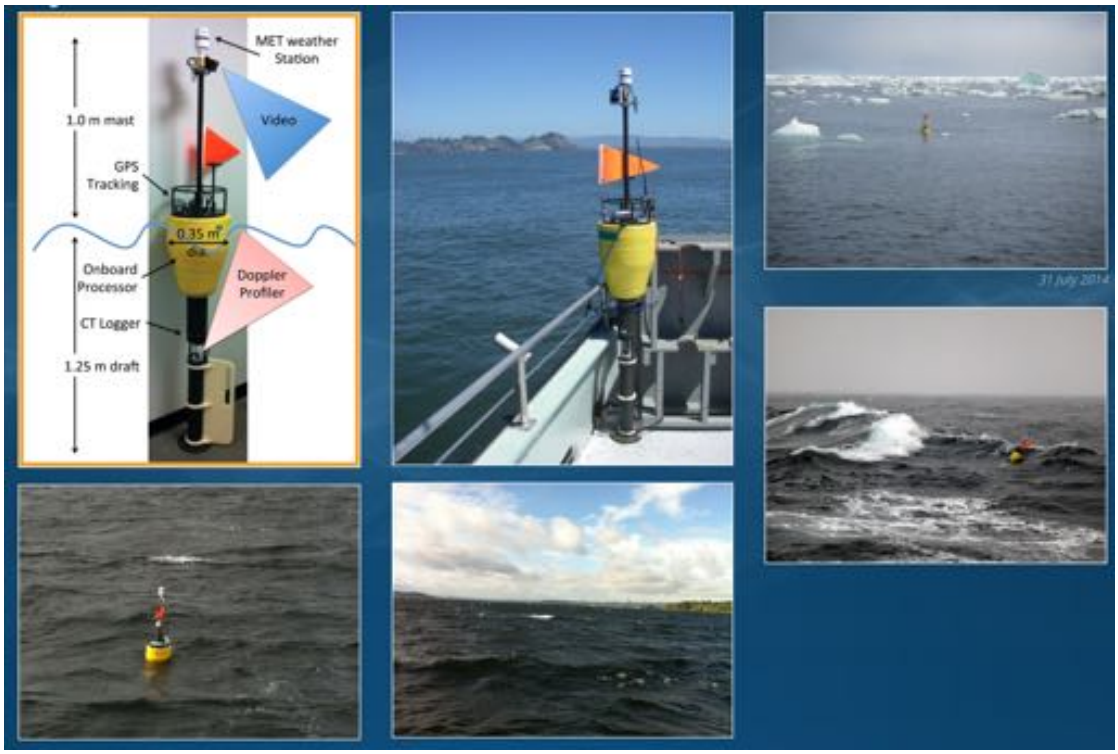

Figure 3.1: Surface Wave Instrument Float with Tracking (SWIFT) – version 3.

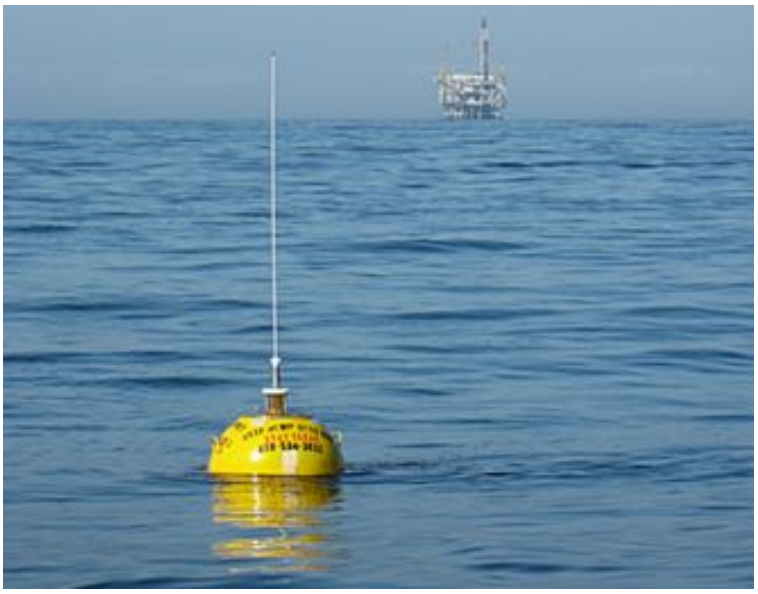

Figure 3.2: A Datawell Waverider from the CDIP wave buoys. Source: cdip.ucsd.edu/

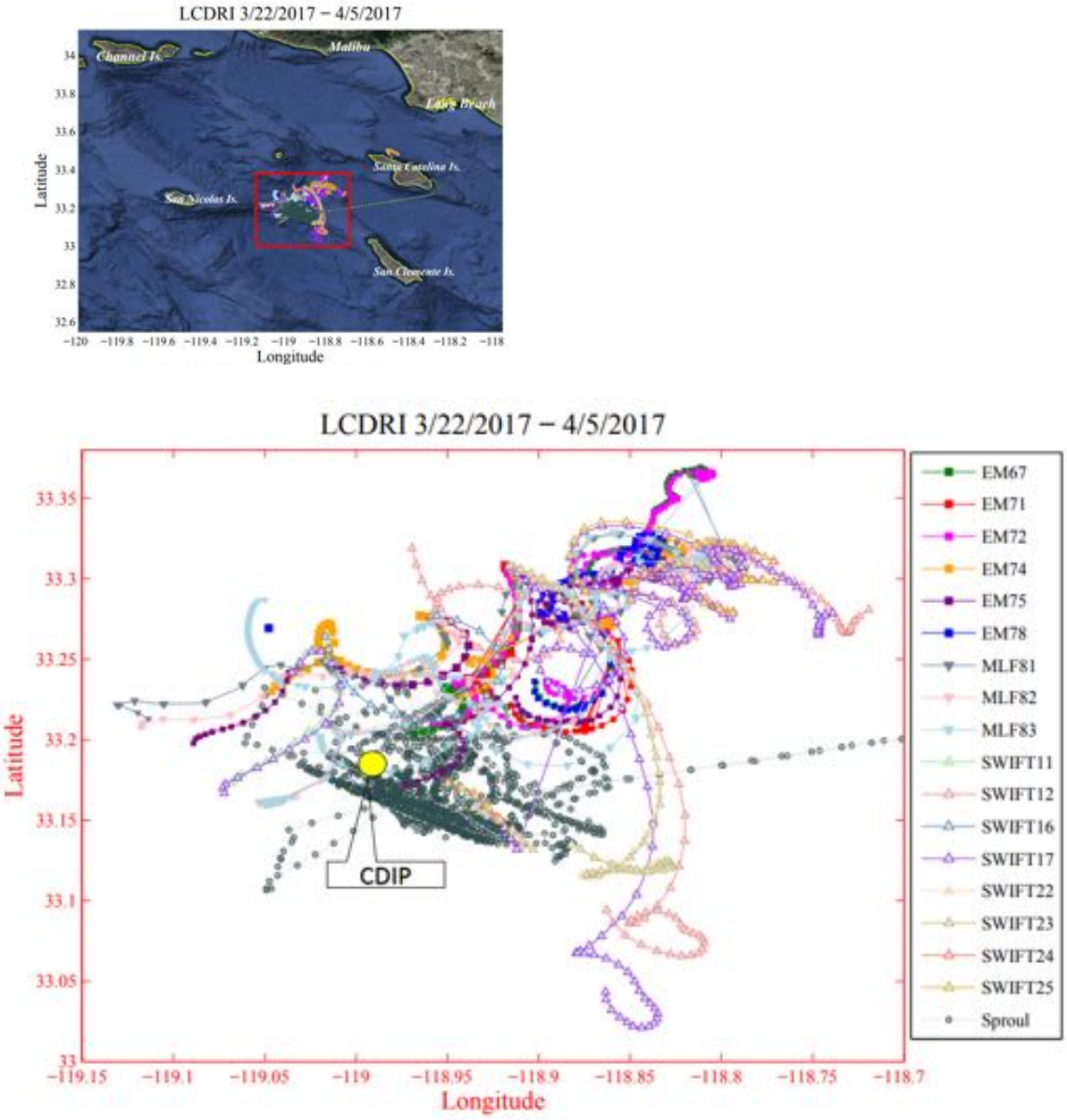

Figure 3.3: LC–DRI SWIFT tracks and CDIP buoy location.

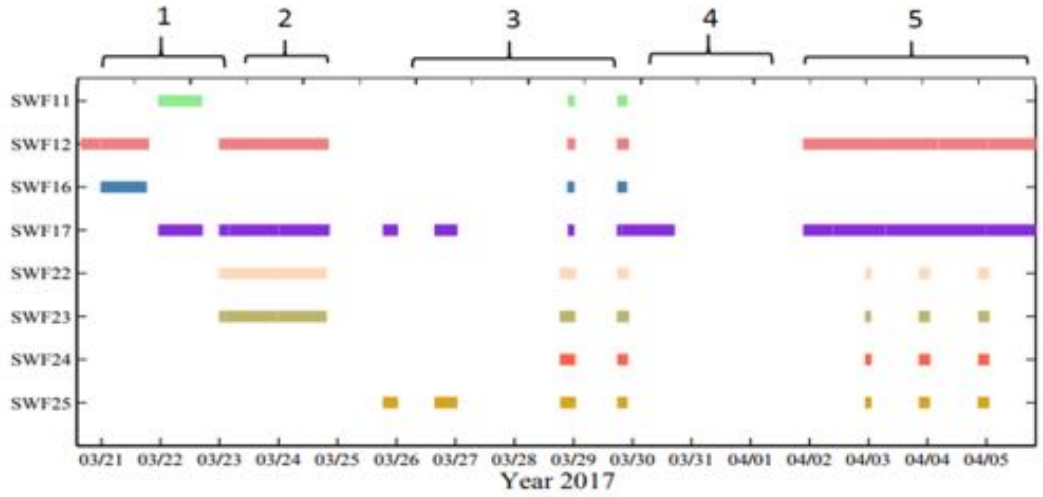

Figure 3.4: SWIFT deployment periods.

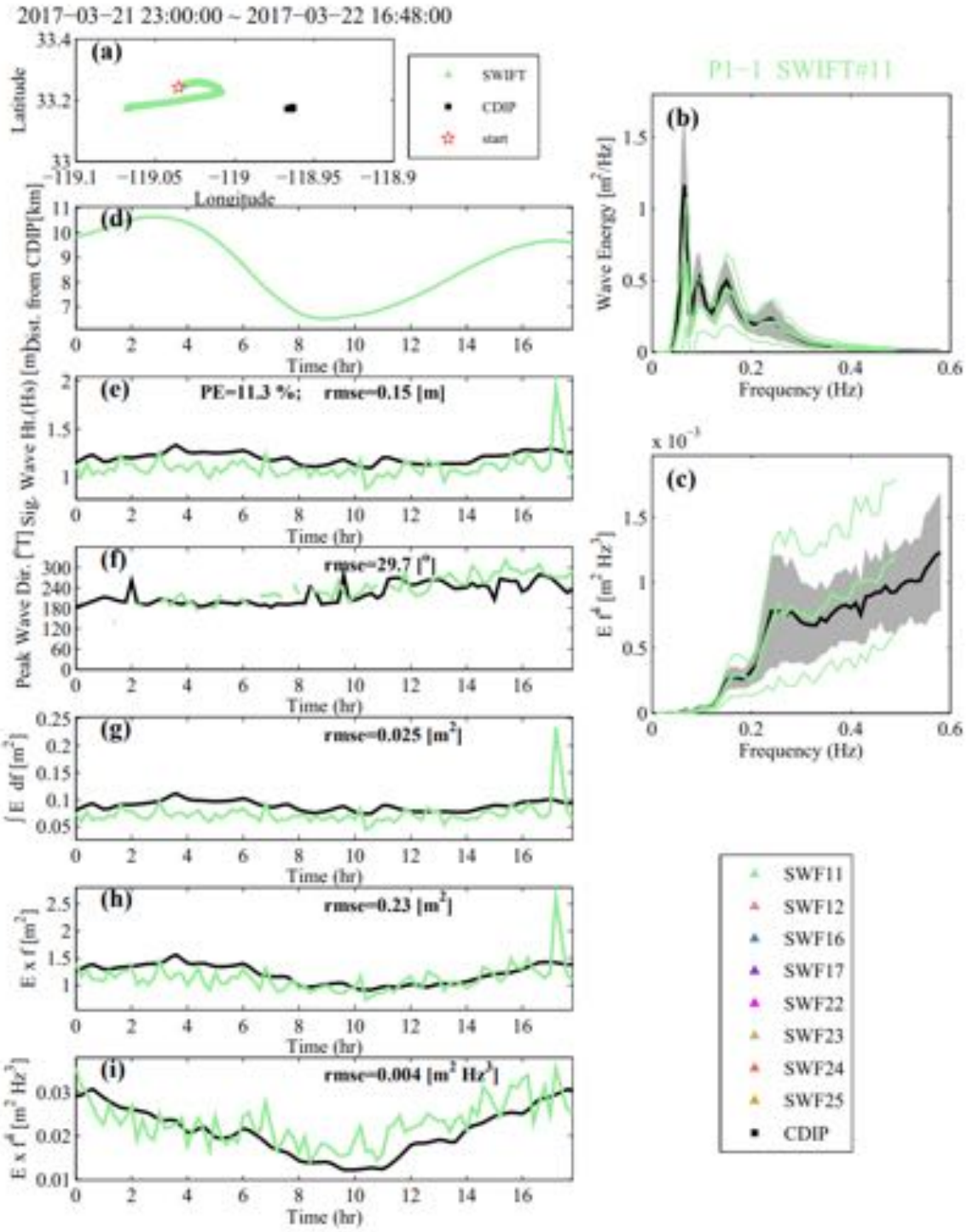

Figure 3.5: SWIFT #11 and CDIP wave energy measurement in period 1–1.

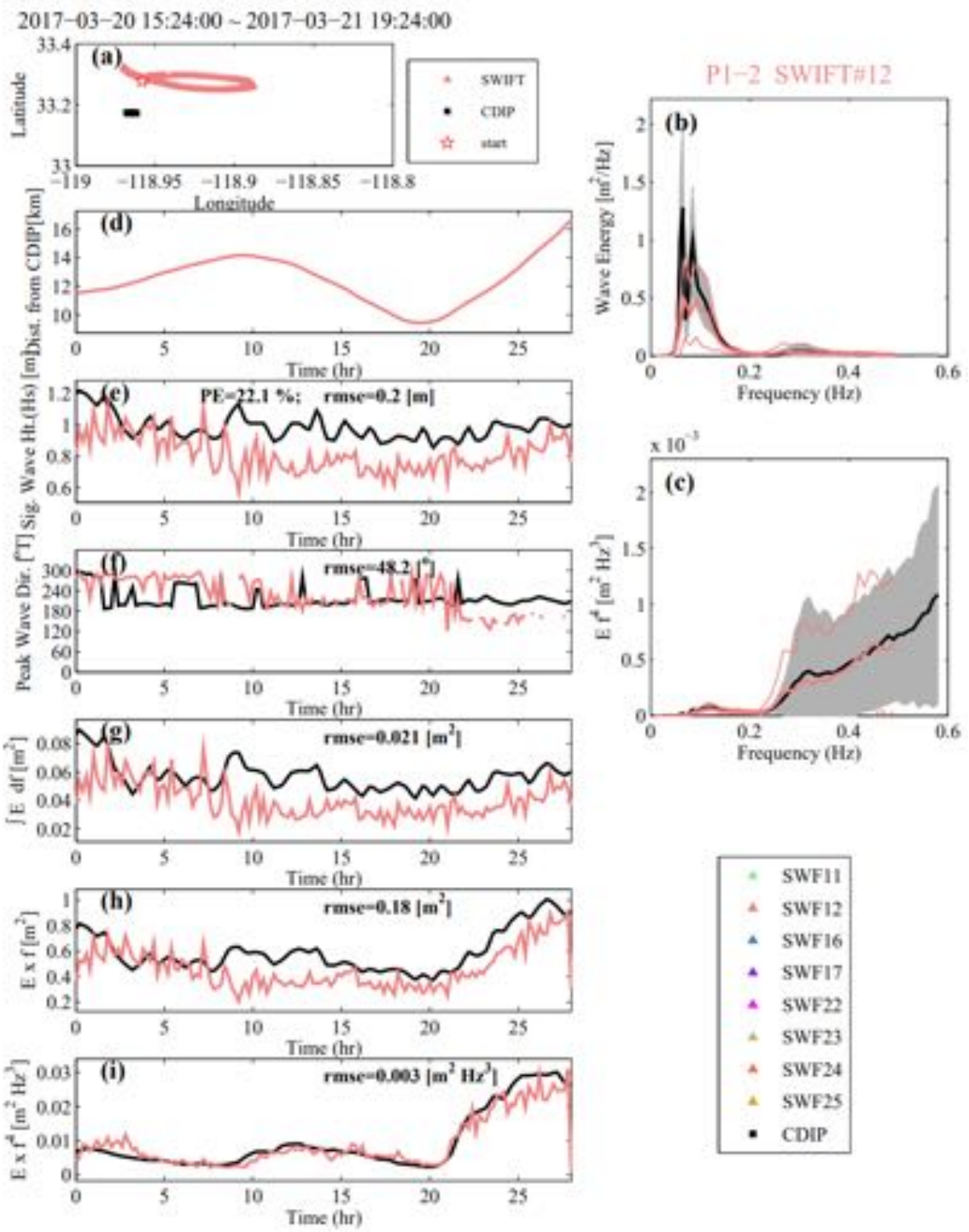

Figure 3.6: SWIFT #12 and CDIP wave energy measurement in period 1–2.

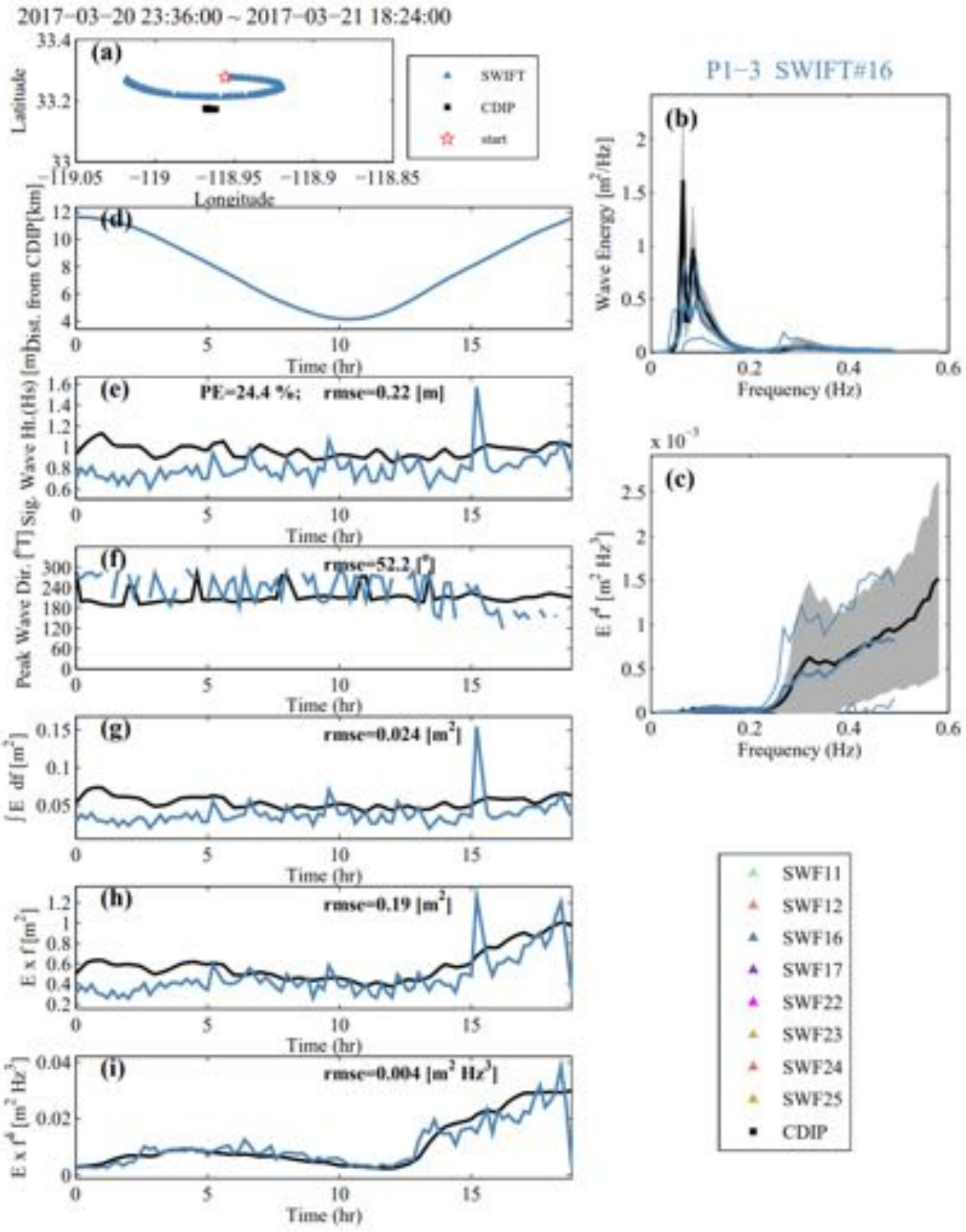

Figure 3.7: SWIFT #16 and CDIP wave energy measurement in period 1–3.

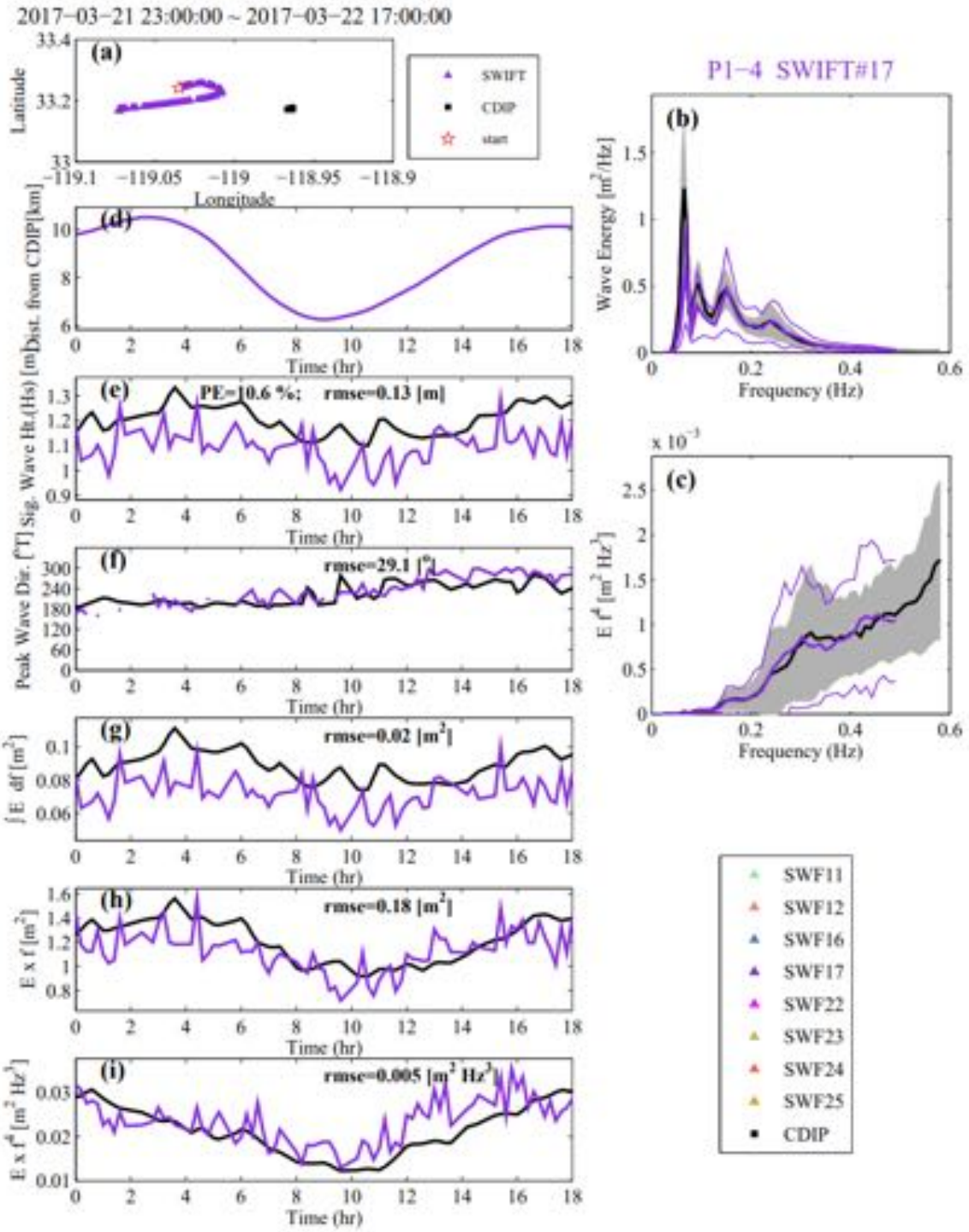

Figure 3.8: SWIFT #17 and CDIP wave energy measurement in period 1–4.

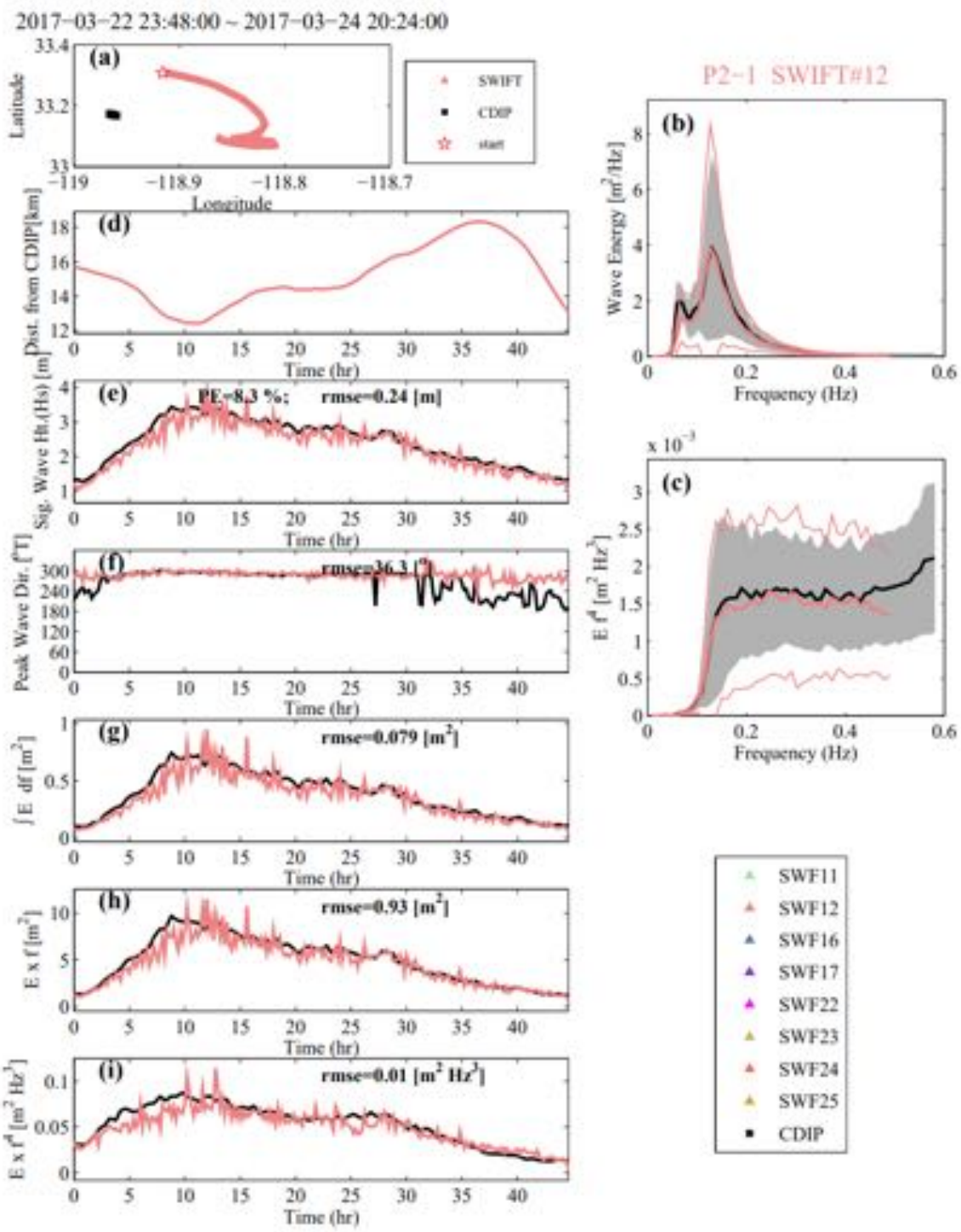

Figure 3.9: SWIFT #12 and CDIP wave energy measurement in period 2–1.

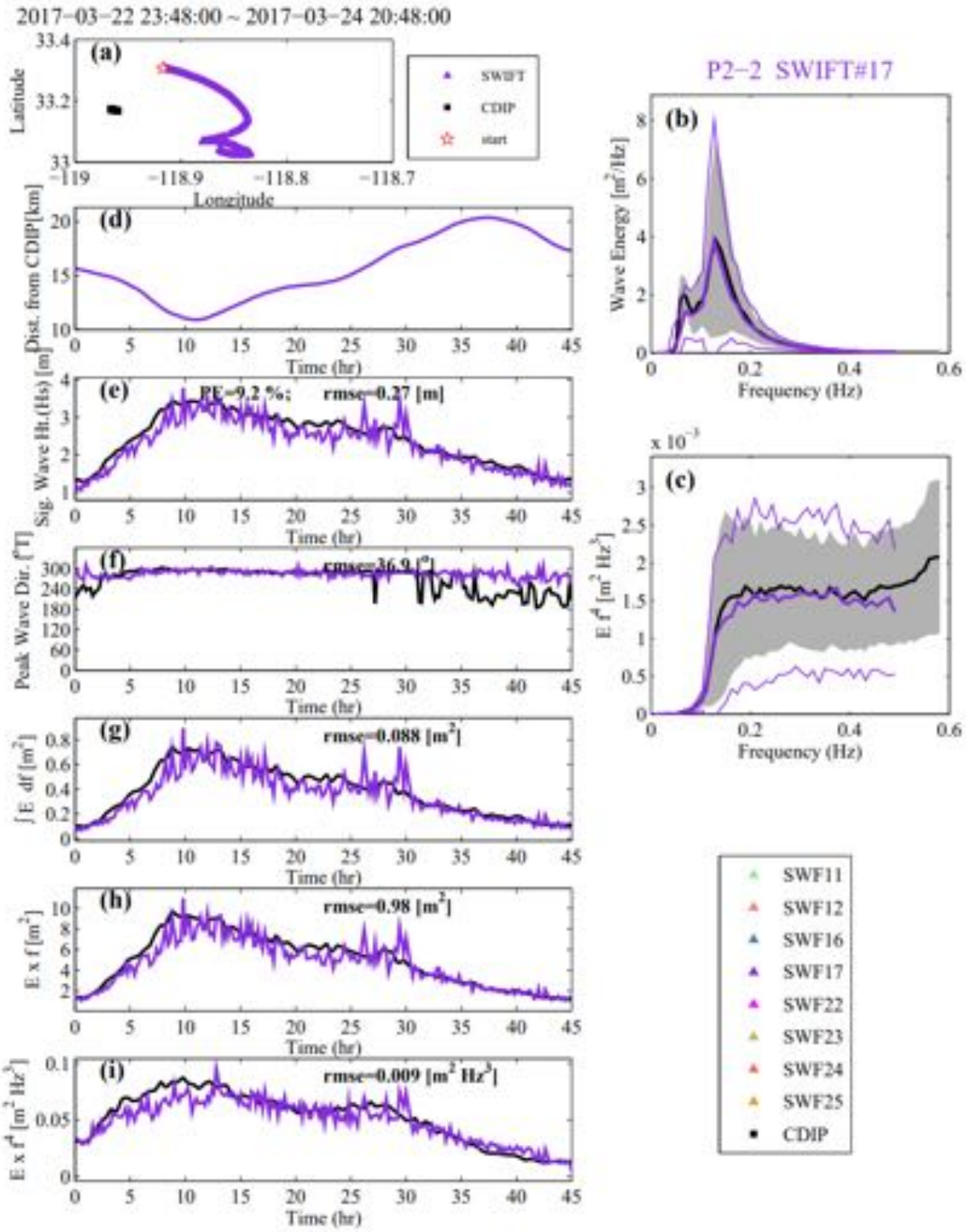

Figure 3.10: SWIFT #17 and CDIP wave energy measurement in period 2–2.

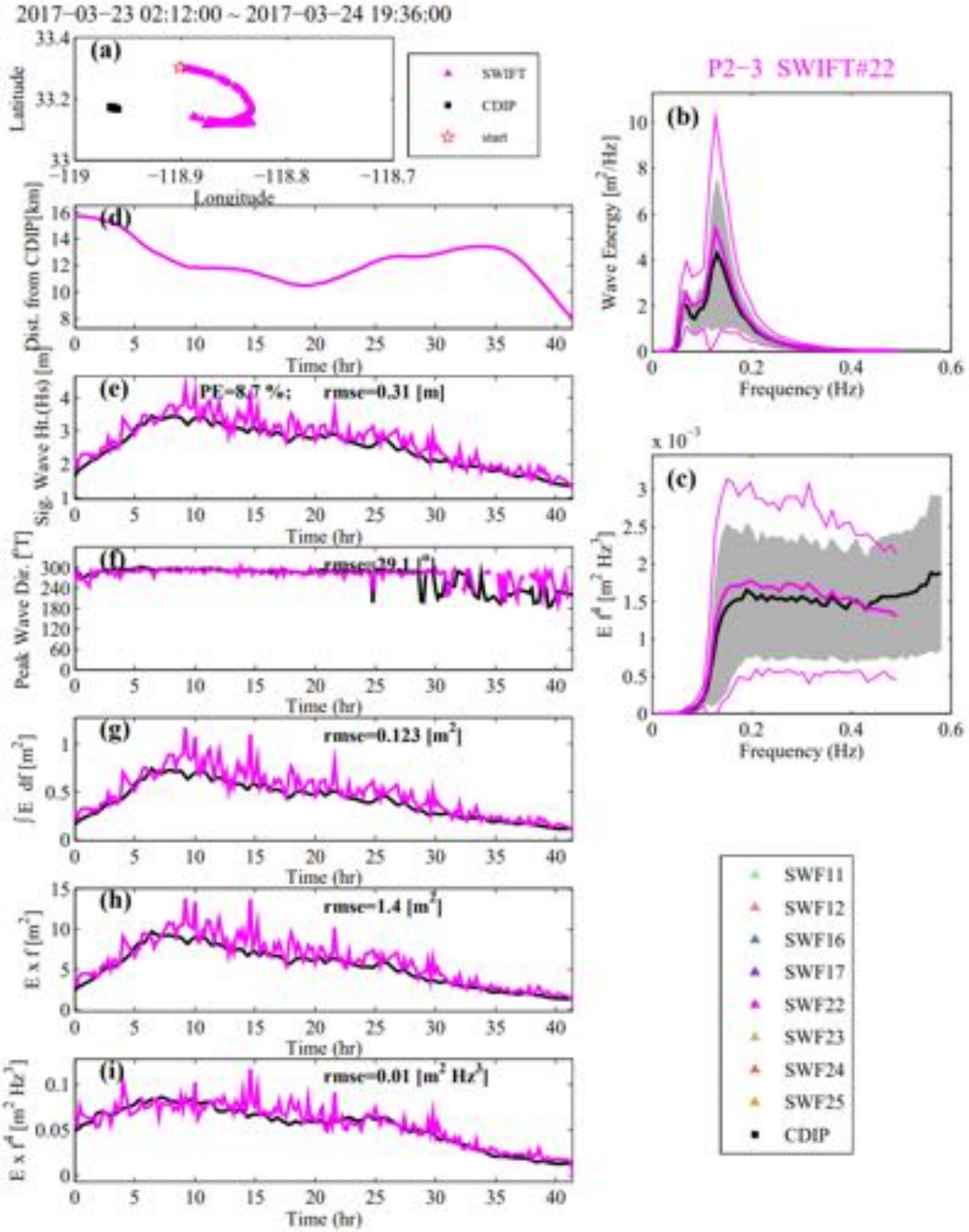

Figure 3.11: SWIFT #22 and CDIP wave energy measurement in period 2–3.

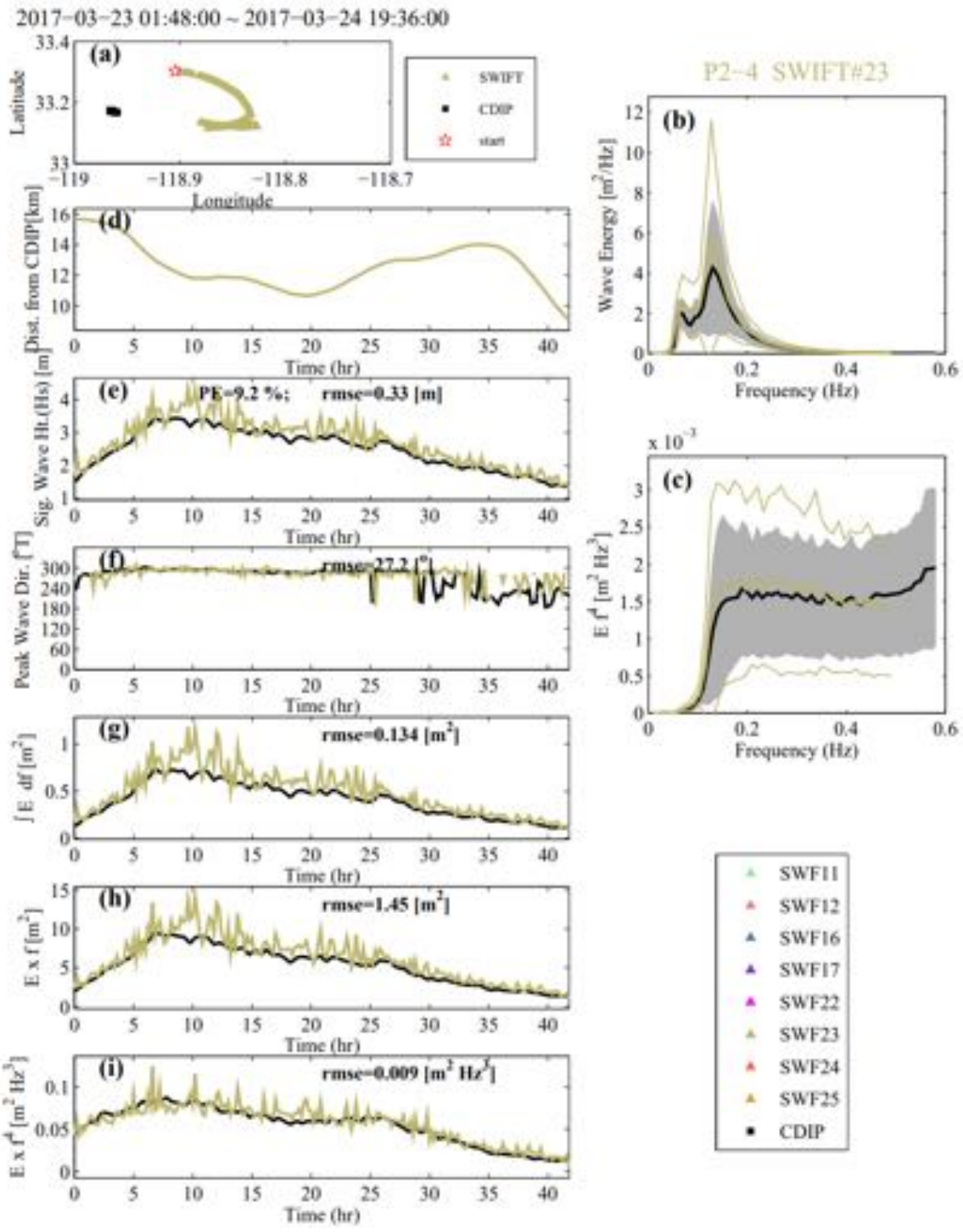

Figure 3.12: SWIFT #23 and CDIP wave energy measurement in period 2–4.

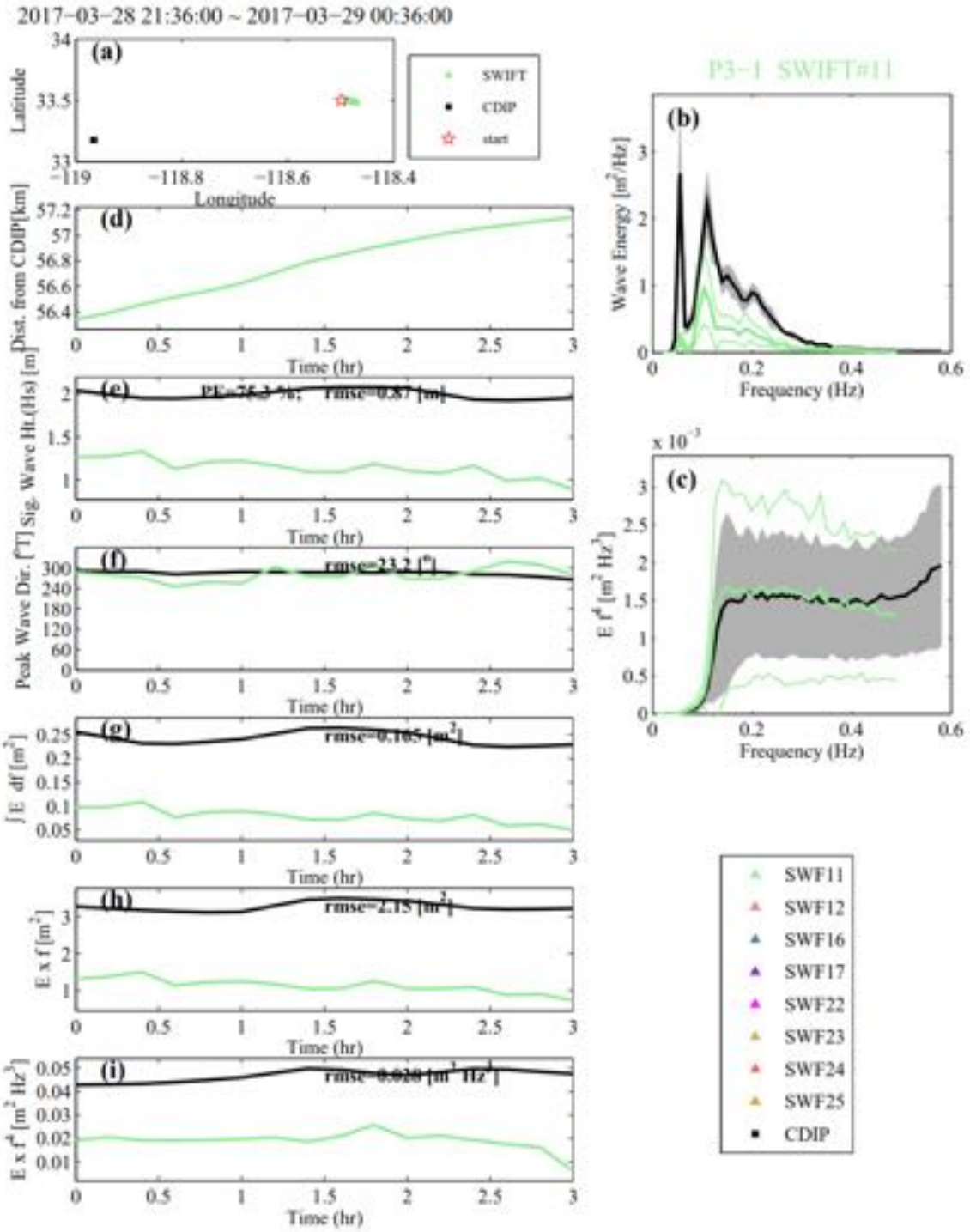

Figure 3.13: SWIFT #11 and CDIP wave energy measurement in period 3–1.

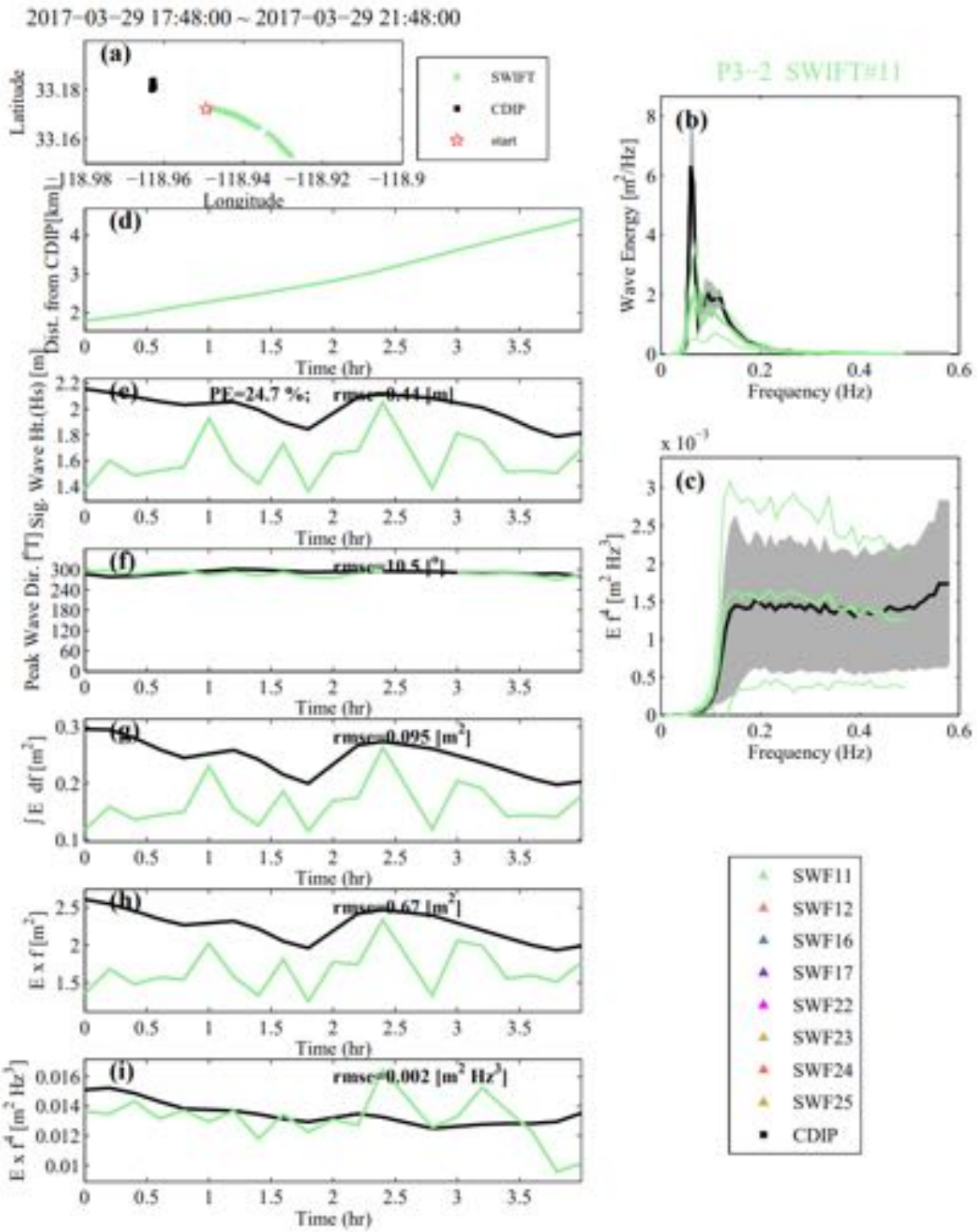

Figure 3.14: SWIFT #11 and CDIP wave energy measurement in period 3–2.

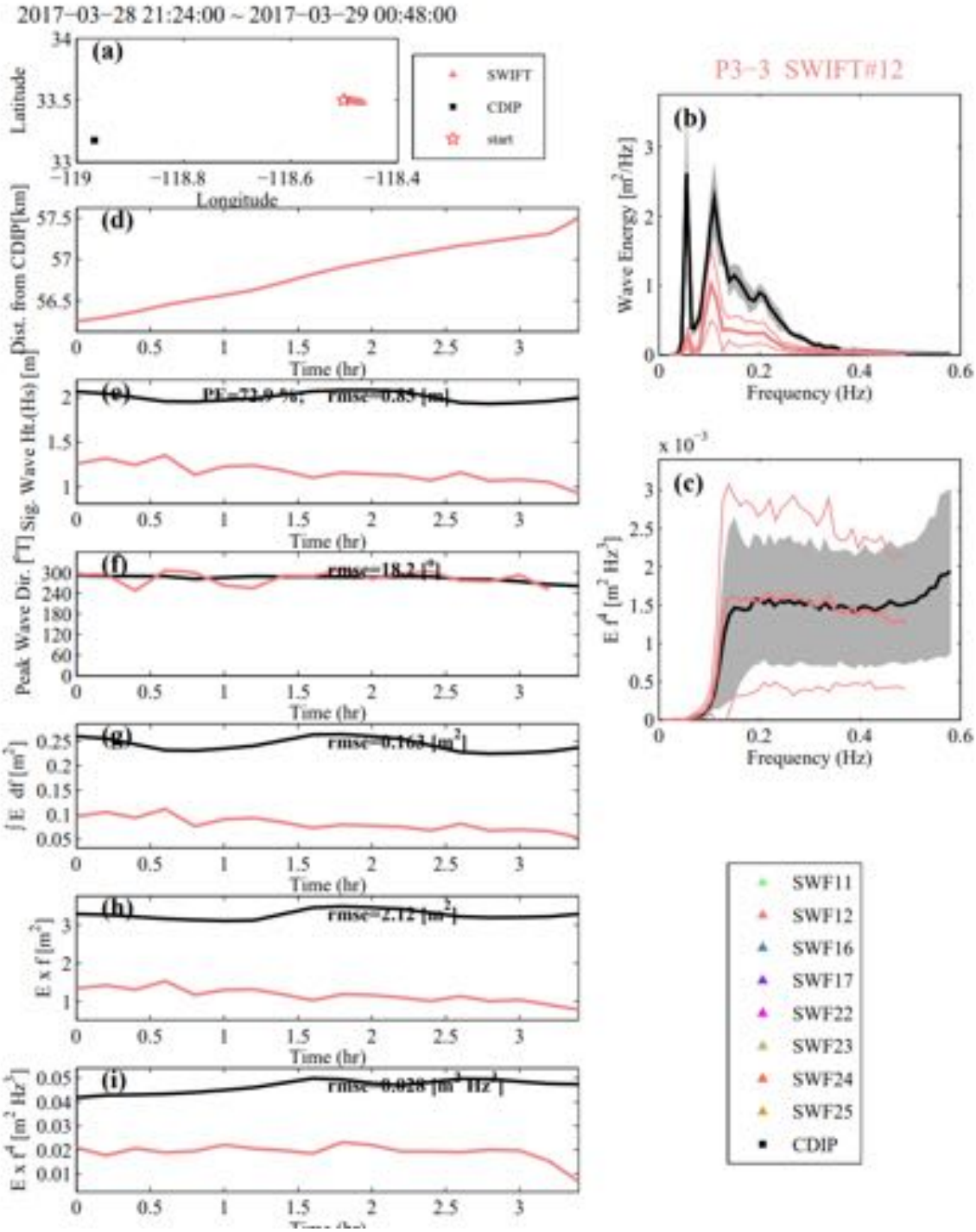

Figure 3.15: SWIFT #12 and CDIP wave energy measurement in period 3–3.

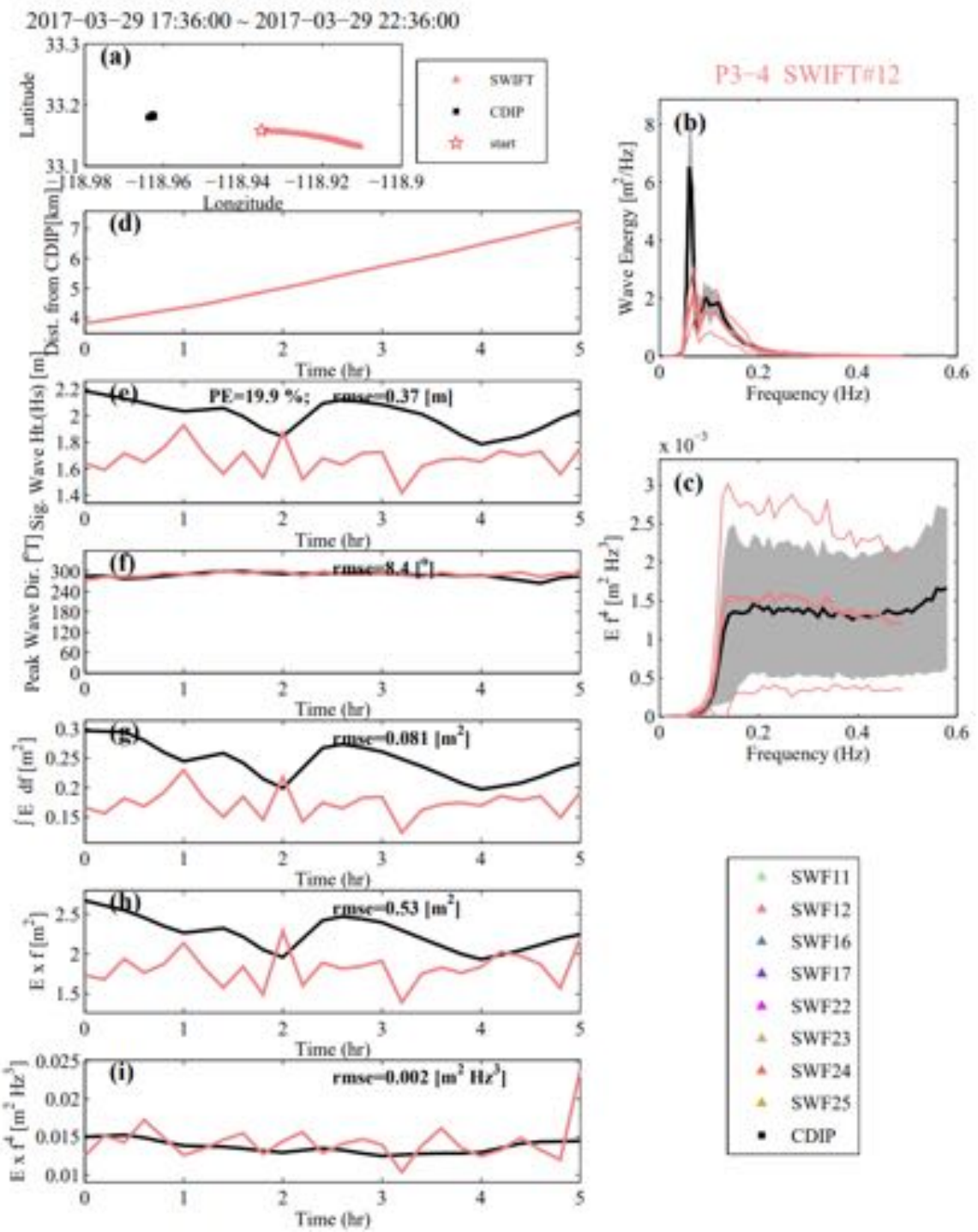

Figure 3.16: SWIFT #12 and CDIP wave energy measurement in period 3–4.

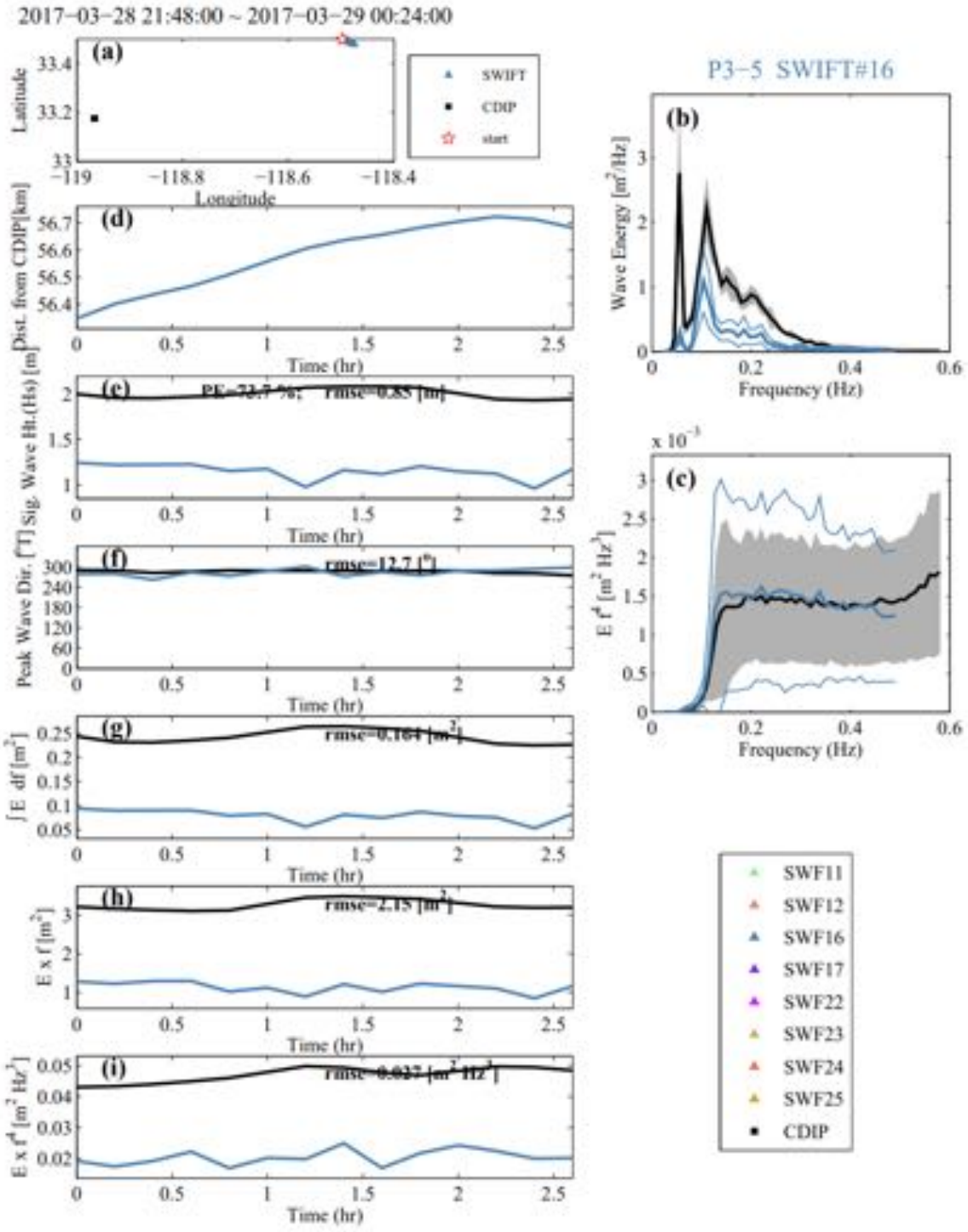

Figure 3.17: SWIFT #16 and CDIP wave energy measurement in period 3–5.

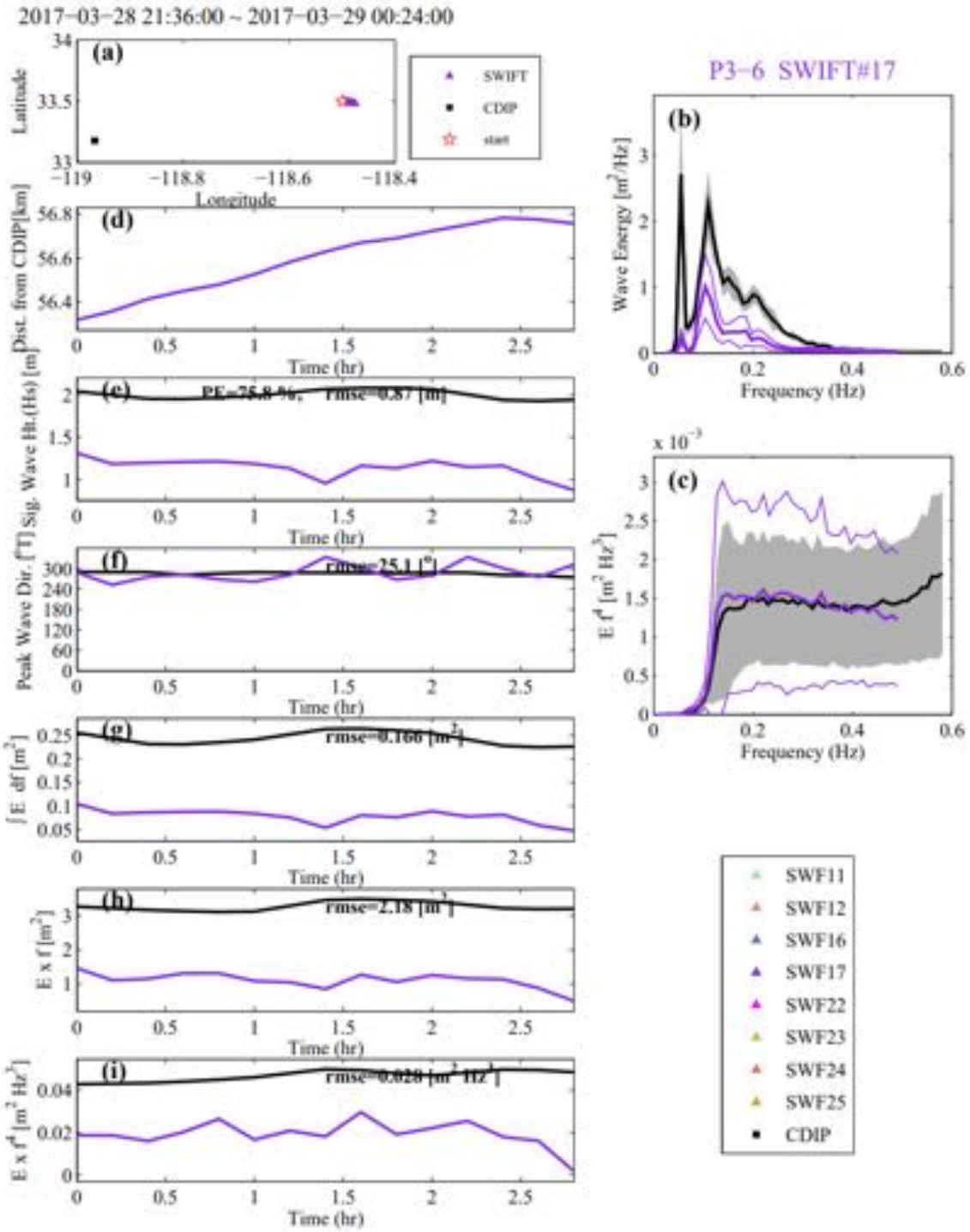

Figure 3.18: SWIFT #17 and CDIP wave energy measurement in period 3–6.

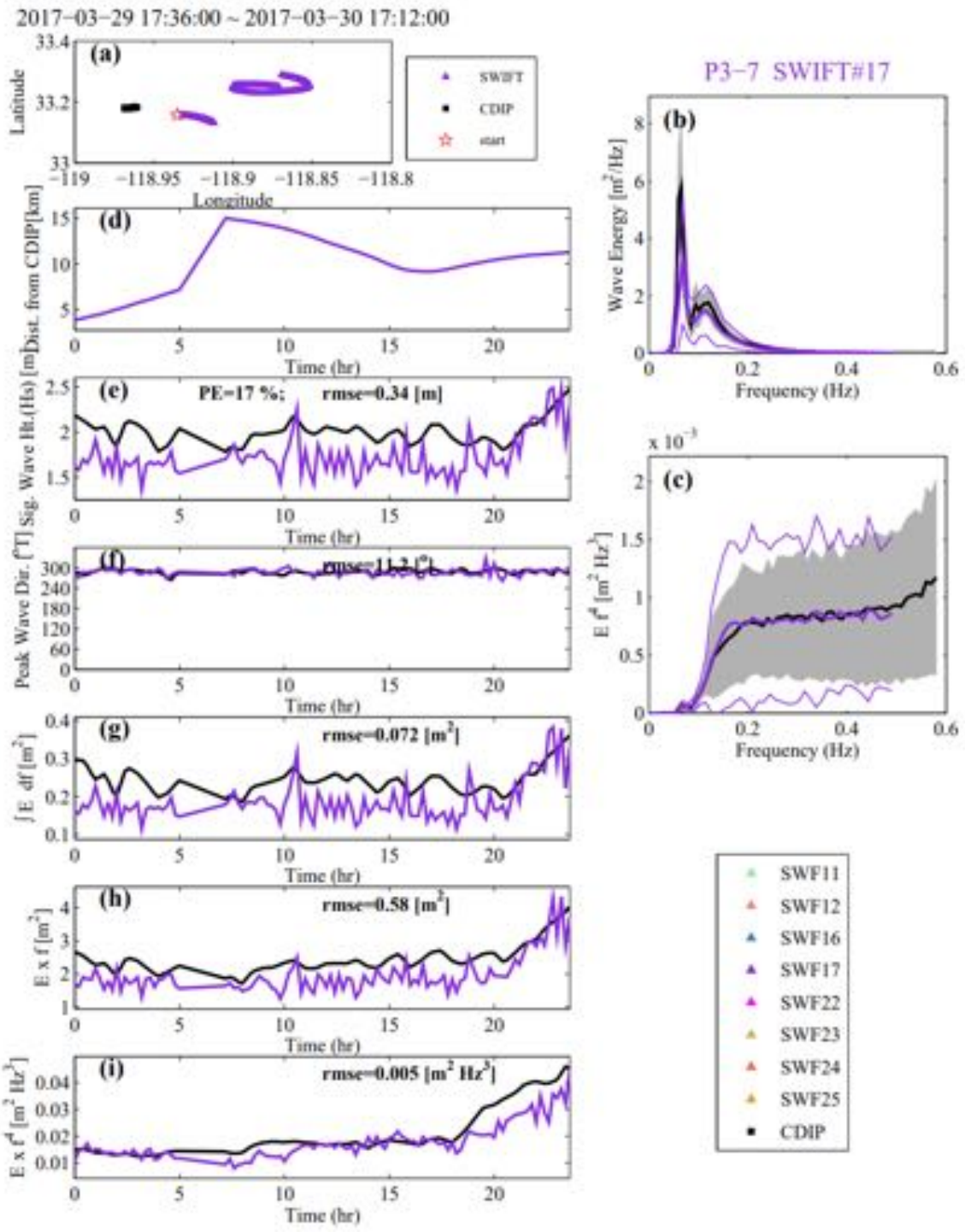

Figure 3.19: SWIFT #17 and CDIP wave energy measurement in period 3–7.

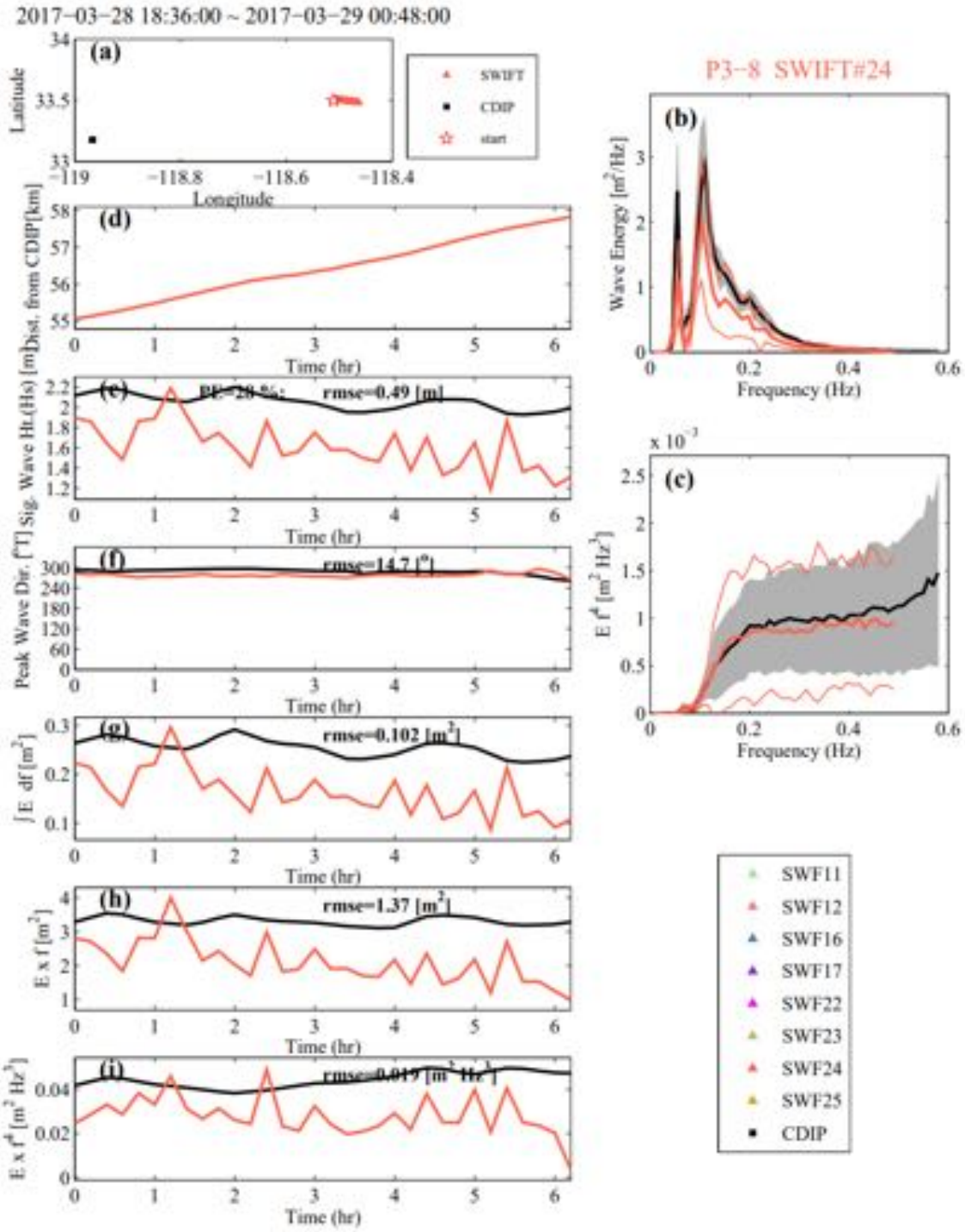

Figure 3.20: SWIFT #24 and CDIP wave energy measurement in period 3–8.

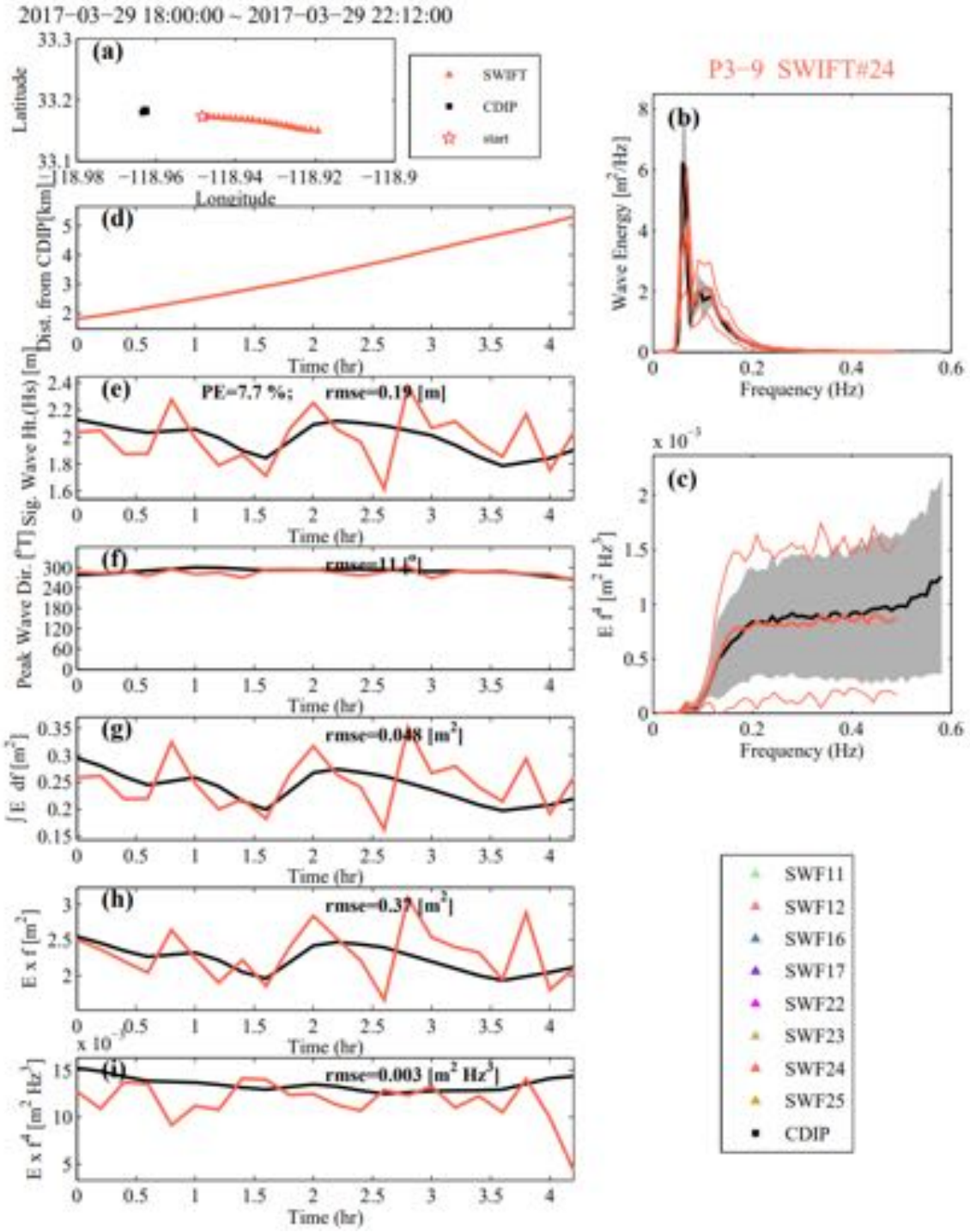

Figure 3.21: SWIFT #24 and CDIP wave energy measurement in period 3–9.

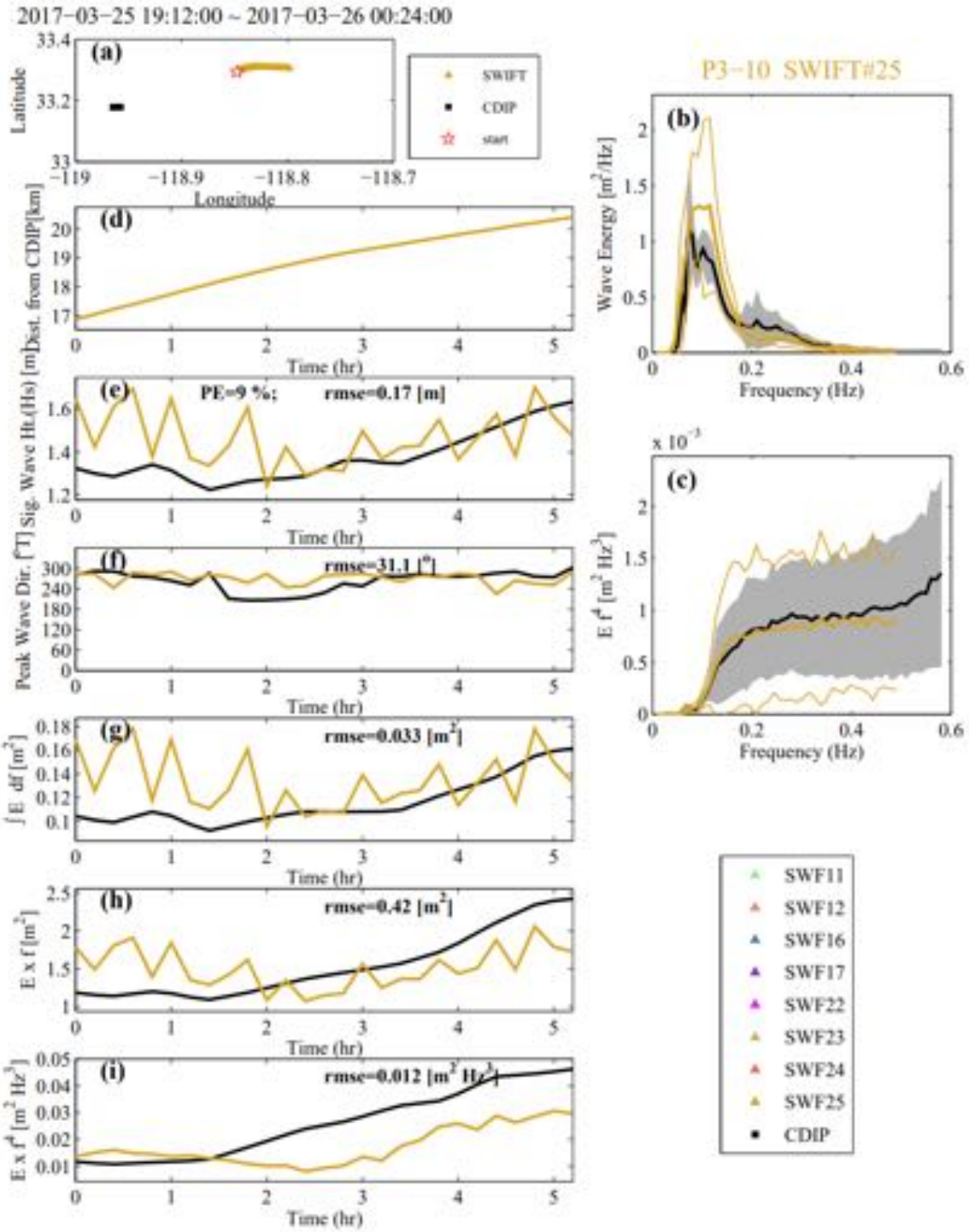

Figure 3.22: SWIFT #25 and CDIP wave energy measurement in period 3–10.

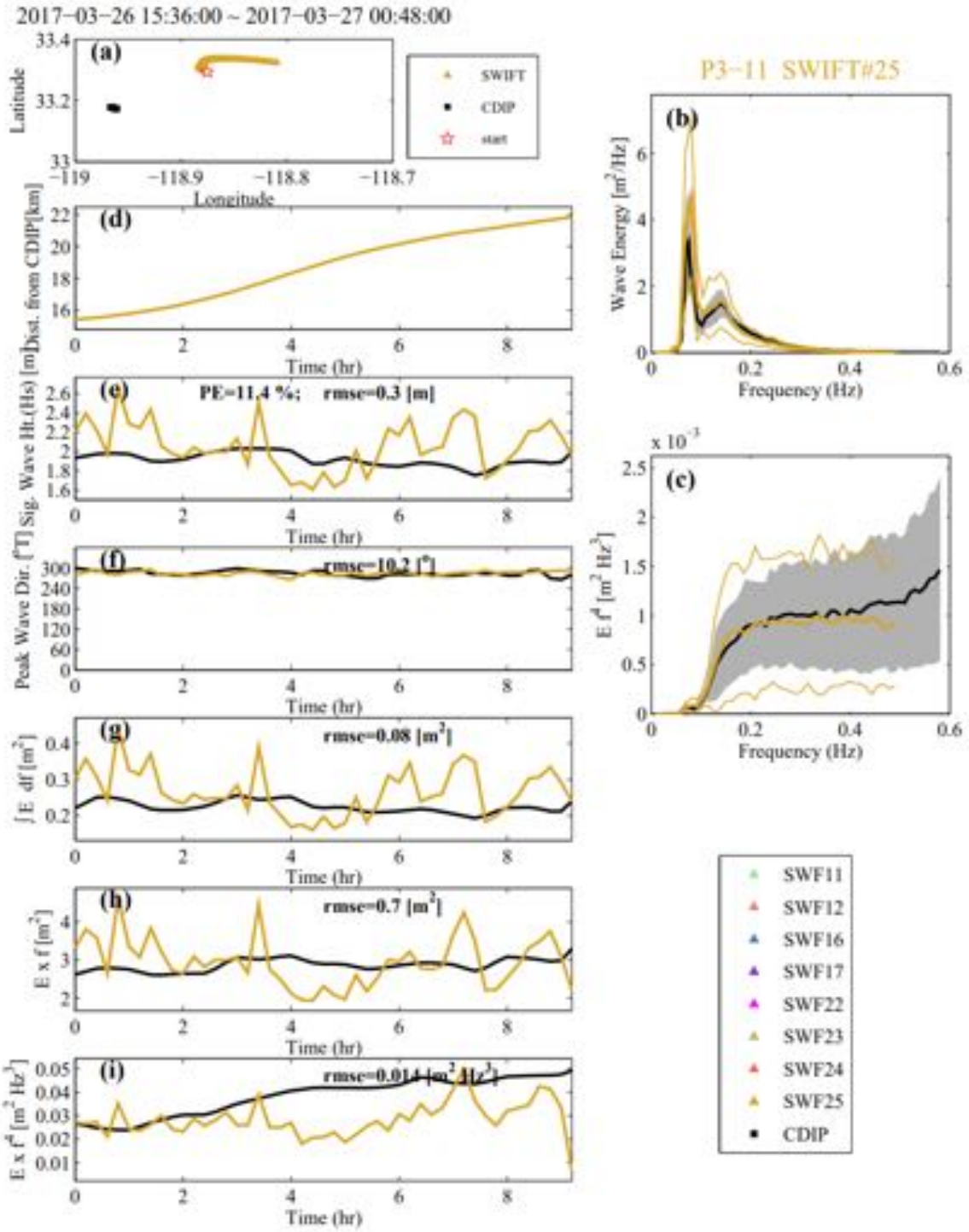

Figure 3.23: SWIFT #25 and CDIP wave energy measurement in period 3–11.

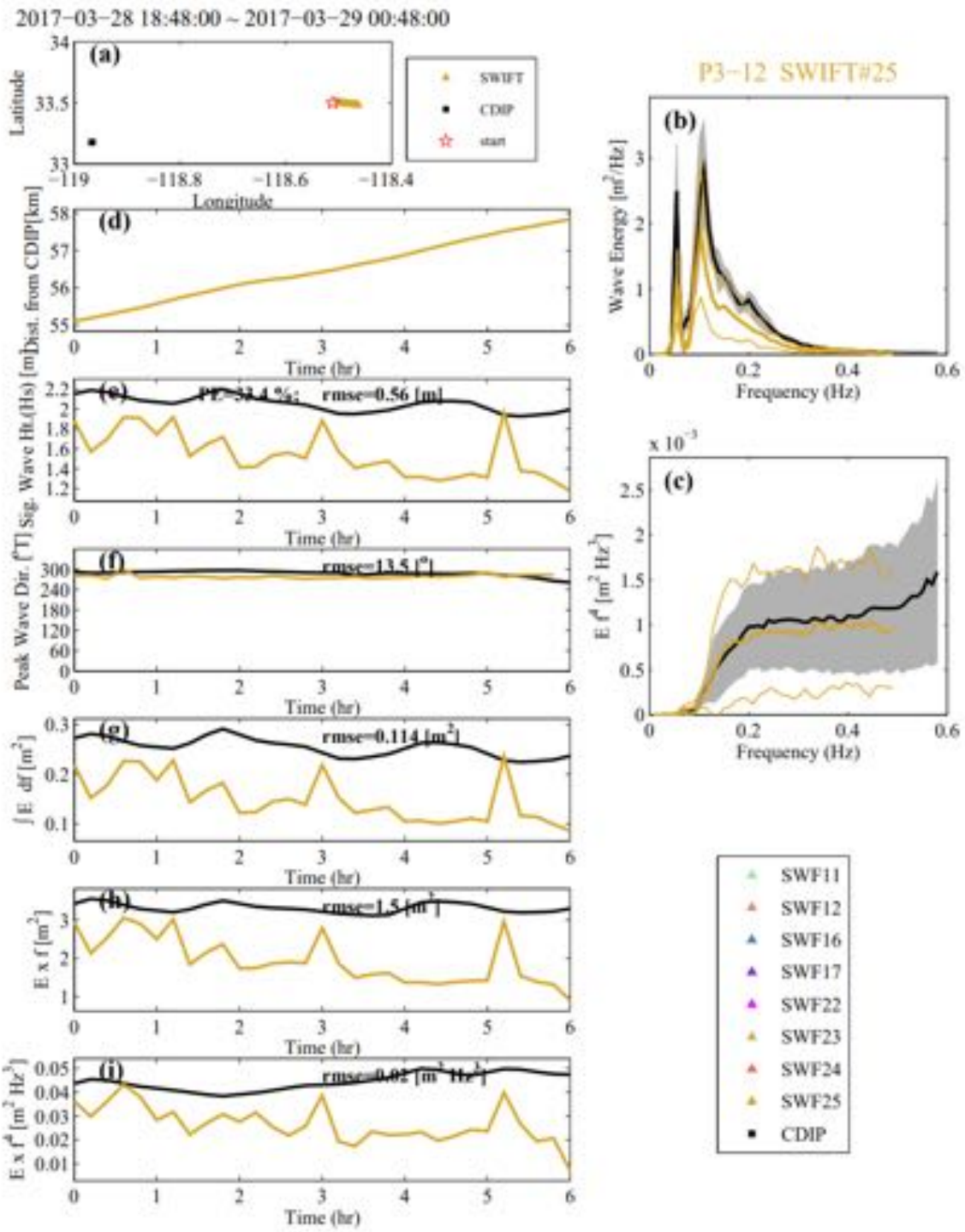

Figure 3.24: SWIFT #25 and CDIP wave energy measurement in period 3–12.

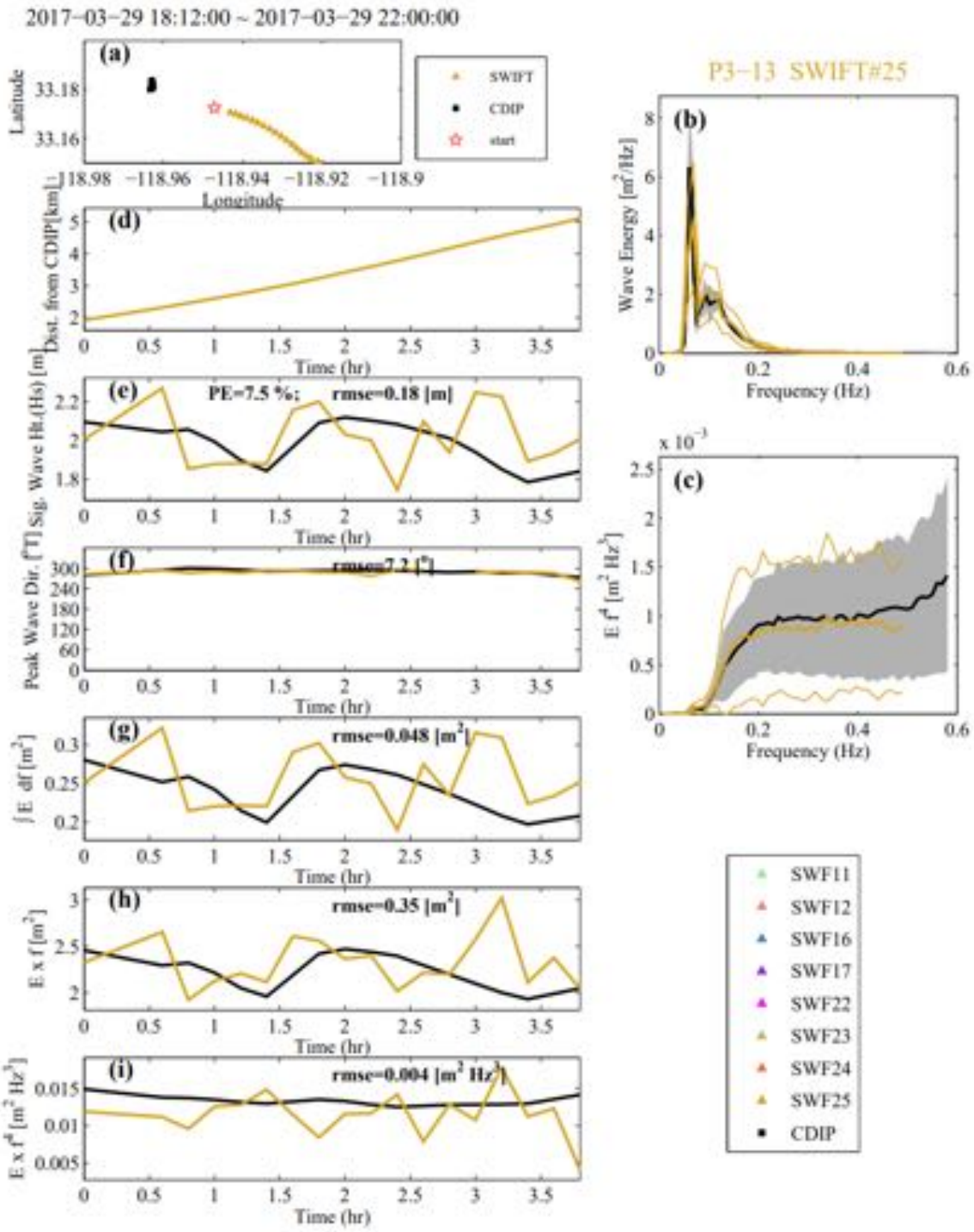

Figure 3.25: SWIFT #25 and CDIP wave energy measurement in period 3–13.

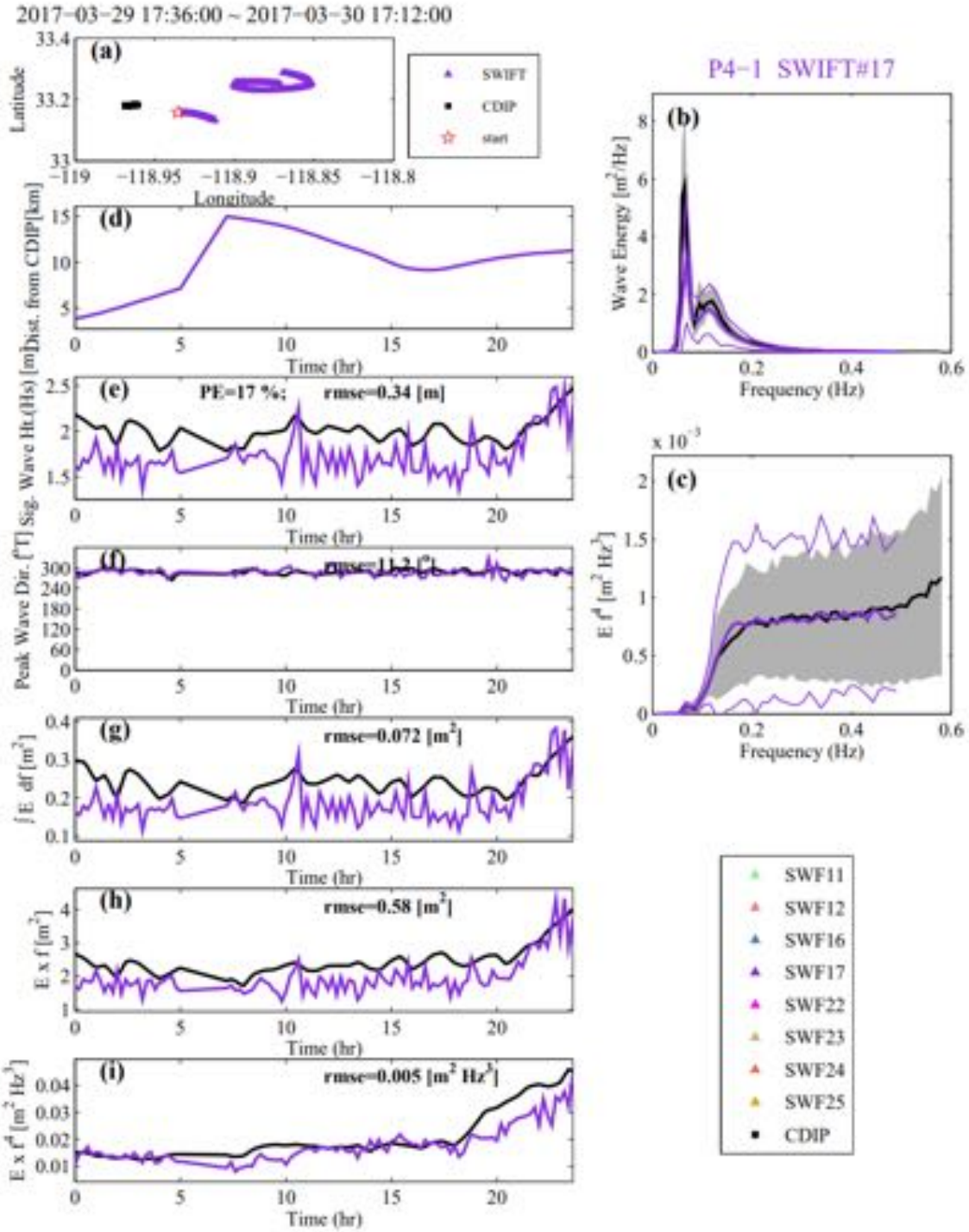

Figure 3.26: SWIFT #17 and CDIP wave energy measurement in period 4–1.

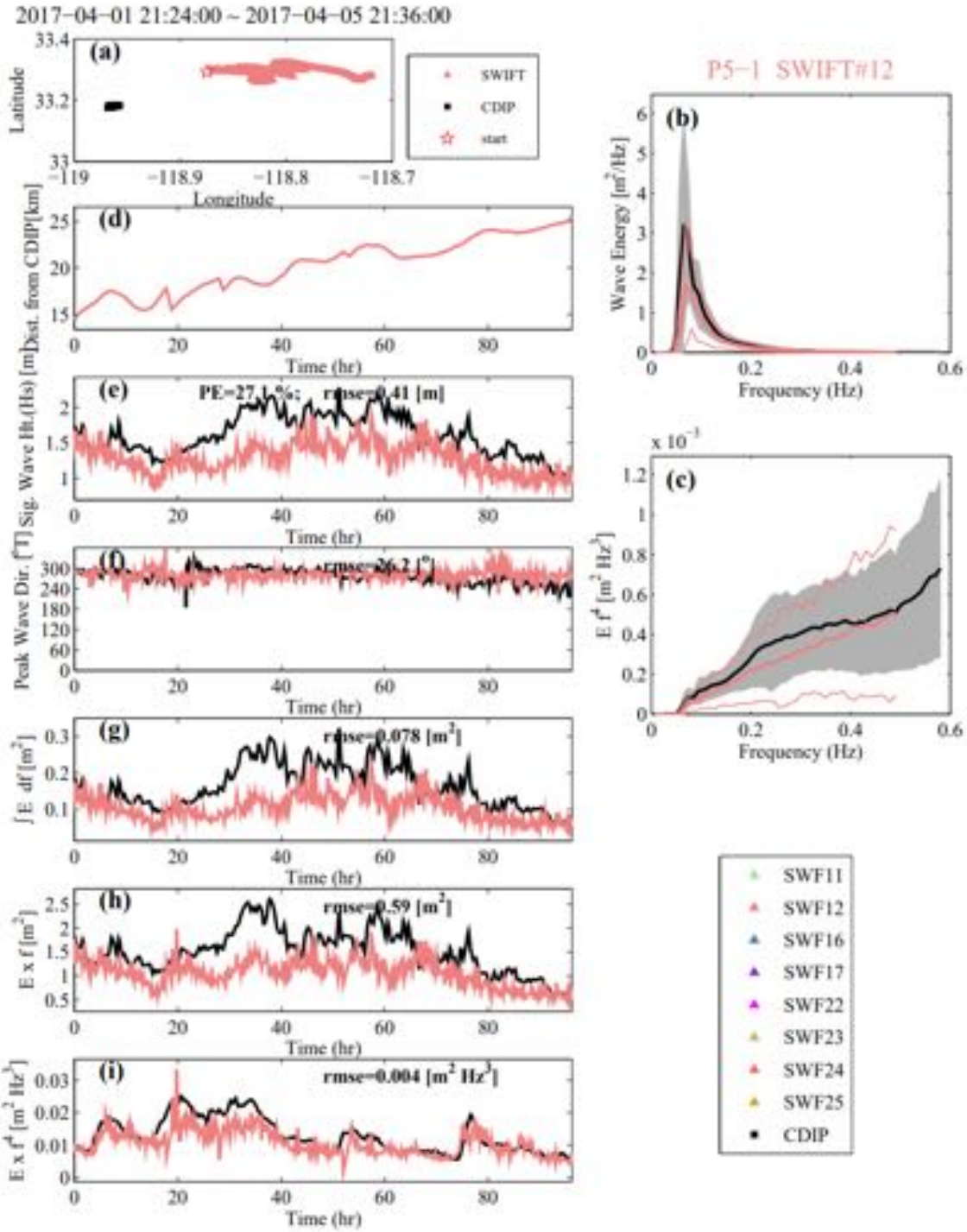

Figure 3.27: SWIFT #12 and CDIP wave energy measurement in period 5–1.

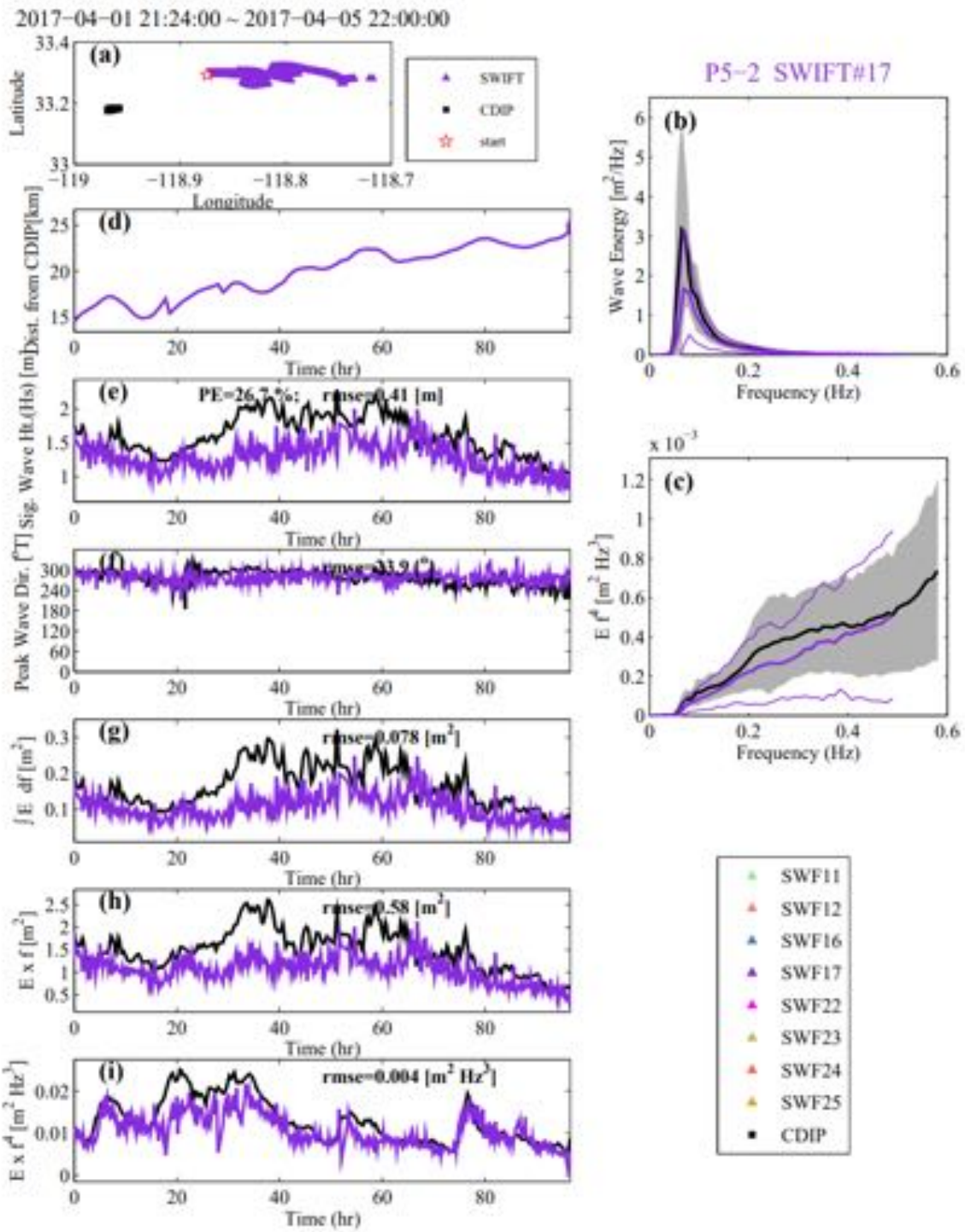

Figure 3.28: SWIFT #17 and CDIP wave energy measurement in period 5–2.

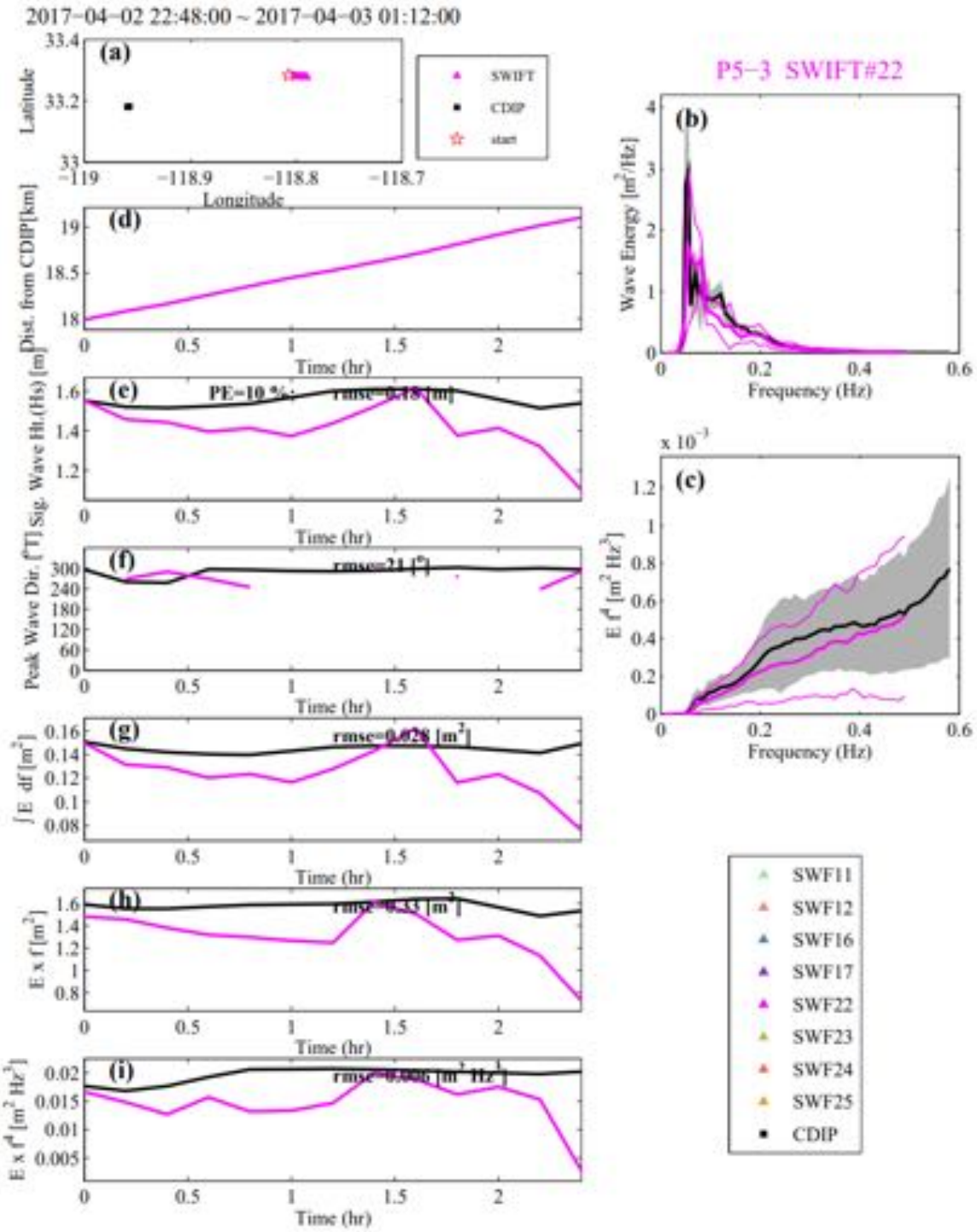

Figure 3.29: SWIFT #22 and CDIP wave energy measurement in period 5–3.

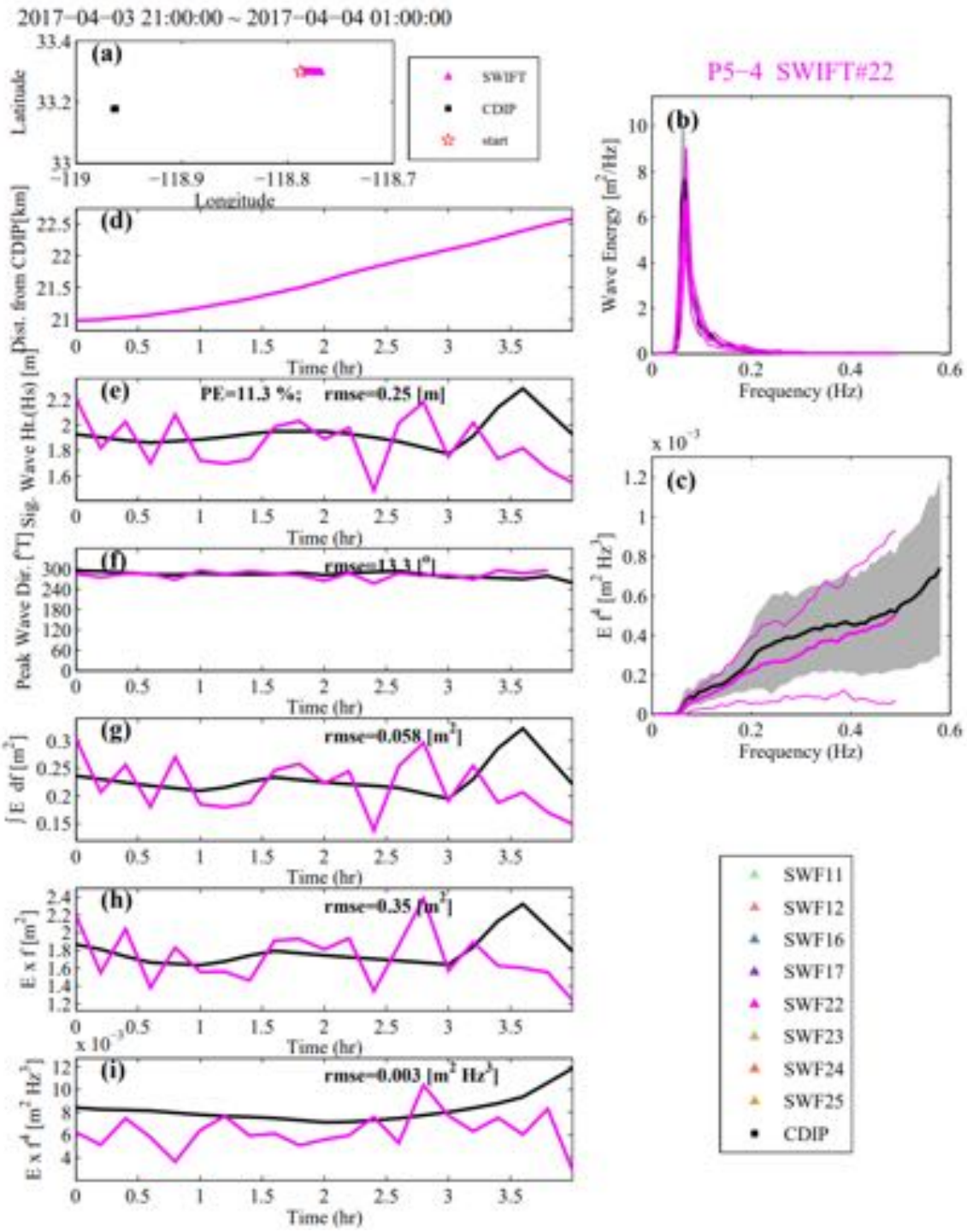

Figure 3.30: SWIFT #22 and CDIP wave energy measurement in period 5–4.

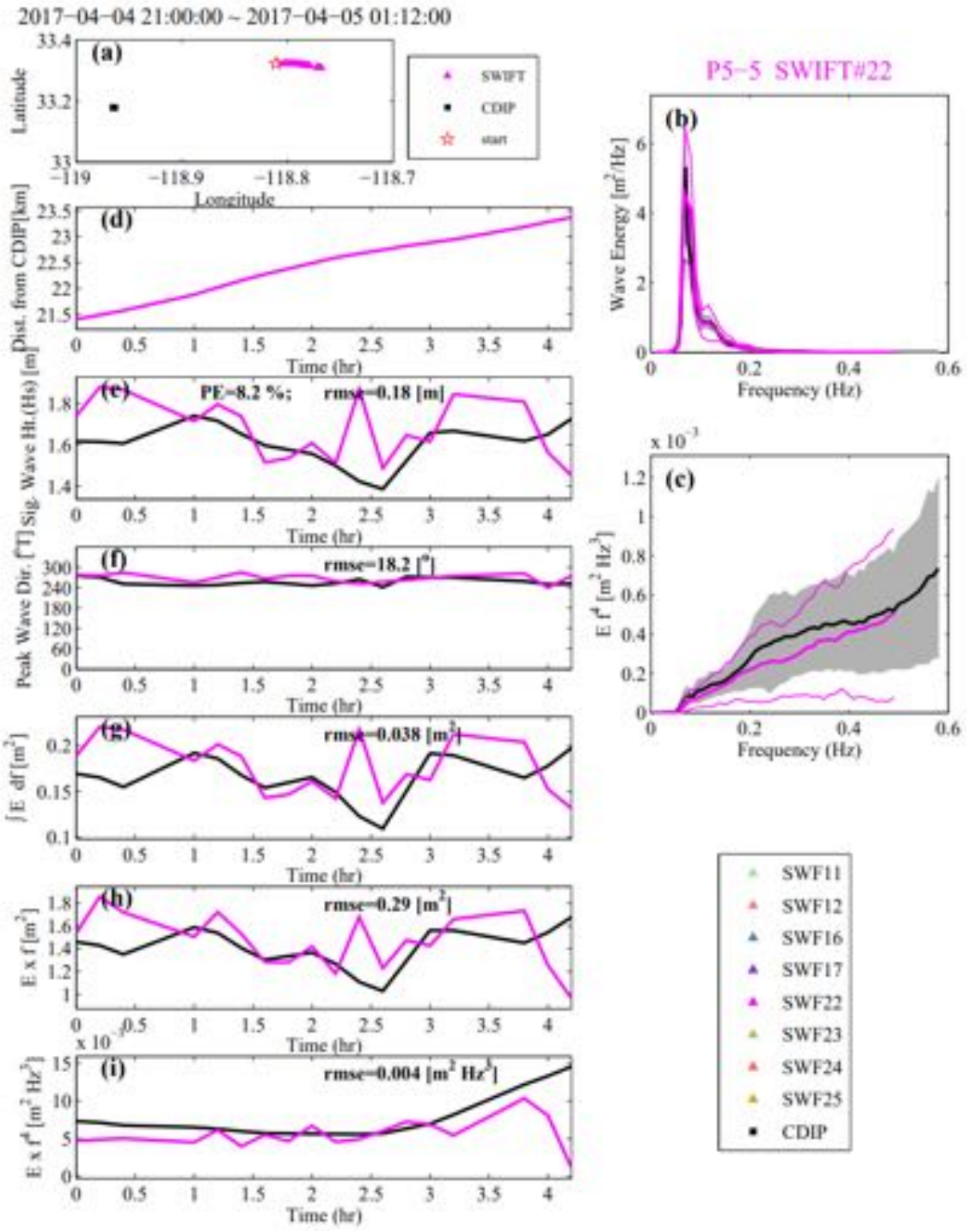

Figure 3.31: SWIFT #22 and CDIP wave energy measurement in period 5–5.

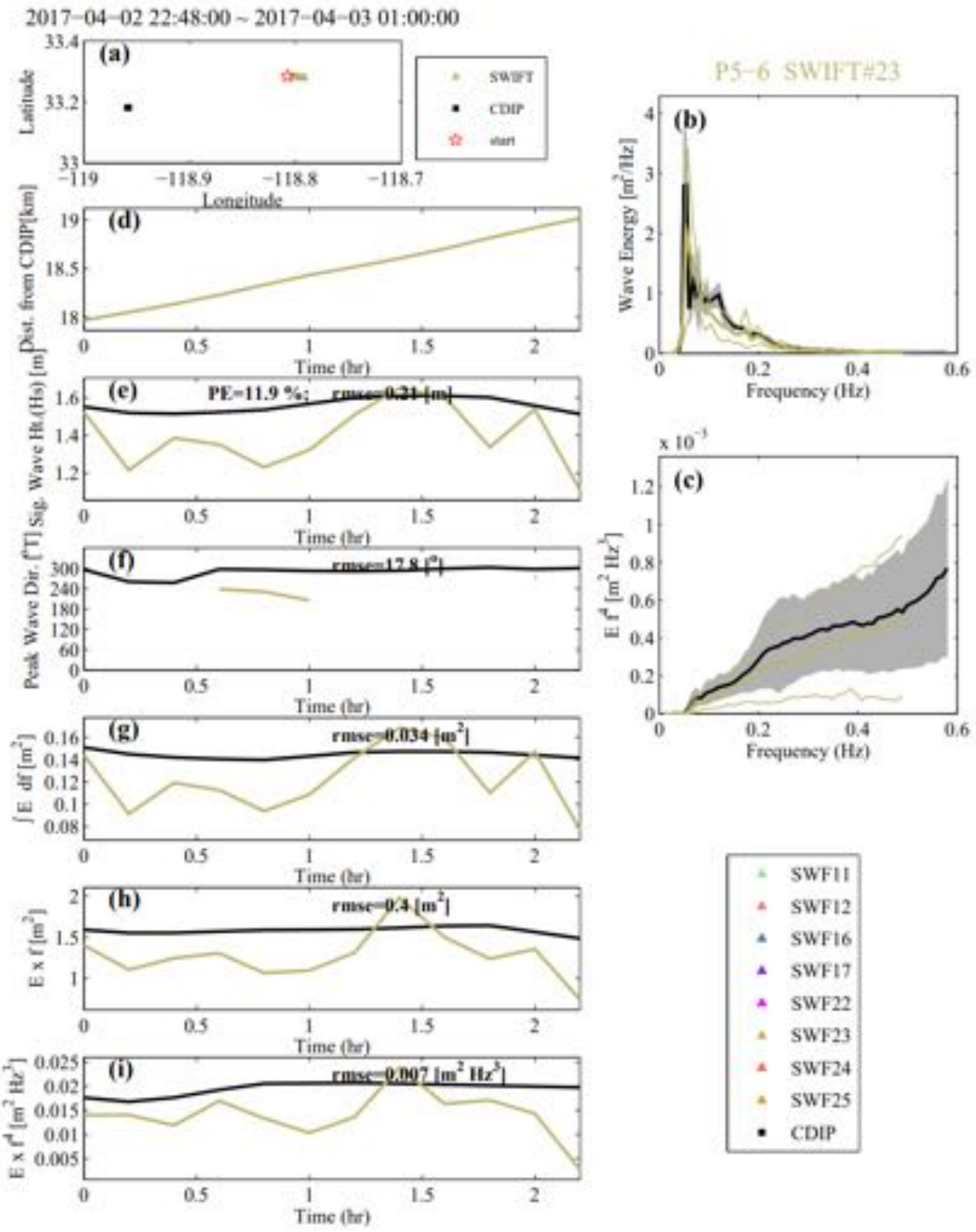

Figure 3.32: SWIFT #23 and CDIP wave energy measurement in period 5–6.

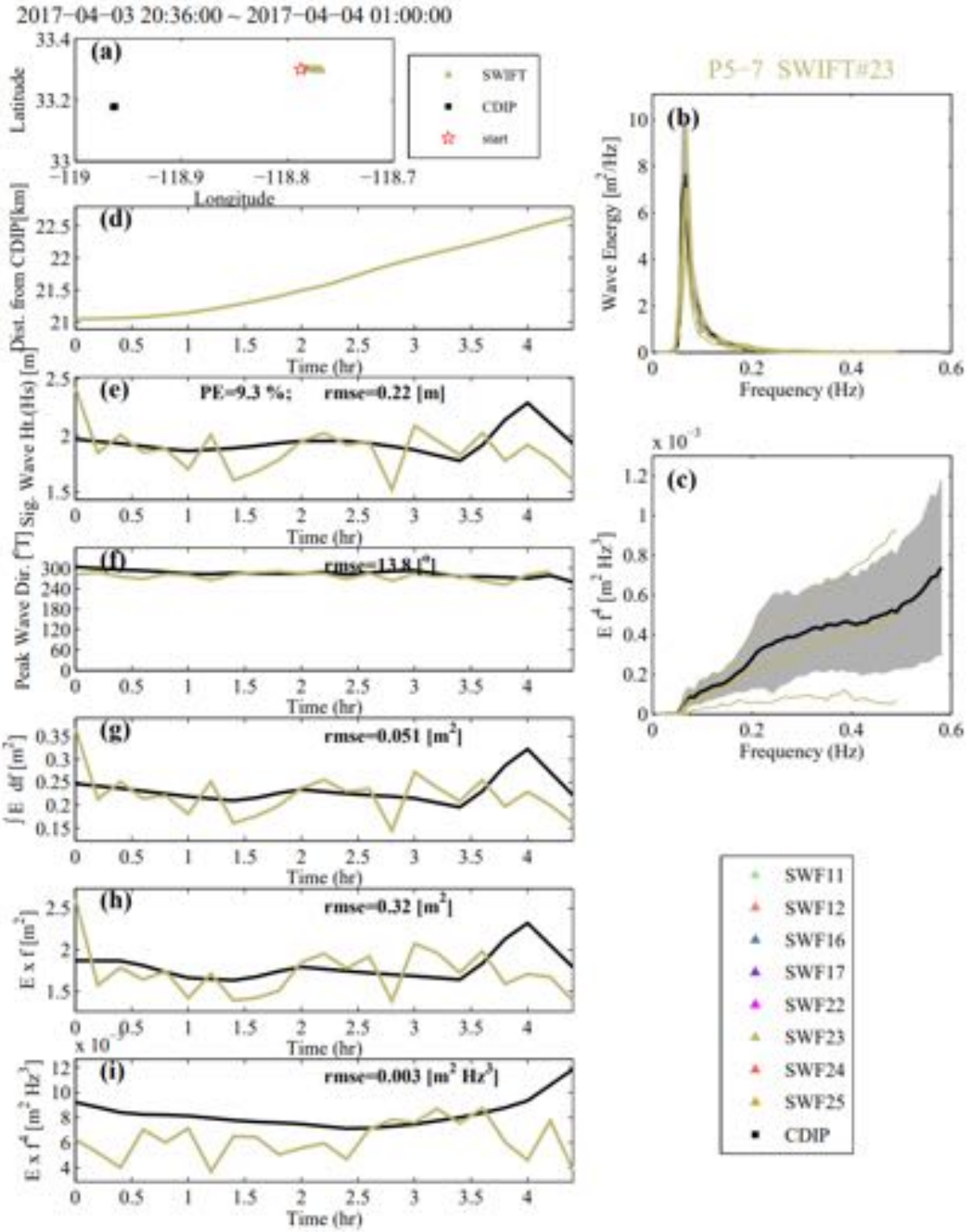

Figure 3.33: SWIFT #23 and CDIP wave energy measurement in period 5–7.

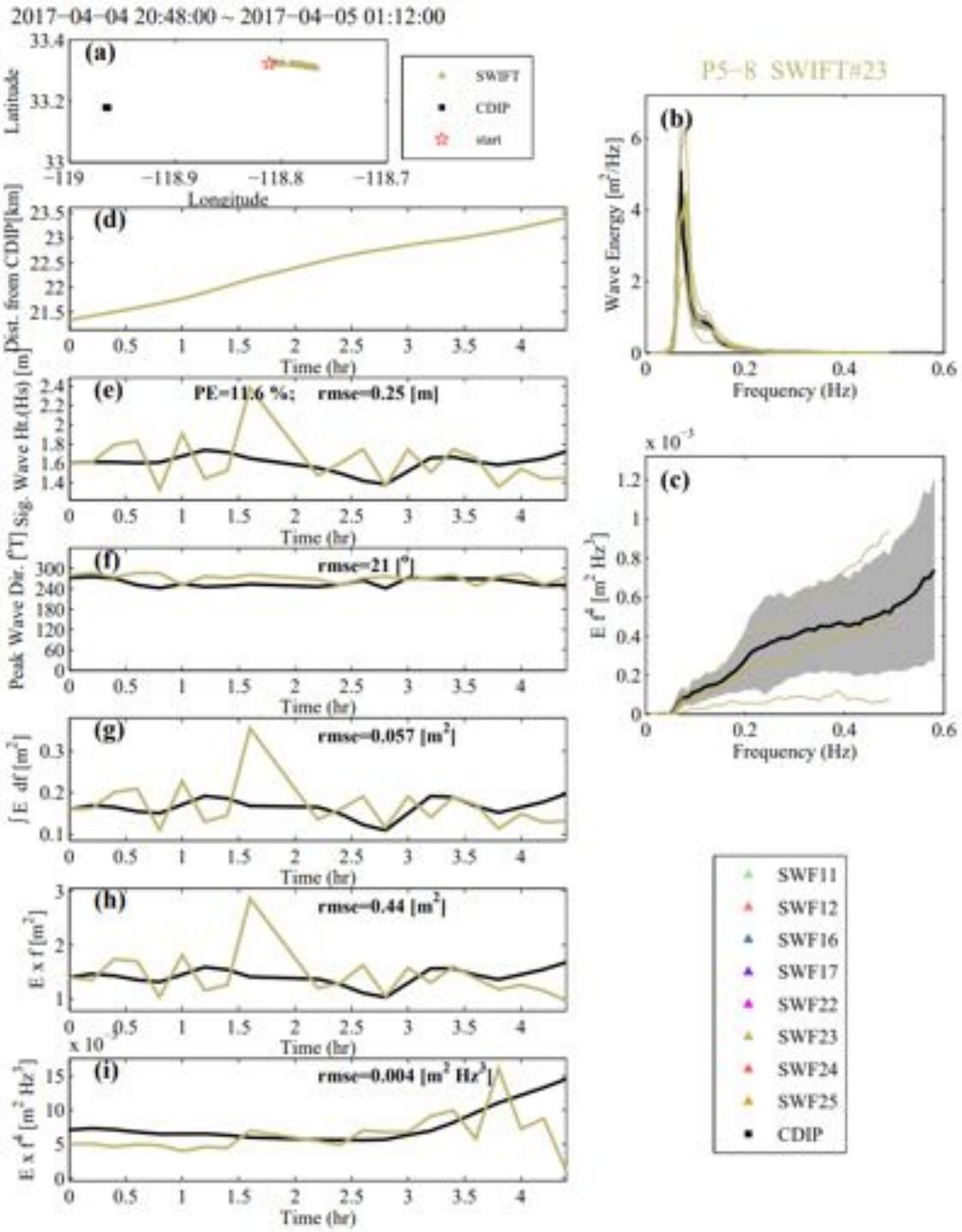

Figure 3.34: SWIFT #23 and CDIP wave energy measurement in period 5–8.

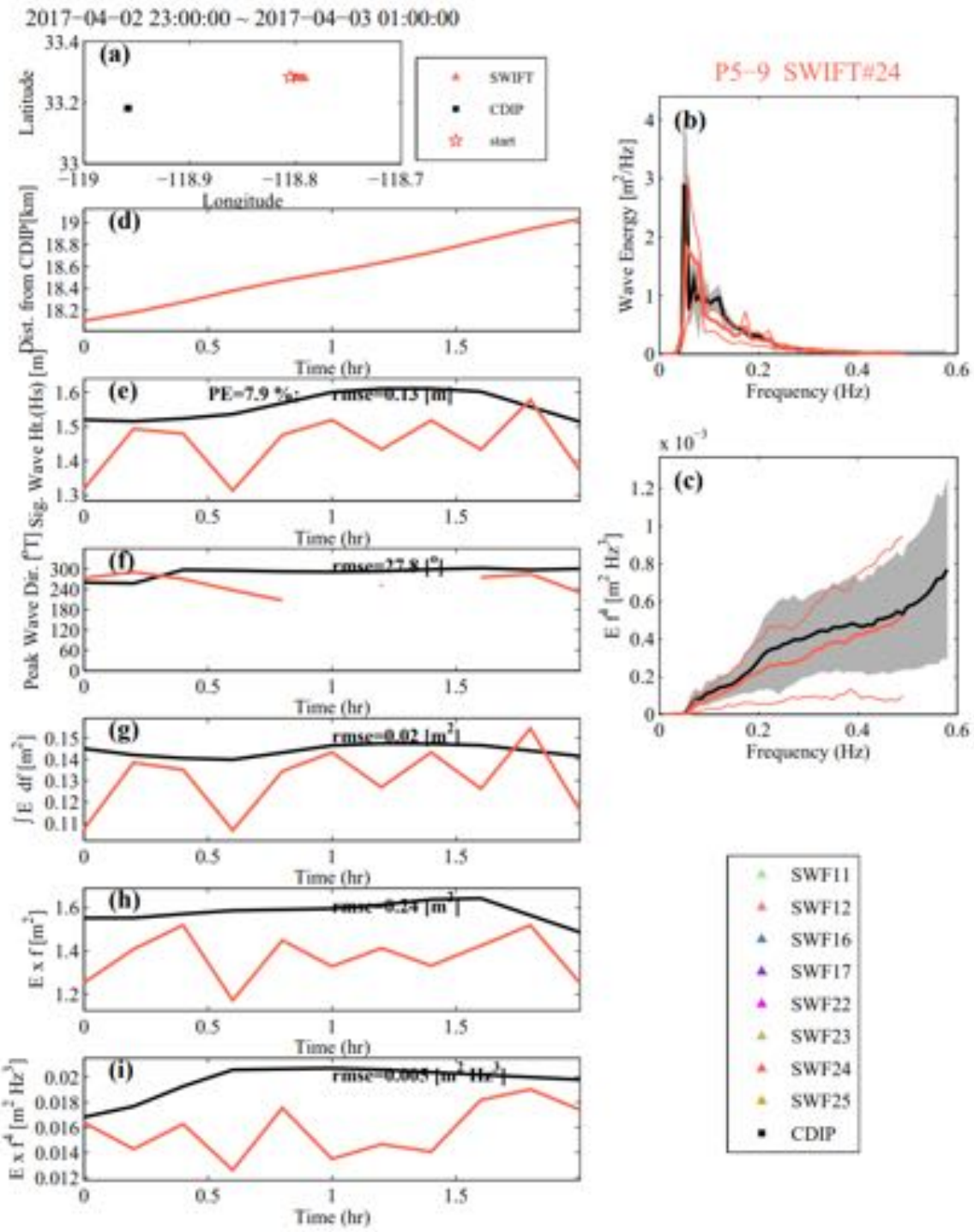

Figure 3.35: SWIFT #24 and CDIP wave energy measurement in period 5–9.

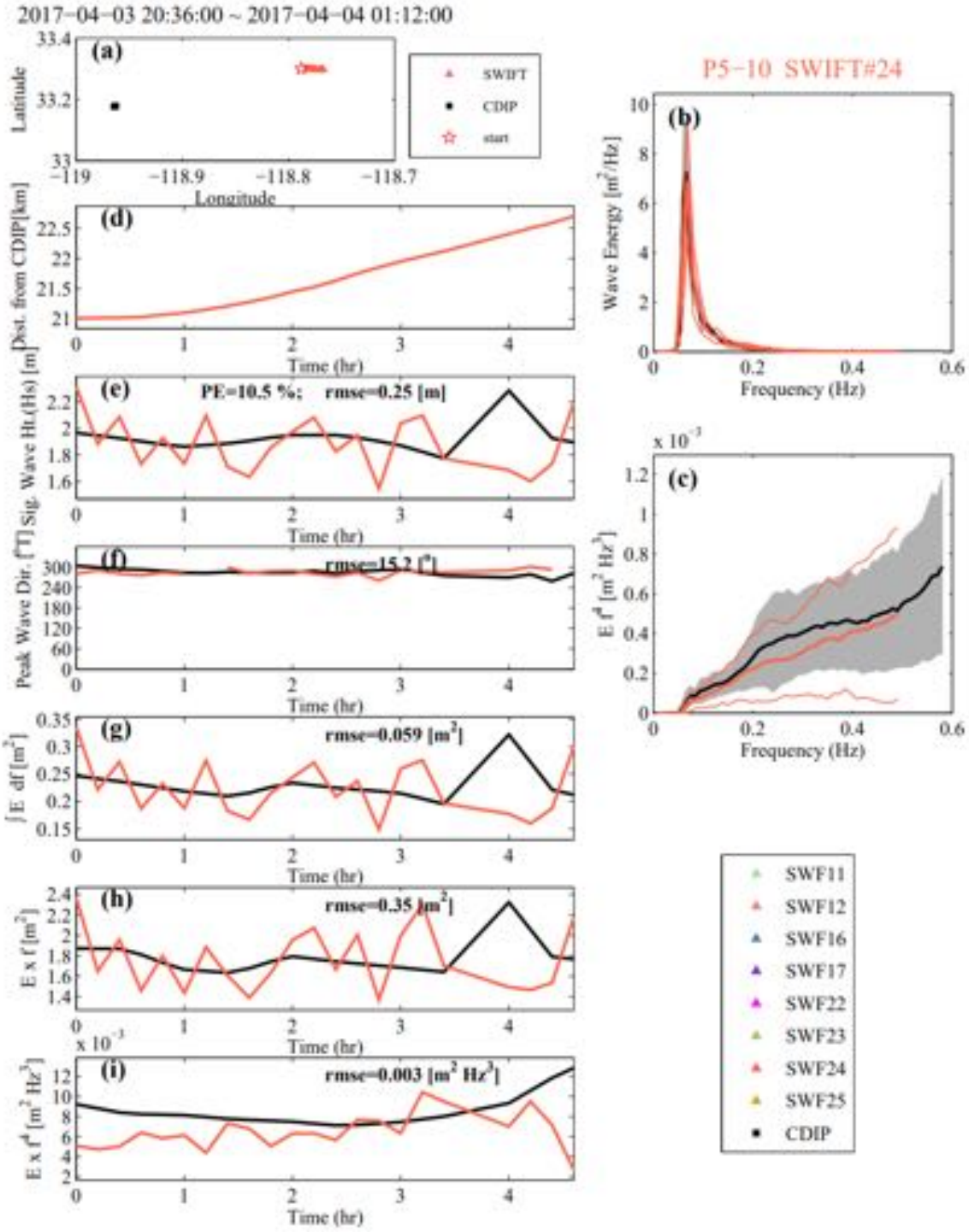

Figure 3.36: SWIFT #24 and CDIP wave energy measurement in period 5–10.

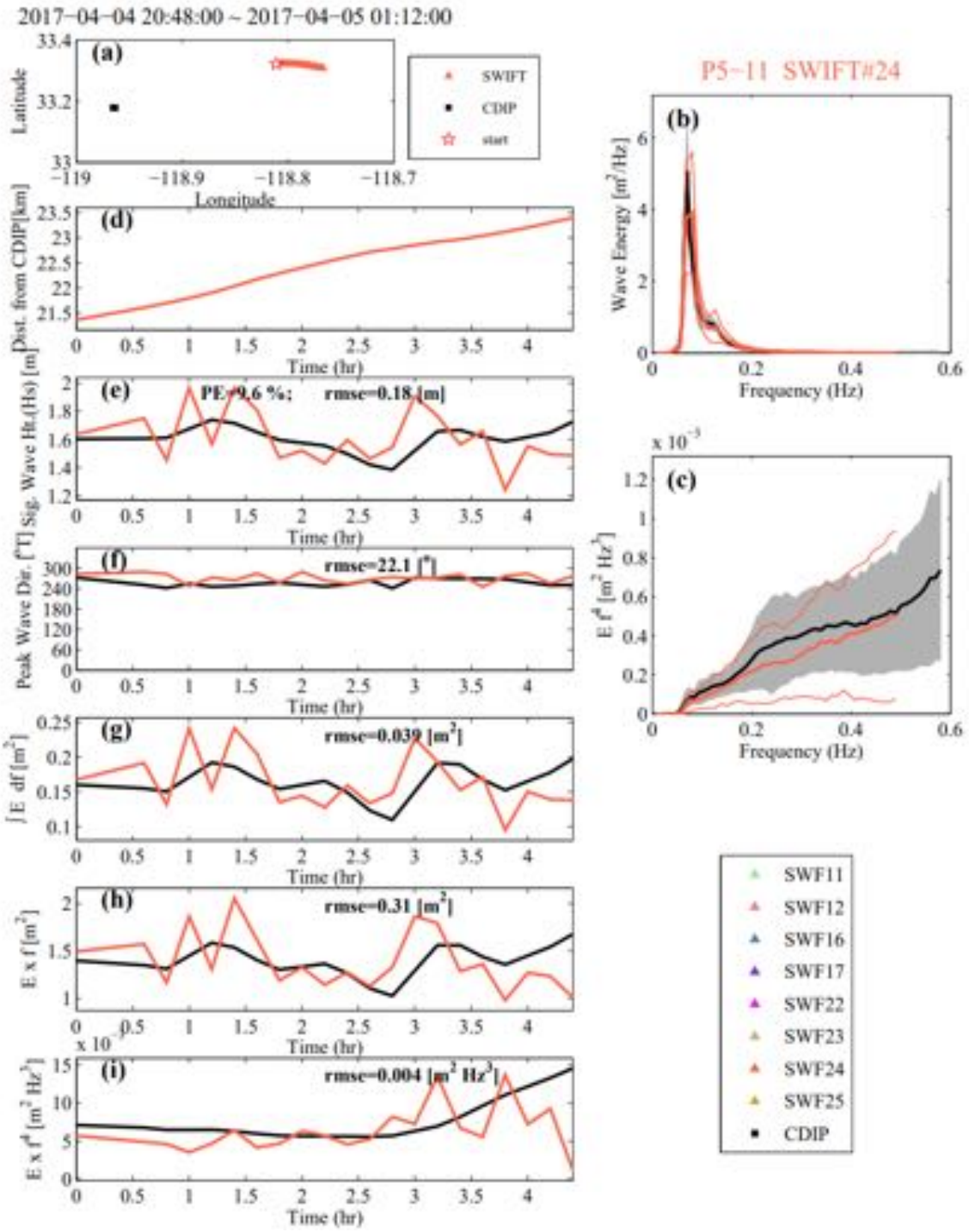

Figure 3.37: SWIFT #24 and CDIP wave energy measurement in period 5–11.

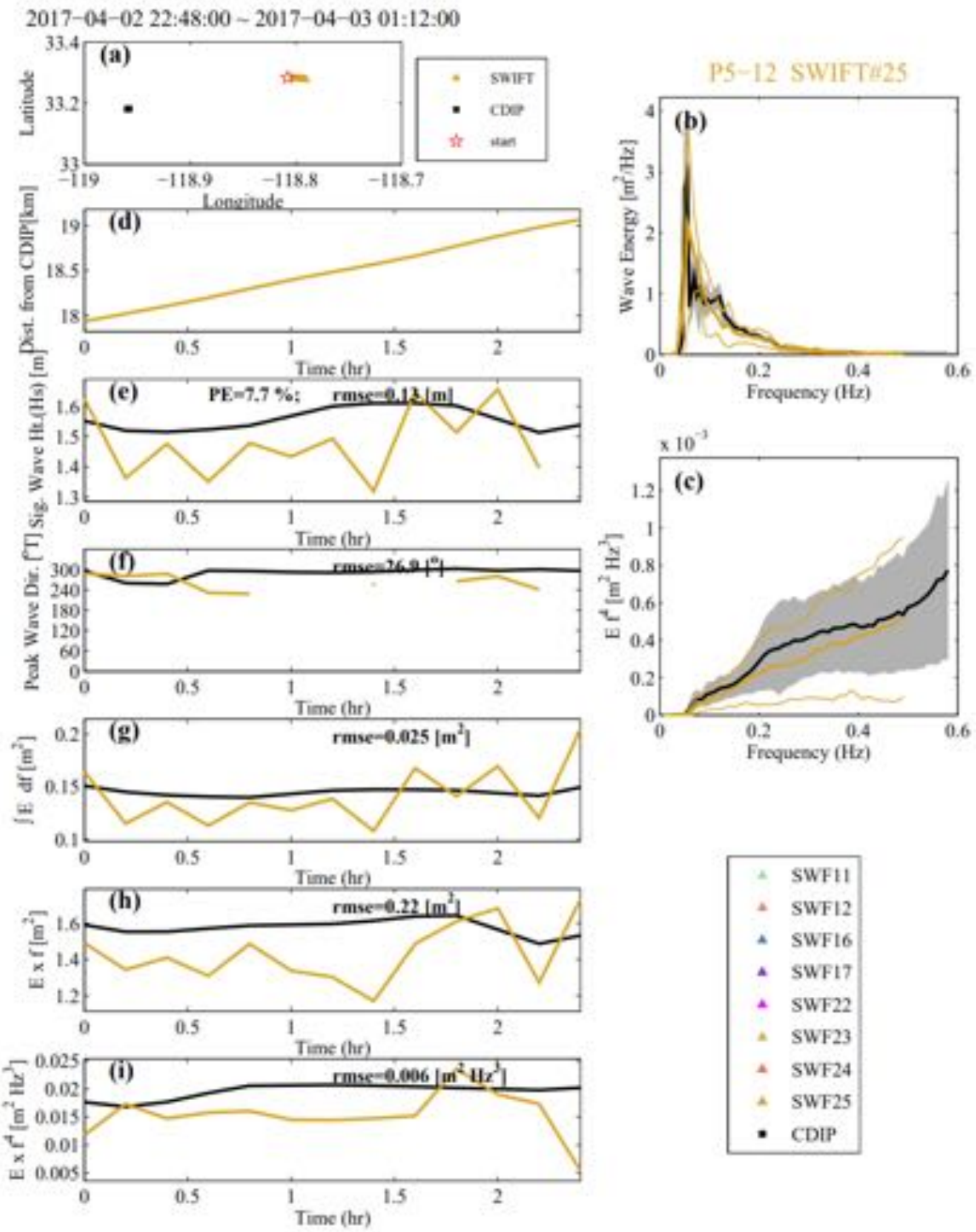

Figure 3.38: SWIFT #25 and CDIP wave energy measurement in period 5–12.

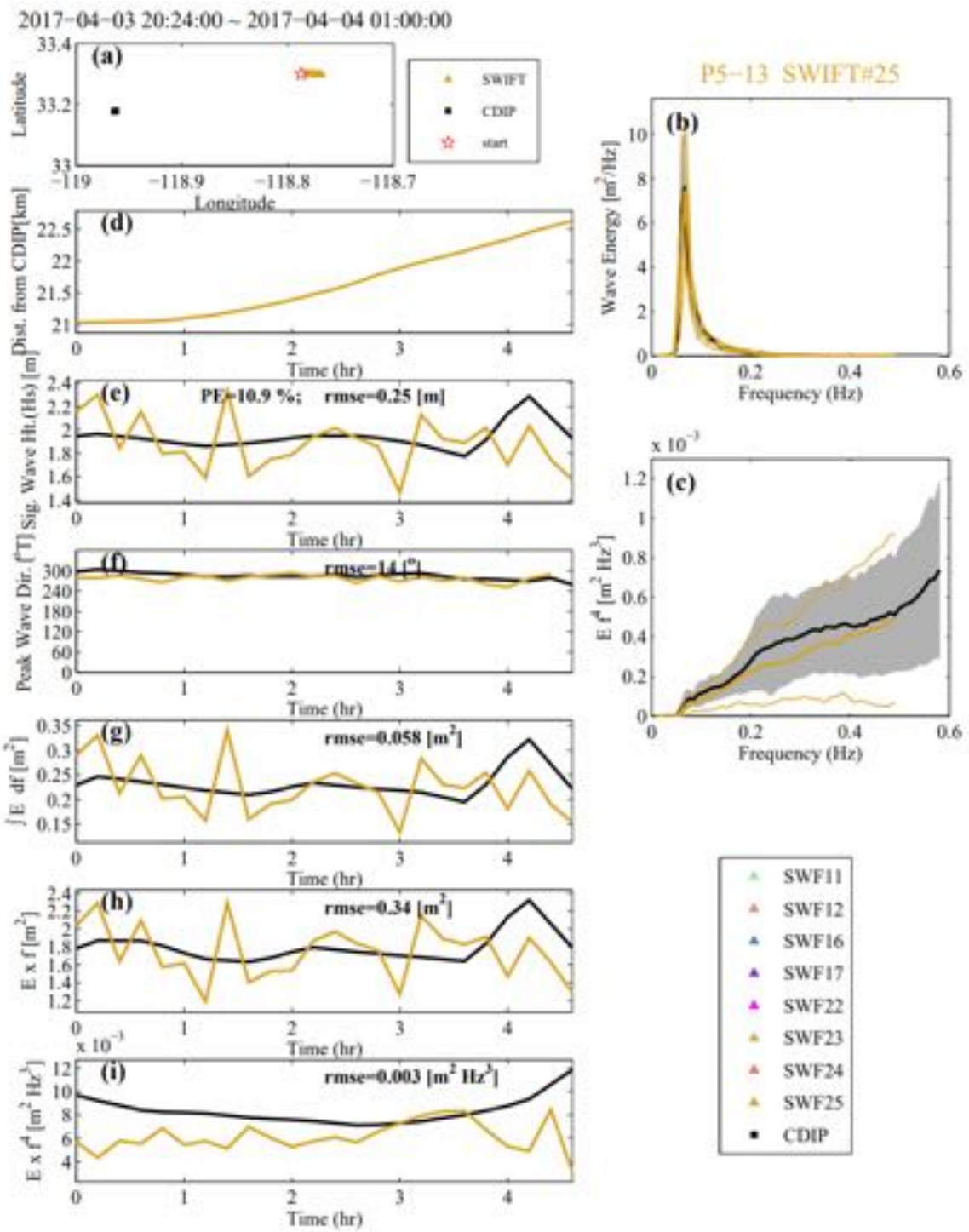

Figure 3.39: SWIFT #25 and CDIP wave energy measurement in period 5–13.

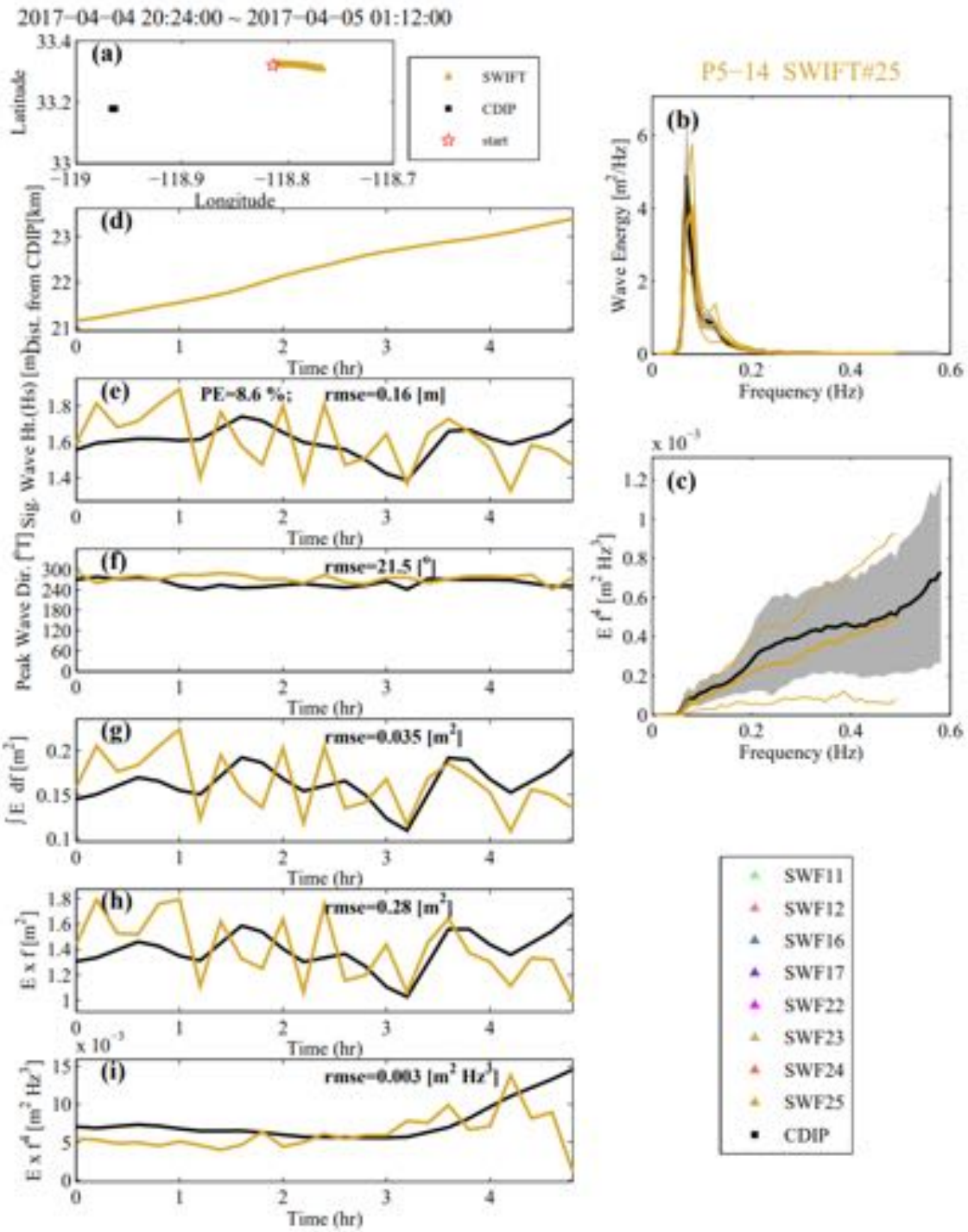

Figure 3.40: SWIFT #25 and CDIP wave energy measurement in period 5–14.

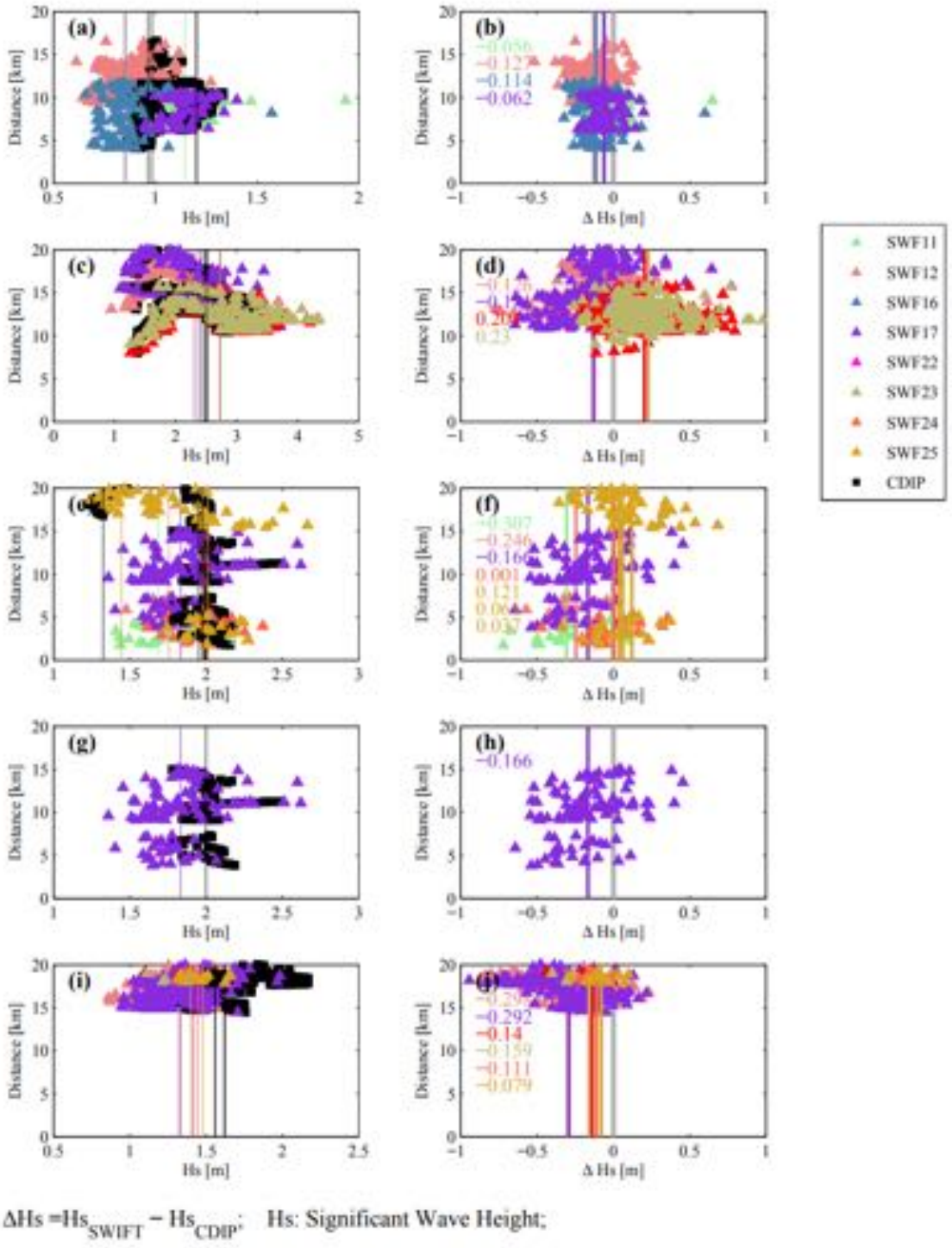

Figure 3.41: Distance vs. significant wave height (Hs) of SWIFTs and CDIP.

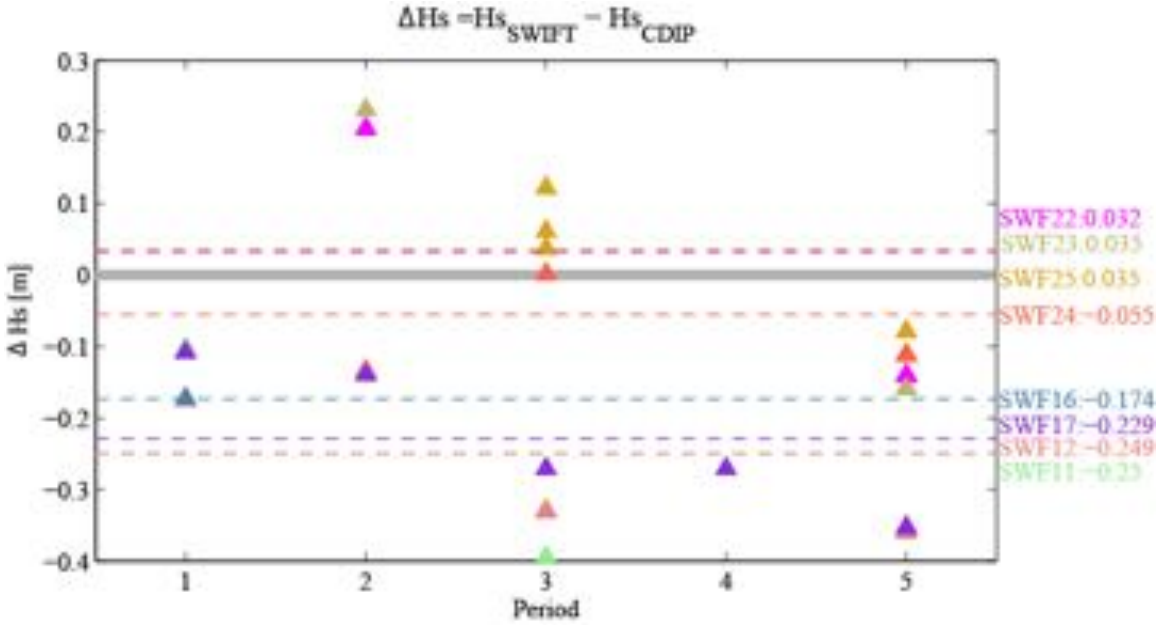

Figure 3.42: The difference of significant wave height period 1–5.

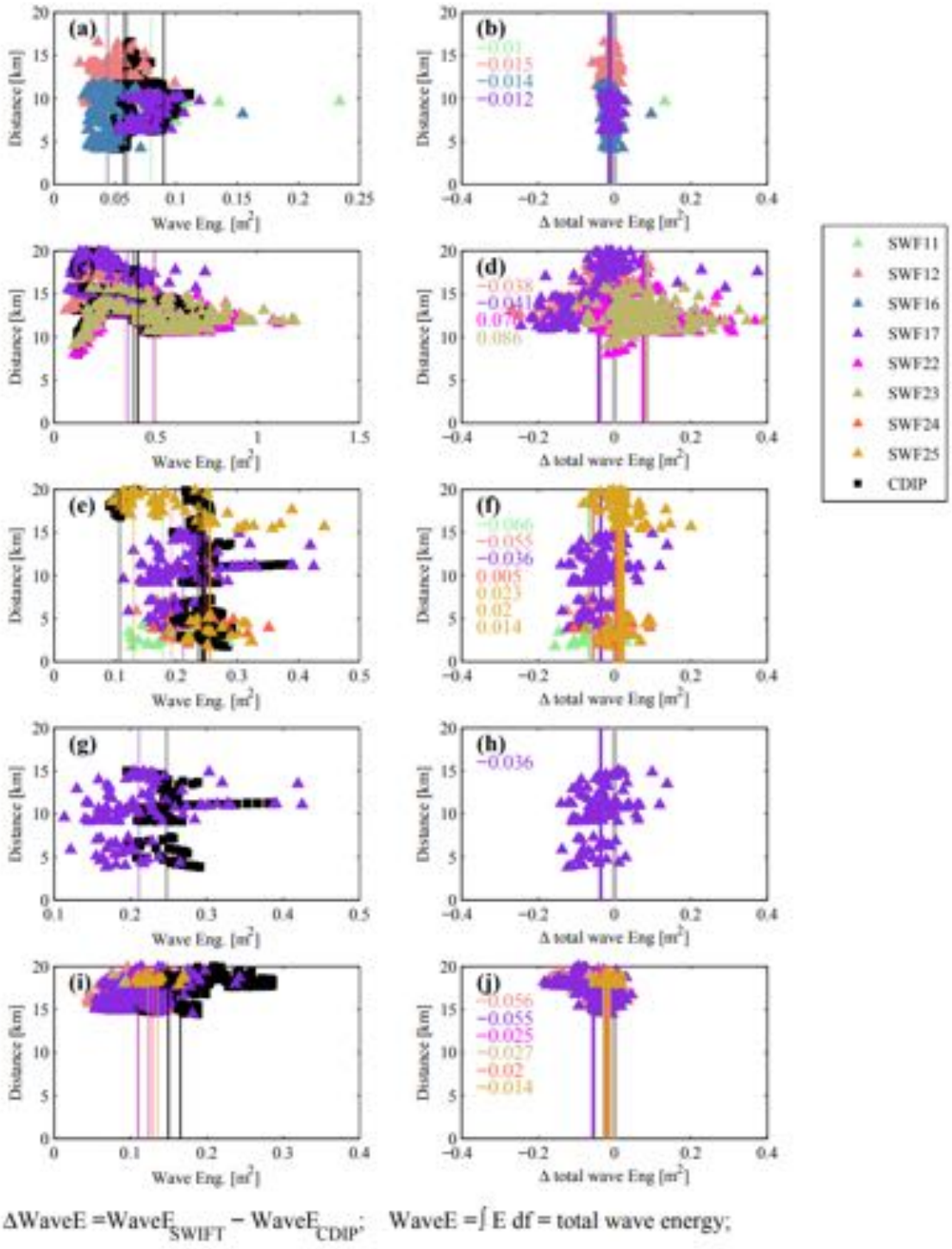

Figure 3.43: Distance vs. total wave energy of SWFITs and CDIP.

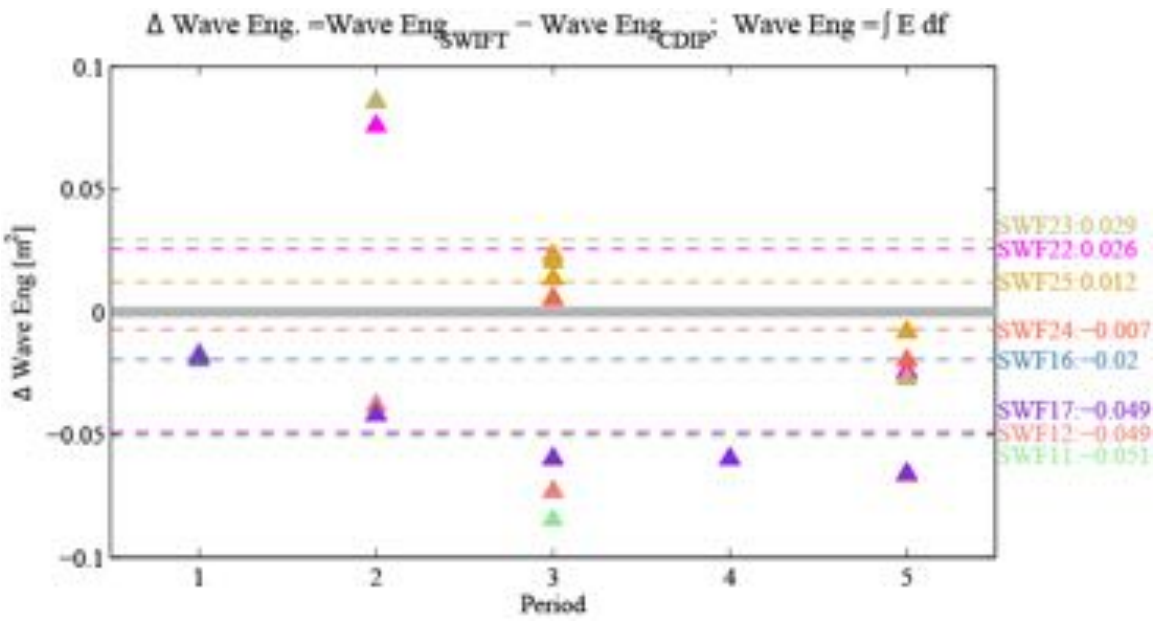

Figure 3.44. The difference of total wave energy over period 1–5.

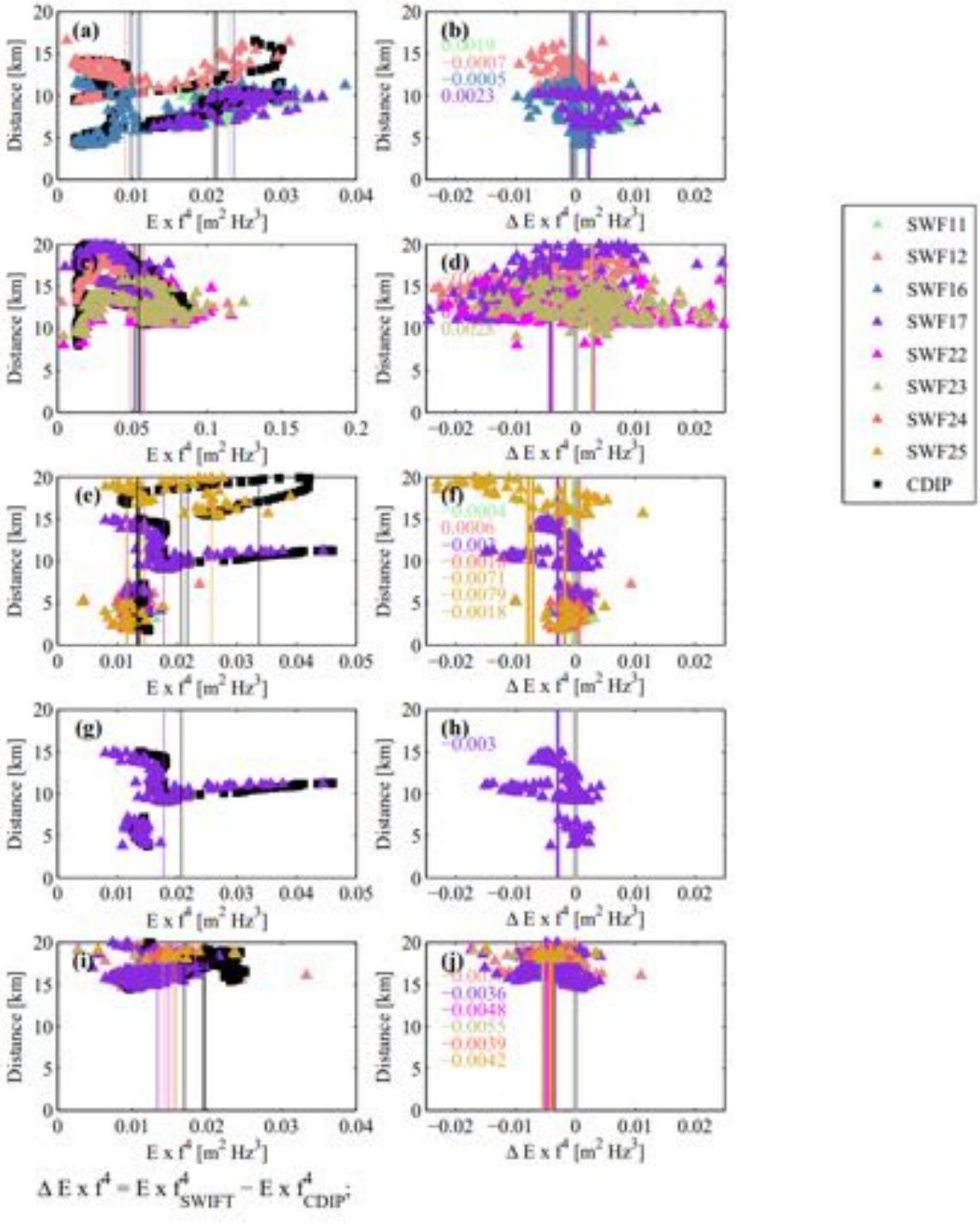

Figure 3.45: Distance vs. compensated wave energy of SWFITs and CDIP.

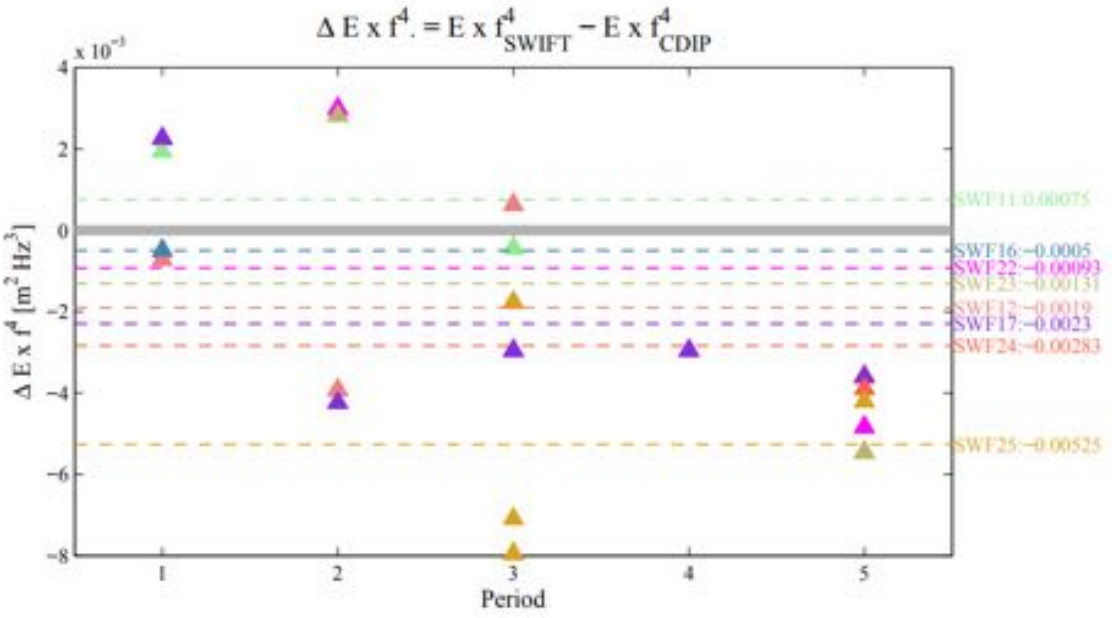

Figure 3.46: The difference between compensated wave energy over period 1–5.

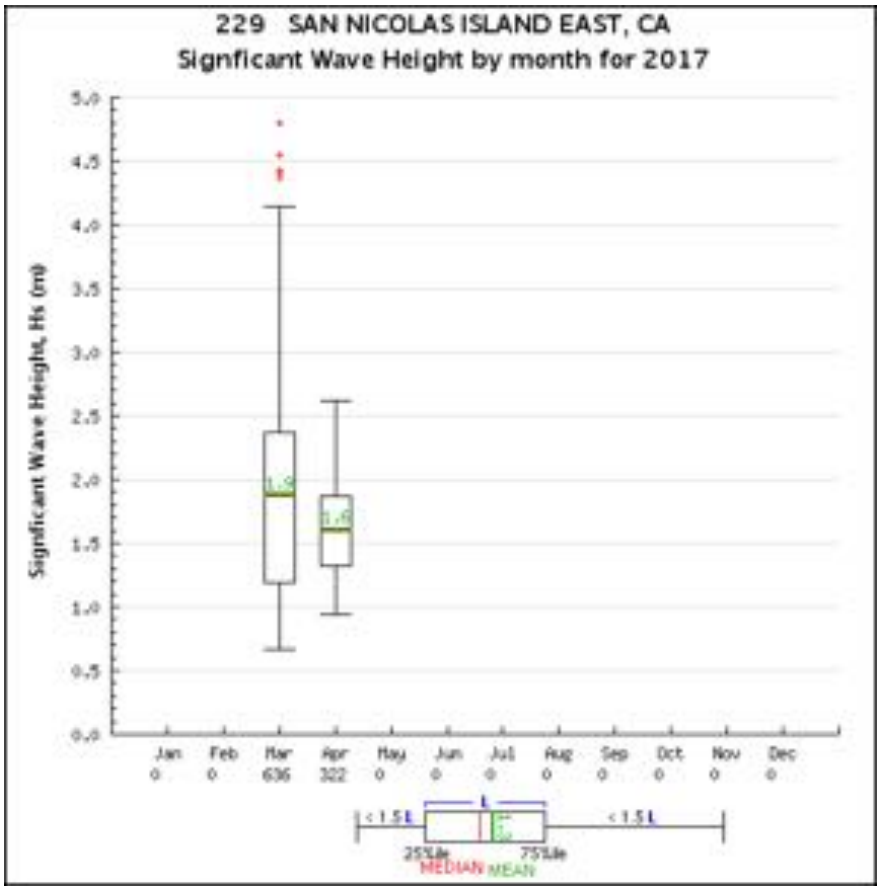

source: http://cdip.ucsd.edu

Figure 3.47: CDIP station 229 significant wave height.

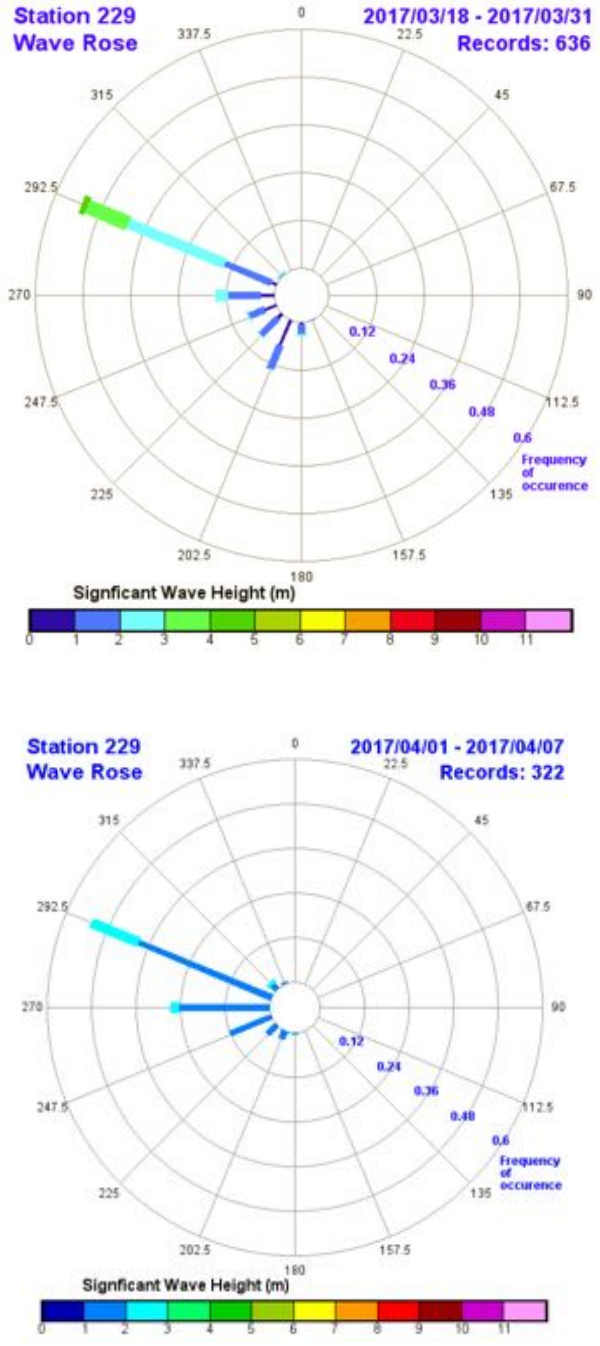

source: http://cdip.ucsd.edu

Figure 3.48: CDIP station 229 San Nicolas Island East wave rose.

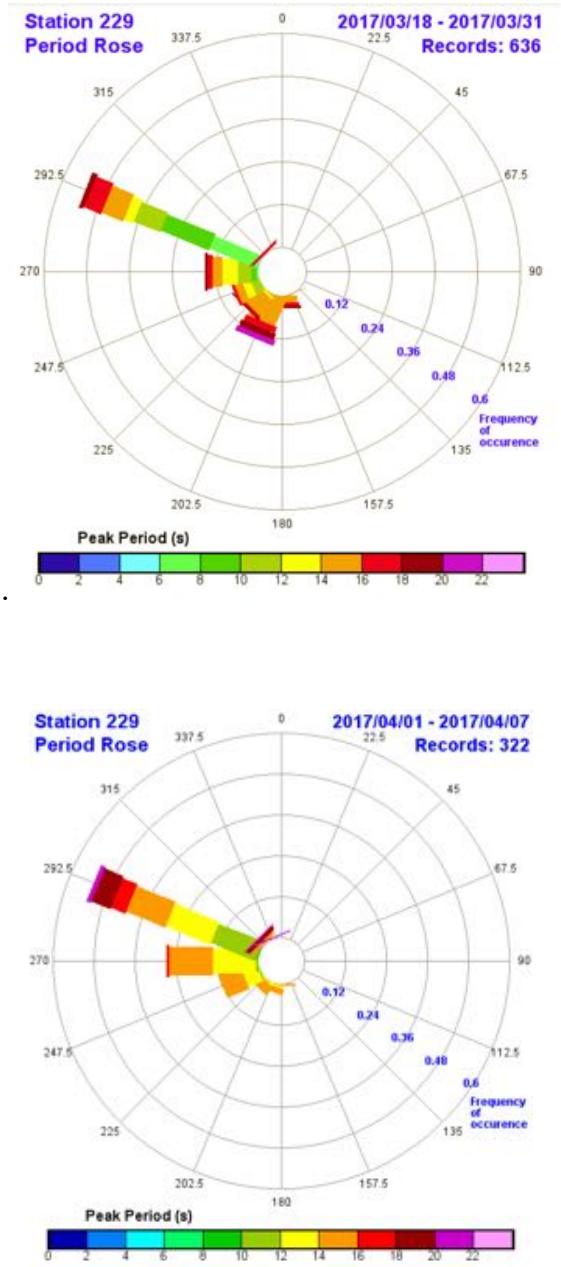

source: http://cdip.ucsd.edu

Figure 3.49: CDIP station 229 period rose.

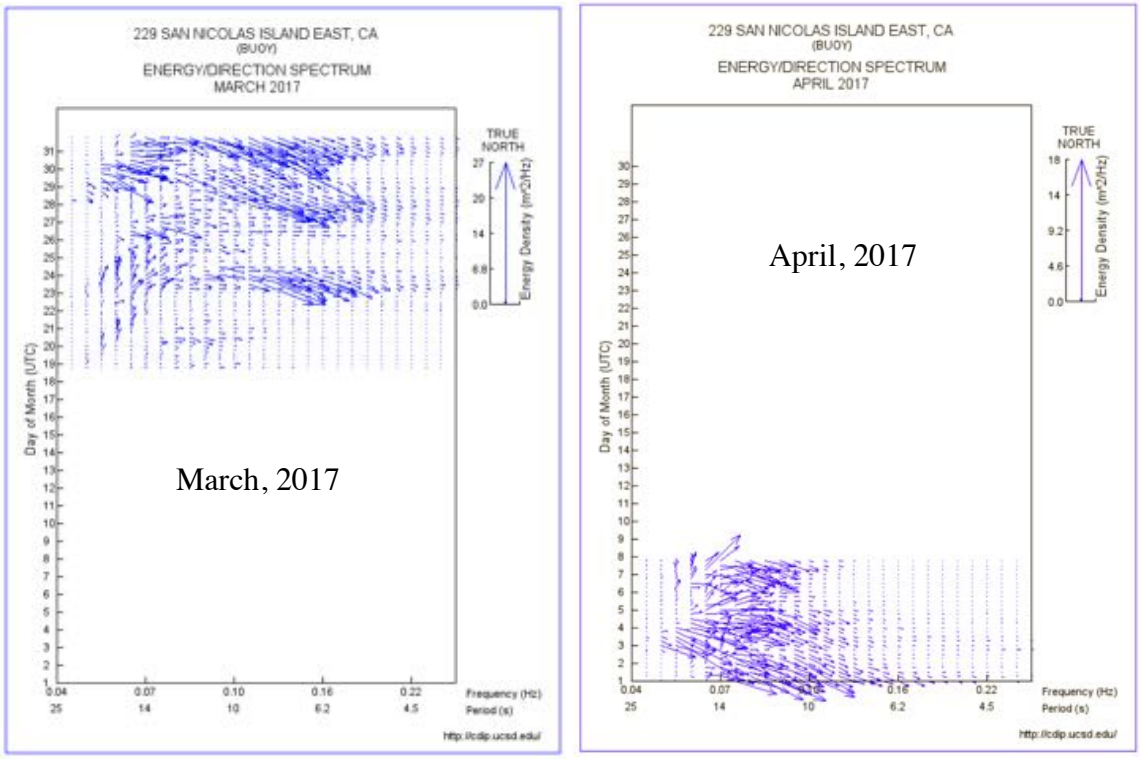

Figure 3.50: CDIP station 229 energy/direction spectrum March 2017.

REFERENCES

D'Asaro, E. A. 2003. Performance of autonomous Lagrangian floats. *J. Atmos. Ocean. Technol.,* 20, 896–911.

Gemmrich, J. 2010. Strong turbulence in the wave crest region. *J. Phys. Oceanogr.,* 40, 583–595.

Herbers, T. H. C., P. F. Jessen, T. T. Janssen, D. B. Colbert, and J. H. MacMahan. 2012. Observing ocean surface waves with GPS tracked buoys. *J. Atmos. Ocean. Technol.,* 29, 944-959.

Sanford, T. B., J. H. Dunlap, J. A. Carlson, D. C. Webb, and J. B. Girton. 2005. Autonomous velocity and density profiler: EM-APEX. *Proceedings of the IEEE/OES Eighth Working Conference on Current Measurement Technology,* 152–156 (IEEE).

Thomson, J. 2012. Wave breaking dissipation observed with SWIFT drifters. *J. Atmos. Ocean. Technol.,* 29, 1866-1882.

Thomson, J., J. Girton, R. Jha, and A. Trapani. 2018. Wave spectra and wind stress measurements from a wave glider autonomous surface vehicle. *J. Atmos. Ocean. Technol.,* 35, 347-363.

Wiles, P., P. Rippeth, J. Simpson, and P. Hendricks. 2006. A novel technique for measuring the rate of turbulent dissipation in the marine environment. *Geophys. Res. Lett.* 33, L21608.

REPORT DOCUMENTATION PAGE

Form Approved
OMB No. 0704-0188

PLEASE DO NOT RETURN YOUR FORM TO THE ABOVE ADDRESS.

1. REPORT DATE *(DD-MM-YYYY)*	2. REPORT TYPE	3. DATES COVERED *(From - To)*
10-03-2020	Technical Report	

4. TITLE AND SUBTITLE
LC – DRI Field Experiment and Data Calibration Report

5a. CONTRACT NUMBER

5b. GRANT NUMBER
N00014-17-1-2859

5c. PROGRAM ELEMENT NUMBER

6. AUTHOR(S)
B. Ma, E. D'Asaro, T. Sanford, and J. Thomson

5d. PROJECT NUMBER

5e. TASK NUMBER

5f. WORK UNIT NUMBER

7. PERFORMING ORGANIZATION NAME(S) AND ADDRESS(ES)
Applied Physics Laboratory – University of Washington
1013 NE 40th Street
Seattle WA 98105

8. PERFORMING ORGANIZATION REPORT NUMBER
APL-UW TR 2002

9. SPONSORING/MONITORING AGENCY NAME(S) AND ADDRESS(ES)
Office of Naval Research
One Liberty Center
875 N. Randolph Street, Suite 1425
Arlington, VA 22203-1995

10. SPONSOR/MONITOR'S ACRONYM(S)

11. SPONSOR/MONITOR'S REPORT NUMBER(S)

12. DISTRIBUTION/AVAILABILITY STATEMENT
Approved for public release; distribution unlimited.

13. SUPPLEMENTARY NOTES

14. ABSTRACT

The goal of the Waves, Langmuir Cells and the Upper Ocean Boundary Layer Departmental Research Initiative (LC – DRI) is to explore the upper ocean physics necessary to advance our understanding of the fluxes into and across the ocean mixed layer, including surface waves and wave breaking, Langmuir cells, and wave – current interaction. A set of comprehensive observational data was collected during the LC-DRI field experiment from various platforms including autonomous floats, drifter, buoys, and shipboard observations. The field campaign was conducted on the coast of Southern California 21 March – 5 April 2017. The fieldwork, including the event log and instrument deployment, is described in Part I. The inter-calibration between observed CTD data from EM-APEX and MLF floats, SWIFT drifters and R/V Sproul are described in Part II. For the MLF vs. EM-APEX calibration, the average salinity of MLF #82 and #83 top and bottom sensors is used as a reference. The calculated salinity offset for EM-APEX #6667, #6672, and #6678 is ~

15. SUBJECT TERMS

16. SECURITY CLASSIFICATION OF:			17. LIMITATION OF ABSTRACT	18. NUMBER OF PAGES	19a. NAME OF RESPONSIBLE PERSON
a. REPORT	b. ABSTRACT	c. THIS PAGE			Barry Ma
unclass	unclass	unclass	unlimited	102	19b. TELEPHONE NUMBER *(Include area code)* 206-221-4720

INSTRUCTIONS FOR COMPLETING SF 298

1. REPORT DATE. Full publication date, including day, month, if available. Must cite at least the year and be Year 2000 compliant, e.g. 30-06-1998; xx-06-1998; xx-xx-1998.

2. REPORT TYPE. State the type of report, such as final, technical, interim, memorandum, master's thesis, progress, quarterly, research, special, group study, etc.

3. DATES COVERED. Indicate the time during which the work was performed and the report was written, e.g., Jun 1997 - Jun 1998; 1-10 Jun 1996; May - Nov 1998; Nov 1998.

4. TITLE. Enter title and subtitle with volume number and part number, if applicable. On classified documents, enter the title classification in parentheses.

5a. CONTRACT NUMBER. Enter all contract numbers as they appear in the report, e.g. F33615-86-C-5169.

5b. GRANT NUMBER. Enter all grant numbers as they appear in the report, e.g. AFOSR-82-1234.

5c. PROGRAM ELEMENT NUMBER. Enter all program element numbers as they appear in the report, e.g. 61101A.

5d. PROJECT NUMBER. Enter all project numbers as they appear in the report, e.g. 1F665702D1257; ILIR.

5e. TASK NUMBER. Enter all task numbers as they appear in the report, e.g. 05; RF0330201; T4112.

5f. WORK UNIT NUMBER. Enter all work unit numbers as they appear in the report, e.g. 001; AFAPL30480105.

6. AUTHOR(S). Enter name(s) of person(s) responsible for writing the report, performing the research, or credited with the content of the report. The form of entry is the last name, first name, middle initial, and additional qualifiers separated by commas, e.g. Smith, Richard, J, Jr.

7. PERFORMING ORGANIZATION NAME(S) AND ADDRESS(ES). Self-explanatory.

8. PERFORMING ORGANIZATION REPORT NUMBER. Enter all unique alphanumeric report numbers assigned by the performing organization, e.g. BRL-1234; AFWL-TR-85-4017-Vol-21-PT-2.

9. SPONSORING/MONITORING AGENCY NAME(S) AND ADDRESS(ES). Enter the name and address of the organization(s) financially responsible for and monitoring the work.

10. SPONSOR/MONITOR'S ACRONYM(S). Enter, if available, e.g. BRL, ARDEC, NADC.

11. SPONSOR/MONITOR'S REPORT NUMBER(S). Enter report number as assigned by the sponsoring/ monitoring agency, if available, e.g. BRL-TR-829; -215.

12. DISTRIBUTION/AVAILABILITY STATEMENT. Use agency-mandated availability statements to indicate the public availability or distribution limitations of the report. If additional limitations/ restrictions or special markings are indicated, follow agency authorization procedures, e.g. RD/FRD, PROPIN, ITAR, etc. Include copyright information.

13. SUPPLEMENTARY NOTES. Enter information not included elsewhere such as: prepared in cooperation with; translation of; report supersedes; old edition number, etc.

14. ABSTRACT. A brief (approximately 200 words) factual summary of the most significant information.

15. SUBJECT TERMS. Key words or phrases identifying major concepts in the report.

16. SECURITY CLASSIFICATION. Enter security classification in accordance with security classification regulations, e.g. U, C, S, etc. If this form contains classified information, stamp classification level on the top and bottom of this page.

17. LIMITATION OF ABSTRACT. This block must be completed to assign a distribution limitation to the abstract. Enter UU (Unclassified Unlimited) or SAR (Same as Report). An entry in this block is necessary if the abstract is to be limited.